the STEEL centre

Steel Centre Engineering Report No. 005 | May 2014

DESIGN AND BEHAVIOUR OF EXTENDED SHEAR TABS UNDER COMBINED LOADS

Kristin Thomas

Robert G. Driver

Logan Callele

Steven Oosterhof

UNIVERSITY OF ALBERTA

cisc icca

Design and Behaviour of Extended Shear Tabs Under Combined Loads

by

Kristin Thomas
Robert G. Driver
Logan Callele
and
Steven Oosterhof

Steel Centre Engineering Report No. 005

Department of Civil and Environmental Engineering
University of Alberta
Edmonton, Alberta, Canada

May 2014

ACKNOWLEDGEMENTS

This research project was funded by the Natural Sciences and Engineering Research Council of Canada (NSERC), the University of Alberta, the Steel Structures Education Foundation, and the Government of Alberta. Donation of the test specimens by Waiward Steel Fabricators, Edmonton, is gratefully acknowledged.

ABSTRACT

Current design procedures for extended shear tab connections tend to be conservative and often do not include considerations for axial load. To address these problems, an investigation into the behaviour of extended shear tabs was completed by testing 23 full-scale specimens. Both unstiffened and stiffened extended shear tab specimens were tested that varied in plate thickness, plate depth, and the number of horizontal bolt lines. The specimens were tested by rotating the beam to 0.03 radians, applying a horizontal load, and then applying vertical load until failure. The horizontal loads varied from 500 kN in compression to 200 kN in tension. Based on the test results, design recommendations were made for both unstiffened and stiffened extended shear tabs. The recommendations include strength equations for bolt group design and plate design, while connection ductility is addressed by ensuring the plate will fail prior to bolt or weld rupture.

TABLE OF CONTENTS

LIST OF TABLES

LIST OF FIGURES

LIST OF SYMBOLS

A_b = bolt cross-sectional area

A_g = gross area

A_{gv} = gross area in shear

A_n = net area

A_{nt} = net area in tension

A_w = weld throat area

B_{BB} = bolt bearing capacity

C = tabulated coefficient for calculating eccentrically loaded bolt group capacity

C' = tabulated coefficient for calculating the moment only bolt group capacity

D = filler weld leg size

d = bolt diameter

d_b = beam depth

d_{bh} = bolt hole diameter

d_c = depth of the plate in compression

d_p = plate depth

d_i = distance from bolt i to the instantaneous centre of rotation

d_{max} = maximum d_i

E = modulus of elasticity

e_{BG} = eccentricity of P

e_g = geometric eccentricity

e_n = end distance

e_{eff} = effective eccentricity

$e_{eff\text{-}cs}$ = clear span effective eccentricity

F_{cr} = critical design buckling stress

F_e = Euler's buckling stress; elastic buckling stress

F_u = ultimate strength of the plate

F_{ub} = ultimate strength of a bolt

F_y = yield strength of the plate

F_{yc} = yield strength of the column

G = shear modulus

I_{BG} = bolt group moment of inertia

I_y = weak-axis moment of inertia

J = St. Venant torsional constant

K = modification factor for critical lateral torsional buckling capacity (Salvadori 1955)

k = plate buckling coefficient, effective length factor

L = unbraced length/clear span

L_o = location of instantaneous centre of rotation perpendicular to P

L_w = weld length

M = moment

M_{BG} = moment about the centroid of the bolt group

M_{CW} = moment capacity of column web

M_{cr} = elastic lateral torsional buckling moment capacity

M_F = factored applied moment

M_{OBG} = Moment-only bolt group capacity

M_p = plastic moment

M_r = factored moment resistance

M_{ta} = Applied nominal torsional moment

M_{tn} = nominal torsional moment resistance

M_y = yield moment

m = number of shear planes

m_o = location of instantaneous centre of rotation parallel to P

m_w = moment capacity of the column web per unit length

N = nominal applied axial load

N_{CW} = axial column web capacity

N_{GS} = axial gross section yielding capacity

N_F = factored applied axial load

N_{NS} = axial net section fracture capacity

n = number of bolts

n_h = number of horizontal bolt lines

P = resultant force on a eccentrically loaded bolt group

Q = non-dimensional yield stress reduction factor for plate buckling

R_i = force on bolt i

R_n = shear capacity of an individual bolt

R_y = factor to approximate probable yield stress

r = radius of gyration

s = bolt spacing

T = clear distance between column web-to-flange fillets for W-shapes

T_{BS} = block shear capacity

t_b = beam web thickness

t_{max} = maximum plate thickness

t_{min} = minimum plate thickness

t_p = plate thickness

U_t = efficiency factor for block shear

V = shear

V_{CW} = shear column web yielding capacity

V_{BG} = shear capacity of a bolt group

V_F = factored applied shear force

V_{GS} = shear gross section yielding capacity

V_{LTB} = nominal shear force that can be applied without stiffeners

V_{NS} = shear net section yielding capacity

V_{MN} = flexural shear capacity of the plate

V_{PB} = shear causing plate buckling

V_r = Factored shear resistance

V_W = fillet weld capacity

V_y = shear causing flexural yielding

v = Poisson's ratio

w = column web thickness

X_{IC} = x-coordinate of the instantaneous centre of rotation

X_i	=	x-coordinate of bolt i
X_u	=	ultimate tensile strength of weld filler metal
Y_{IC}	=	y-coordinate of the instantaneous centre of rotation
Y_i	=	y-coordinate of bolt i
β	=	angle of resultant load
Δ_i	=	deformation of bolt i
Δ_{max}	=	theoretical maximum bolt deformation
θ	=	End Rotation
θ_i	=	angle of force for bolt i
θ_w	=	orientation of applied force with respect to the weld axis
κ	=	ratio of smaller end moment to larger, positive for double curvature
λ	=	non-dimensional slenderness parameter for plate buckling
σ_n	=	normal stress
τ	=	shear stress
ϕ	=	plate resistance factor
ϕ_b	=	bolt resistance factor
ϕ_w	=	weld resistance factor
ω_2	=	coefficient to account for moment gradient in lateral-torsional buckling capacity

CHAPTER 1: INTRODUCTION

1.1 Statement of the Problem

A shear tab is a type of shear connection commonly used in steel building construction, wherein a plate is welded in the vertical orientation to a column or girder, and bolted to the supported beam. As demonstrated in Figure 1-1, "extended" shear tabs have the same configuration as conventional shear tabs, but normally frame into the supporting member's web and extend beyond its flanges. This creates a larger geometric eccentricity, the distance between the bolt group centroid and weld (denoted as "a" in Figure 1-1), that must be accounted for explicitly in design. The recommended limit on eccentricity for conventional shear tabs is typically between 75 mm (3 in), according to the Canadian Institute of Steel Construction's Handbook of Steel Construction (CISC 2010), and 89 mm (3.5 in), according to the American Institute of Steel Construction's Steel Construction Manual (AISC 2011). The extended configuration is also known as an extended single plate connection or a long fin plate.

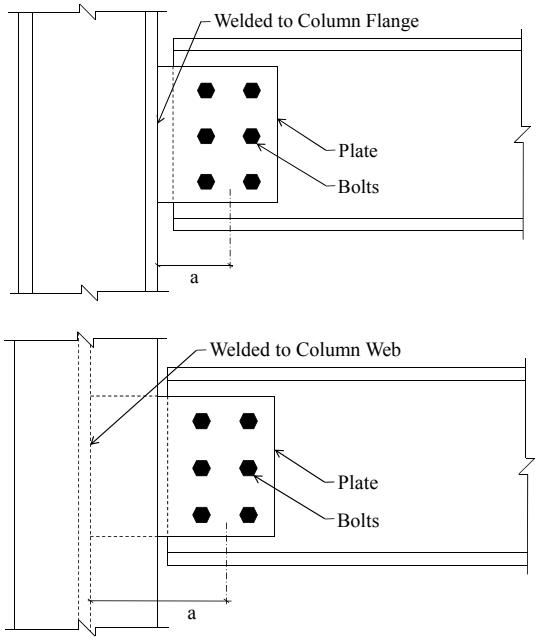

Figure 1-1: (a) conventional shear tab and (b) extended shear tab geometry

Extended shear tabs are either unstiffened, like conventional shear tabs, or stiffened by welding the plate either directly to the flanges of a girder or to perpendicular stiffeners, or stabilizer plates, located between the flanges of a column. The stiffener plates may be required for the extended shear tab only or also as part of the connection to the column strong axis and can be located directly above and below the plate or offset from the plate. Examples of unstiffened and stiffened extended shear tabs framing into a column are shown schematically in Figure 1-2. The stiffeners in this figure are offset from the top and bottom of the by increasing the plate depth near the column web.

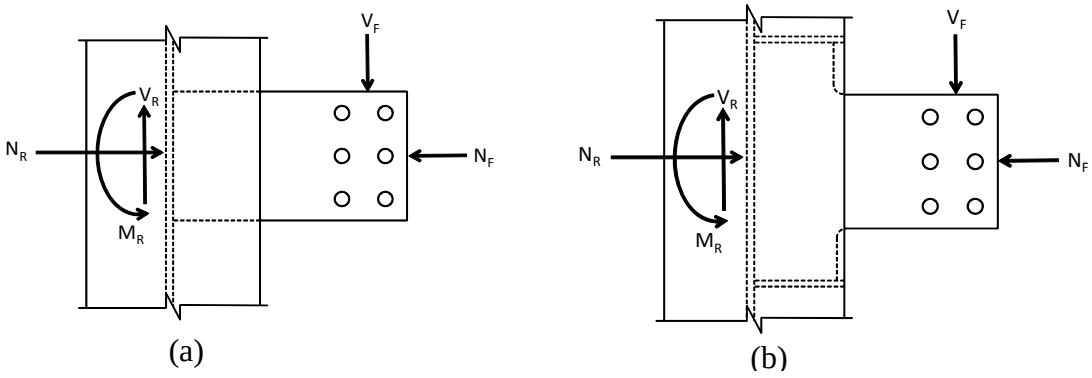

Figure 1-2: Combined loading on (a) unstiffened and (b) stiffened extended shear tabs

Extended shear tabs are advantageous when framing a beam into the web of either a column or girder as they eliminate the need for coping the beam, normally making for a more economical connection. Typical coped beams, connected to the support using an end-plate or angle (a conventional shear tab could also be used), are compared to an equivalent unstiffened extended shear tab connection in Figure 1-3. By using the extended shear tab, the beam can more easily be positioned during construction, improving both speed and safety during assembly of the structural components. Despite their relatively common use, extended shear tab behaviour is not well understood. As such, conservative procedures and assumptions are commonly adopted for expediency, leading to excessively conservative connection designs.

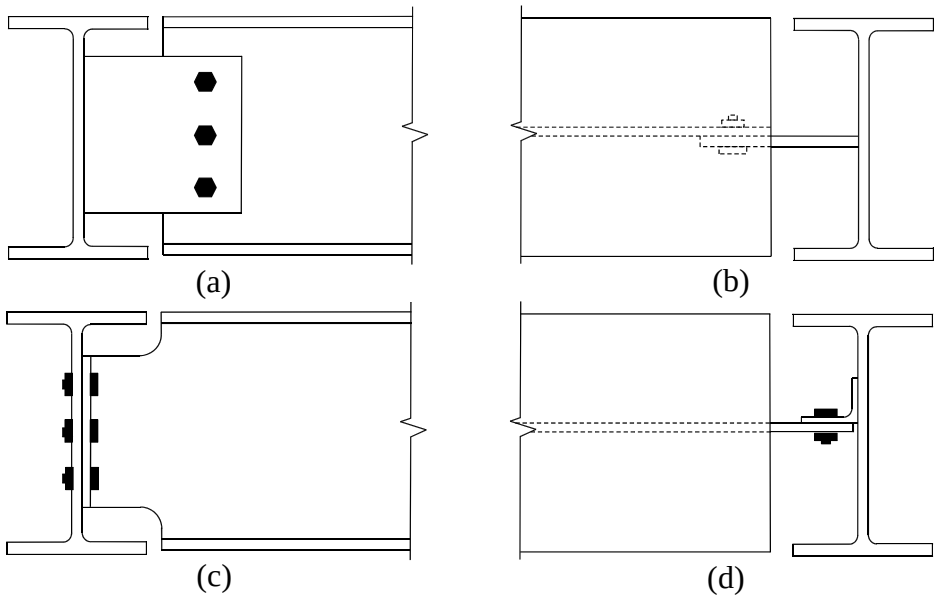

Figure 1-3: (a) extended shear tab connection to girder (elevation); (b) extended shear tab connection to column (plan); (c) double-coped beam and end plate connection to girder (elevation); (d) double-coped beam and single angle connection to column (plan)

Because the extended shear tab plates are slender, one main consideration for design is the stability of the connection. Plate buckling becomes an even larger concern when the connection is loaded under both shear and compression. However, the manner in which shear, axial load, and moment interact on the plate is complex, particularly after significant inelastic action has taken place.

The requirement for connections to transfer axial load, either compressive or tensile, in addition to shear is becoming more common. These loads may originate from the building shape, as is the case for gable-framed buildings, from industrial equipment supported by the structure, or as part of the lateral load resisting system for wind or earthquake loading. Connections may also be required to have a certain degree of axial load capacity to ensure robustness of the structure or, in other words, to prevent collapse due to abnormal loading such as blast or impact.

1.2 Objectives and Scope

The objective of this work is to examine the behaviour of extended shear tab connections, both with and without the presence of axial load. By varying a number of geometric parameters, as well as the magnitude and direction of the horizontal load, current design procedures were evaluated to determine their validity. This was completed by conducting full-scale laboratory tests and comparing the measured capacities with those predicted by the design procedures. Ultimately, a recommendation of an appropriate design model was made for the failure modes observed in the laboratory.

A limited number of research programs have studied the behaviour of extended shear tabs, especially those connected to a flexible support such as a column or girder web. A total of 23 full-scale unstiffened extended shear tab tests were found in literature, with 17 framing into the weak axis of a column. Results of 29 stiffened extended shear tabs were found, including 20 framing into the column web. None of these tests examined the effect of horizontal loading, nor have any of the tested connections had more than one vertical bolt line.

To expand the available test results, this research program includes 23 specimens, 13 without stiffeners and 10 stiffened configurations. All had two vertical lines of bolts and the beam was braced laterally to isolate the local connection behaviour. The specimens differed in four geometric characteristics in addition to varying the magnitude and direction of the applied horizontal load: the number of horizontal bolt lines, plate depth, plate thickness, and use of stiffeners. The effect of beam end rotation was also examined to determine the sensitivity of the connection behaviour to a moderate beam rotation. In addition to determining the capacity of each connection, its behaviour was also characterised in terms of the sequence of development of the various limit states. The test specimen capacities and critical failure modes were compared to those predicted by current design procedures. Due to the difference in behaviour, the unstiffened and stiffened configurations

were analyzed separately and design recommendations were developed for both configurations.

1.3 Organization of Thesis

This thesis consists of six chapters. Chapter 2 contains a literature review of areas pertaining to this research including shear connections, shear tabs, extended shear tabs, and axially loaded shear connections. Capacity equations related to extended shear tab design, as well as an overview of design standards from North America and Europe, are also presented in the second chapter. The experimental program is discussed in Chapter 3. Details of the specimen geometry and design are given, followed by an overview of the material properties, test set-up, instrumentation, and test procedures. Following the experimental design, a summary of the test results is presented by giving the maximum recorded vertical load and observed failure modes for each specimen. Chapters 4 and 5 discuss the behaviour and design of unstiffened and stiffened extended shear tabs, respectively. Each proposes design recommendations based on observations made from the results of the testing program. Finally, a summary of the research is presented in Chapter 6 and conclusions about the behaviour and design of extended shear tabs are made, as well as recommendations for future work. Appendix A includes sample calculations. Appendix B contains shear-deformation graphs for the unstiffened specimens, while those for the stiffened test specimens are given in Appendix C.

CHAPTER 2: BACKGROUND AND LITERATURE REVIEW

2.1 Introduction

Extensive research on the behaviour of shear connections has been conducted in North America and Europe over the past fifty years. Much of this research concentrated on the behaviour and design of shear tabs due to their economy in terms of fabrication. However, despite their relatively common use, a limited number of research programs have investigated the behaviour of extended shear tabs and, therefore, no comprehensive limit states design procedure has been widely accepted. As such, elastic procedures are commonly adopted for expediency, leading to excessively conservative connections.

In the following sections, an overview of existing knowledge related to the behaviour and design of extended shear tabs is given. First, a review of significant general research on shear connections and research specific to conventional and extended shear tabs is presented. Next, capacity equations for the limit states identified during the experimental program that forms part of this research project are explained. Finally, current design guidelines in Canada, the United States, and Europe, are discussed.

2.2 Previous Research

2.2.1 Shear connections

Steel framing connections can be broken into three categories depending on their stiffness and bending moment capacity: moment, shear, and semi-rigid. A connection is typically classified into one of these groups using beam line theory. The beam line is drawn on a graph of moment versus rotation as a straight line connecting the beam's fixed end moment on the vertical axis and its simple span end rotation on the horizontal axis. The moment–rotation curve of a given connection can then be plotted on the same graph. The intersection point of the beam line and moment–rotation curve gives the demand on the connection for a beam under conventional gravity loading (Richard et al. 1980).

Astaneh (1989) proposed that moment connections be classified as those that develop at least 90% of the fixed end moment, while not rotating by more than 10% of the simple span end rotation. The proposed limit for shear connections was given as a moment less than or equal to 20% of that for a fixed end and a rotation greater than or equal to 80% of that for a simple span. Connections that are subjected to a combination of moment and rotation that falls between these moment and shear limits were defined as semi-rigid. This theory can be used in conjunction with beam line theory, as shown in Figure 2-1. Depending on the zone in which the moment–rotation curve and beam line intersect, the connection can be placed into the appropriate category. In the figure, two moment–rotation curves are given: curve "a" and "b". Curve "a" intersects the beam line in the moment zone and is therefore a moment connection. The moment–rotation curve "b" represents a simple connection. However, because elastic beam lines are non-conservative when the beam behaves inelastically, Astaneh (1989) expanded the theory to include inelastic behaviour.

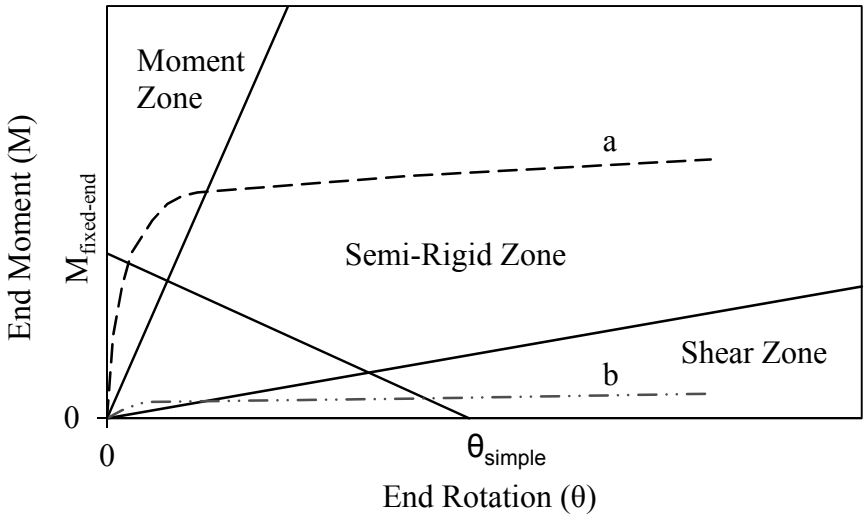

Figure 2-1: Classification of connections based on beam line theory

Using inelastic beam line theory, Astaneh (1989) completed a numerical study to determine the rotational demand on connections at critical loads, such as when the

beam begins to yield in flexure or when its plastic moment is reached. Hundreds of beams were analyzed, varying in section geometry and span length. A "typical" shear–rotation relationship for simple beams, shown in Figure 2-2, resulted from the study. In this figure, the end shear, V, is normalized based on the shear that causes flexural yielding, denoted as V_y. This relationship has been widely accepted and is commonly used to study shear connection behaviour.

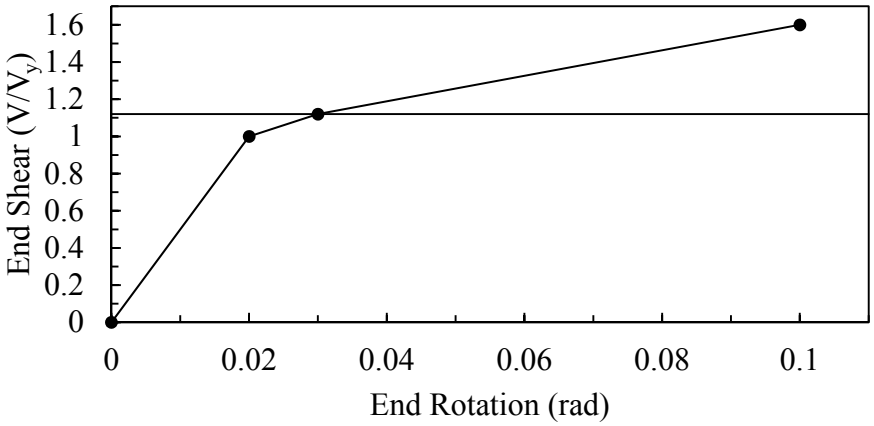

Figure 2-2: Typical shear–rotation behaviour of simple connections

As indicated in Figure 2-2, the rotational demand on a shear connection when the plastic moment is reached in a beam is typically approximately 0.03 radians. Because beams are not designed to resist a load that will cause its plastic moment to be exceeded, this rotation can be considered a reasonable upper limit for shear connections. Among others, Creech (2005), Metzger (2006), and Guravich and Dawe (2006) targeted this value as the maximum rotation during their test programs. To allow any combination of moment, rotation and shear to be applied to the connection, Astaneh (1989) proposed a test set-up consisting of two vertical actuators connected to a beam that is cantilevered from the connection. One force-controlled actuator is positioned next to the connection to apply primarily shear and another is placed near the end of the beam to maintain a specified rotation.

Although the theory and testing procedures that have been developed for shear connections ignore the influence of axial load, Astaneh et al. (1989) recognized

that “major forces present in a simple connection can be shear force, bending moment, and axial load”. However, until recently, most research concentrated on the moment–rotation behaviour as well as shear capacity of connections. After the collapse of the World Trade Center in 2001, research into progressive collapse prevention has increased the number of tests done on connections subjected to axial tension, although axial connection forces are also commonplace under normal service conditions, particularly in industrial structures. On the other hand, demands on connections in a progressive collapse scenario involve rotations far greater than those discussed above for conventional loading.

2.2.2 Shear Tabs

Research into the behaviour of shear tab connections has a long history, and design procedures began to be developed in the mid-1900s. Although a previous design procedure had been proposed by Lipson (1968) and another by Richard et al. (1980; 1982) that were verified and refined by other researchers, the experimental program and design procedure proposed by Astaneh et al. (1993) laid the foundation for the design methods used today.

Astaneh et al. (1989) began an extensive research program into the behaviour of shear tabs that was continued by Porter and Astaneh (1990) and Shaw and Astaneh (1992). The first phase of the research included six tests and resulted in a design procedure that focused on six limit states: shear yielding of the gross area, fracture of the net section, fracture of the end distance of the plate, bolt bearing, bolt fracture, and weld fracture. Shear tabs with three, five, seven, and nine bolts were tested. The rotational stiffness of the connections was reduced as shear yielding began, releasing moment to the centre of the beam and allowing the shear tabs to be sufficiently ductile to accommodate end rotation. The ductility increased with the depth of the connection. Porter and Astaneh (1990) also tested shear tabs with short slotted holes and found that the limit states were unaffected. Beam-to-girder connection tests were completed by Shaw and Astaneh (1992), who observed that shear tab behaviour was most sensitive to the number of bolts

and the support condition, either rigid or flexible. The flexible support allowed larger rotations to occur due to deformation of the girder web. A change in failure mode was also evident when results from tests with rigid and flexible support conditions were compared. Bolt fracture was more common for rigidly supported shear tabs, whereas weld fracture was often observed when the plate was connected to a girder web. In one case, the failure mode was girder web yielding, which was not included as a limit state in the design procedure (Astaneh et al. 2002).

Additional shear tab research was completed by Creech (2005). A total of ten full-scale specimens were tested. The specimens varied in a number of parameters, including support type and number of bolts. Creech found that consideration of the eccentricity of the shear force was only required when calculating the bolt group capacity for two or three bolt connections and, therefore, connections with more than three bolts could be designed by calculating the direct shear capacity of the bolt group. However, the support type was found to reduce the bolt group capacity due to the additional rotation from the girder web.

Metzger (2006) conducted four additional shear tab tests. However, only two were loaded to failure. Through these tests, Metzger studied the effective eccentricity acting on the bolt groups and found that using nominal bolt strengths, without the bolt group action factor, and the distance from the weld to the vertical bolt line gave the best approximation. The bolt group action factor is used to account for non-uniform load distributions in a connection by reducing the bolt strength by 20%.

A series of eight specimens with more than one vertical bolt line was tested by Marosi et al. (2011a). Although a larger number of bolts was used, the connections were able to reach rotations comparable with those of single-line connections. The connection strength was conservatively predicted by a design procedure proposed by Marosi et al. (2011b), which was a modified version of the American Institute of Steel Construction (AISC) procedure for extended single

plate connections (AISC 2005), in which the bolt shear capacity was calculated using 0.62 of the ultimate tensile stress rather than 0.5.

2.2.3 Extended Shear Tabs

The critical limit states for extended shear tabs are similar to those observed for conventional shear tabs. However, due to the complex behaviour introduced by the increased load eccentricity and extended plate, research programs to determine additional design parameters have been completed. These include investigations of both stiffened and unstiffened geometries, as well as physical and numerical testing.

Moore and Owens (1992) conducted a series of tests that mimicked realistic shear tab connections in order to verify a design model proposed by the Steel Construction Institute and the British Constructional Steelwork Association in their design guide (BCSA and SCI 2002). The tests were completed by connecting a shear tab to both ends of a test beam. The compression flange of the beam was laterally restrained along its length at regular intervals and, using two hydraulic jacks, the test beams were loaded in two phases. First, the nominal live and dead loads were applied to determine the elastic characteristics of the connections. The load was then removed and reapplied until failure occurred. Although these beam-to-column connection tests included both regular and extended shear tabs, only the results from the specimens with the extended configuration are included in this discussion.

From the first phase completed at working loads, Moore and Owens (1992) found that the deflection of the beams at mid-span was much larger than that permitted for serviceability, 1/360 of the beam length. The large deformation was caused by a combination of vertical plate deformation and rotation. The rotation was significantly larger when the connection was made to the column web. From these results, Moore and Owens (1992) suggested that serviceability may be the governing limit state for extended shear tab connections.

Assuming a constant shear along the length of the shear tabs, Moore and Owens (1992) found that the moment varied significantly. At the ultimate load, they found that two locations were particularly important for describing the moment at failure: the weld line and the bolt line. The location of failure depended on the length of the plate. Extended shear tabs were more likely to fail at the weld line, whereas shorter plates tended to fail at the bolt line. The extended shear tabs also had a tendency to twist.

The behaviour of extended shear tabs connected to both interior and exterior columns were included in the test program. The interior column connection test was conducted by loading a cantilevered section on the opposite side of the column web, maintaining an equal moment on both sides of the web. As a result, the interior and exterior connections developed similar moments, but the interior connection had a much lower rotational ductility (Moore and Owens 1992).

Sherman and Ghorbanpoor (2002) conducted an extensive testing program on extended shear tabs for AISC. A total of 31 tests were completed, including six unstiffened beam-to-column, two unstiffened beam-to-girder, 14 stiffened beam-to-column, and nine stiffened beam-to-girder connections. Variations in the number of horizontal bolt lines, plate dimensions, support members, beam sizes, lateral braces, and bolt hole types were accompanied by changes in how the plates were welded to the support, the size of stiffener plates used, and the method of bolt installation. A number of observations, geometric restrictions, and design suggestions were given for extended shear tabs:

1. Pretensioned bolts do not influence connection behaviour.
2. Short slotted holes and standard holes can both be used and do not influence the strength of the connection.
3. Bracing the beam laterally does not affect connection capacity.
4. Both sides of the plate must be welded to the supporting member.
5. Stiffener plates need not be thicker than the shear tab.
6. Stiffeners need not be welded to the column web.

Based on their results, Sherman and Ghorbanpoor (2002) recommended the consideration of plate twisting and web yielding as possible failure modes. Plate twisting was observed during many of the unstiffened extended shear tab tests, as was column web yielding for the supports with thinner webs. Buckling of the plate was also observed for two connections in beam-to-girder tests when the connection was made to both the top and bottom girder flanges. However, checks for these three observed failure modes were not included in their proposed design method.

Sherman and Ghorbanpoor (2002) also observed that unstiffened extended shear tabs have "excessive" vertical deflections. Therefore, to reduce the mid-span beam deflections, connection capacities were given as the load that caused a reasonable level of deflection, considered by the researchers to be a quarter-inch of total vertical connection deformation.

A research program on the design of stiffened beam-to-column extended shear tabs was completed by Goodrich (2005). In both physical tests and finite element simulations, the shear tab plates were stiffened at the top and bottom to determine how stiffeners influence the connection behaviour and if a reduced eccentricity can be used in design instead of the actual. The capacities of the three geometries tested were more than twice those predicted by the design procedure proposed by Goodrich, and exceeded the AISC allowable stress design safety factor of 1.67.

All of the extended shear tab tests described above used specimens with only one vertical bolt line. The use of multiple vertical bolt lines was investigated by Metzger (2006). Four beam-to-column connection tests were completed to assess the validity of the AISC extended configuration design procedure, three of which had two bolt lines and the other, one. However, unlike the majority of the tests discussed above and extended shear tabs typically used in construction, the plates were welded to the column flange in lieu of the column web.

The specimens tested by Metzger (2006) were designed according to AISC's extended configuration guidelines (AISC 2005). Although the measured

connection capacities exceeded the design capacities, the predicted failure mode—bolt shear fracture for all four tests—was incorrect. The connections either failed due to weld fracture or the beam failed prior to connection failure. The welds that failed were smaller than those recommended by AISC for shear tab design, but the capacities calculated using the AISC equation for weld design over-predicted the strength when the eccentricity was ignored. Although the AISC design procedure ignores the load eccentricity on the weld, Metzger (2006) recalculated the weld strength using the geometric eccentricity, the distance from the weld to the centroid of the bolt group, and found these values were lower than the tested capacity. This suggests that, although the eccentricity of the load must be considered when designing the weld, the effective eccentricity is likely less than the total eccentricity.

2.2.4 Combined Loading

When simple connections are required to resist a tensile or compressive force in addition to shear, they tend to be rotationally stiffer (Thornton 1997). This increased stiffness may cause fracture of the weld or bolt(s) and lead to a progressive failure. Using an approximation of the maximum possible moment that the connection will attract, Thornton (1997) proposed equations for tee, angle, and end-plate connections to ensure progressive failure of the connection will not occur. These equations are used to ensure the less ductile connection elements, like the bolts or welds, have sufficient ductility to preclude premature failure. Thornton (1997) also proposed an equation for tensile capacity that was based on prying action and accounted for shear–tension interaction.

Guravich and Dawe (2006) examined the behaviour of common shear connections, including shear tabs, when subjected to combined shear and tension. This research was partly in response to evolving requirements to design connections for tensile "tie-forces", which are intended to improve overall structural integrity. They found that, similar to shear tabs without axial load,

ductility was provided by yielding of the plate and bolt bearing. They also found that the nominal bolt bearing resistance, B_{BB}, given by:

2-1 $$B_{BB} = t_p n e_n F_u$$

where t_p is the plate thickness, n is the number of bolts, e_n is the end distance (perpendicular to the vertical edge of the plate), and F_u is the ultimate strength of the plate, gave a consistent approximation of the resultant force on the connection at failure, with an average experimental-to-predicted capacity ratio of 0.94. Therefore, the end distance becomes critical to connection behaviour.

Guravich and Dawe (2006) also studied the effect of shear force on the connection's ability to resist tension. The tensile capacities of shear tab connections were found after zero, fifty, and one hundred percent of the factored bolt shear capacity was applied in shear. These tests showed that as long as the shear stress in the plate is less than approximately 50% of the yield stress, the tensile capacity of the connection does not decrease.

Research into the prevention of progressive collapse of structures has focused on the ability of connections to allow floor and roof structures to bridge over a failed column. In this column-removal analysis, the connections are subjected to high tensile forces as well as moment and shear. However, much higher rotations than expected under normal loading conditions are applied to the connections and, therefore, this aspect is outside of the scope of this project.

A design procedure for extended shear tabs subjected to axial load is given by Tamboli (2010). The procedure is similar to that in the AISC Steel Construction Manual (2011), described in Sections 2.4.2 and 2.4.3, but includes a buckling check of the plate, treating it as a column subjected to a compressive load. The interaction of the shear, moment and axial load is also taken into consideration. The detailed procedure is shown in Appendix A.

2.3 Capacity Equations

Capacity equations for limit states associated with shear connections and members under axial load have been developed that are widely accepted for use in design. The equations related to extended shear tabs and axially loaded connection elements are presented in the following sections.

2.3.1 Gross Section Yielding

Gross section yielding occurs when a member has yielded along the depth of its cross-section, allowing for gradual failure as the material deforms plastically. While often treated as an ultimate limit state, particularly for member design, gross section yielding in connection elements differs from many of the other such limit states. When gross section yielding occurs, the connection deforms and, therefore, this limit state can be used instead as a means of controlling the overall connection behaviour by ensuring a ductile failure. When a plate is subjected to axial load only, the nominal capacity of the gross section in tension or compression, N_{GS}, is calculated as follows, barring instability failure:

2-2 $$N_{GS} = A_g F_y = d_p t_p F_y$$

where A_g is the gross cross-sectional area, F_y is the yield strength, and d_p is the plate depth. Using the von Mises yield criterion for pure shear, the nominal shear resistance, V_{GS}, is:

2-3 $$V_{GS} = 0.577 A_g F_y = 0.577 d_p t_p F_y$$

The 0.577 shear coefficient is often increased in design to account for strain hardening; for example, CSA standard S16 (CSA 2009) uses a value of 0.66. Under bending, the moment at which the plate begins to yield at the extreme fibres, M_y, is:

2-4 $$M_y = \frac{d_p^2 t_p F_y}{6}$$

The plate reaches its plastic moment capacity, M_p, when it has yielded through its full depth:

2-5 $$M_p = \frac{d_p^2 t_p F_y}{4}$$

2.3.2 Net Section Fracture

Net section fracture occurs when the connection plate begins to tear along the bolt line. For plates under tension, without significant shear lag, the capacity is given by:

2-6 $$N_{NS} = A_n F_u$$

where A_n is the minimum net area of all possible failure paths and F_u is the ultimate tensile strength of the plate material. For a plate with a regular bolt pattern, the net area is:

2-7 $$A_n = \left[d_p - n_h d_{bh}\right] t_p$$

where d_{bh} is the bolt hole diameter and n_h is the number of horizontal bolt lines. The shear capacity is similar to Equation 2-6, but with the 0.577 shear coefficient added, which assumes that the von Mises yield criterion for pure shear applies also at the ultimate stress. Flexural rupture of connection plates was investigated by Mohr (2005). Based on test results, he suggested that this moment capacity was closely approximated by the plastic moment on the gross cross-section:

2-8 $$M_p = \frac{F_y t_p d_p^2}{4}$$

2.3.3 Column Web Yielding

Because extended shear tabs are usually connected to a flexible web, if unstiffened the strength of the supporting member's web must be evaluated. Yield line theory can be used to find the web's capacity. This theory is applied by assuming a failure geometry and equating the internal work required to cause this

failure mode and the applied or external work done on the system. However, the results from yield line analysis are dependent on the assumed failure mechanism and, if incorrect, they provide an upper bound solution.

For cases where shear tab connections transfer tensile or compressive forces to the column web, Kapp (1974) proposed the failure geometry shown in Figure 2-3.The yield line capacity, N_{CW}, is given by:

2-9
$$N_{CW} = \frac{F_{yc} w^2 d_p}{b} + 4 F_{yc} w^2 \sqrt{1 + \frac{c}{2b}}$$

where F_{yc} is the yield strength of the column web and the values for a=2b+c and c (see Figure 2-3) should be determined by the engineer based on design assumptions. However, Kapp mentions that the clear distance between column web-to-flange fillets, T, could be used for a, and c could be taken as zero or as the plate thickness plus an eighth of an inch to account for the welds.

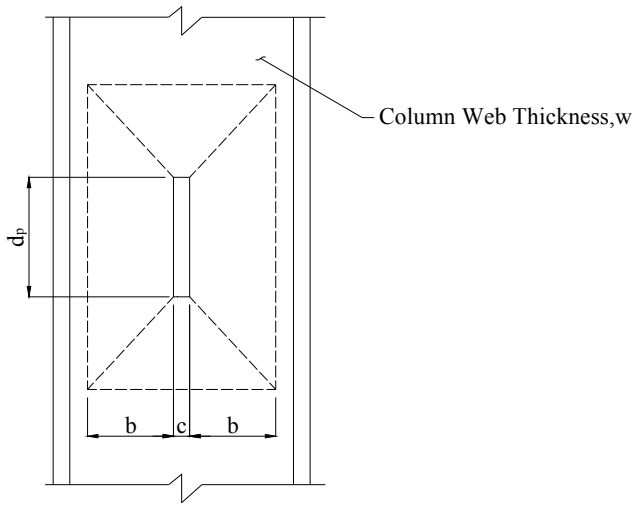

Figure 2-3: Assumed yield pattern in column web subjected to transverse tension or compression from shear tab plate

Two failure geometries were proposed by Abolitz and Warner (1965) to describe the yielding of column webs when subjected to out-of-plane moment. Sherman and Ghorbanpoor (2002) recommended the failure geometry shown in Figure 2-4 for extended shear tabs.

The corresponding capacity equation is:

2-10 $$M_{CW}=m_w d_p \left[\frac{2a}{d_p}+\frac{4d_p}{a}+4\sqrt{3}\right]$$

where m_w is the moment capacity of the column web per unit of length and, similar to Equation 2-9, the a dimension should be determined based on design assumptions.

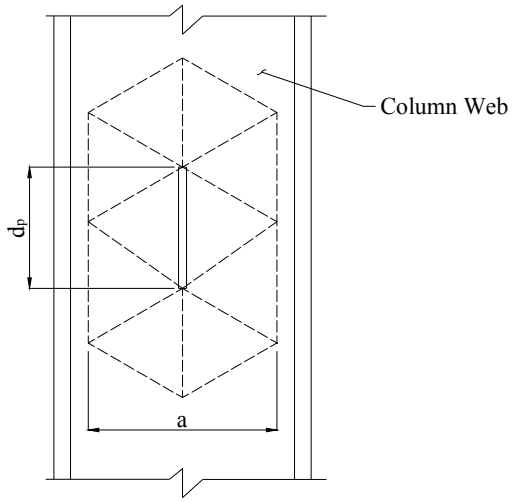

Figure 2-4: Assumed yield pattern in column web subjected to moment from shear tab plate

2.3.4 Out-of-plane Deformation

Out-of-plane deformation of an extended shear tab could occur due to instability related either to lateral–torsional buckling or plate-type buckling. The elastic lateral–torsional buckling capacity of any flexural member with a rectangular cross-section can be represented by its critical moment capacity, M_{cr}, as follows:

2-11 $$M_{cr}=\frac{\pi}{L}\sqrt{EI_yGJ}$$

where E is the modulus of elasticity, I_y is the weak-axis moment of inertia, G is the shear modulus, J is the St. Venant torsional constant, and the warping torsional constant is considered negligible for a thin rectangular section. The

unbraced length, L, for an extended shear tab supporting a laterally-braced beam would be from the weld line to the first vertical line of bolts.

While Equation 2-11 assumes that the member is loaded by a constant moment along its length, Salvadori (1955) proposed interaction curves that accounts for the effect of axial load and a linear moment gradient for wide-flange members of a wide variety of geometries, with plates constituting the limiting case of zero flange width. The member capacity is quantified in terms of a non-dimensional factor, K, that modifies the critical moment. Using Equation 2-12, simplified to apply only to rectangular sections (plates) under a moment gradient, the K values can be converted into ω_2 values, used in S16 (CSA 2009) to account for the moment gradient in unbraced flexural members:

2-12 $$\omega_2 = \frac{K}{\pi}$$

A simple, conservative approximation to Equation 2-12 is provided in S16 (CSA 2009). Applying the modifier ω_2 to Equation 2-12 gives the elastic lateral–torsional buckling equation for an extended shear tab with a linear moment gradient:

2-13 $$M_{cr} = \frac{\omega_2 \pi}{L}\sqrt{EI_y GJ}$$

Because the slender extended shear tab plate is typically subjected to compressive stress resulting from the applied axial load and/or bending from eccentric shear, plate buckling also becomes a concern. The classical plate buckling equation is based on calculating the critical stress, F_e, at which buckling will occur:

2-14 $$F_e = \frac{k\pi^2 E}{12(1-v^2)}\left(\frac{t_p}{d_c}\right)^2$$

where v is Poisson's ratio and d_c is the depth of the plate in compression. The k factor varies depending on the loading and boundary conditions.

2.3.5 Weld Rupture

Shear tabs are connected to the supporting member with a double-sided fillet weld. The capacity of a fillet weld, V_W, depends on the area of the weld throat, A_w, the ultimate tensile strength of the filler metal, X_u, and the orientation of the load with respect to the weld axis, θ_w (CSA 2009):

2-15 $$V_W = 0.67A_wX_u\left(1.00+0.5\sin^{1.5}\theta_w\right)$$

where the coefficient 0.67 relates the filler metal tensile strength to its shear strength. The area of the weld throat is the product of 0.707 times the weld leg dimension, D, and the weld length, L_w:

2-16 $$A_w = 0.707DL_w$$

2.3.6 Bolt Group Capacity

The capacity of a bolt group loaded in shear, V_{BG}, is found by multiplying the number of bolts by the strength of an individual bolt, as follows for a concentric load:

2-17 $$V_{BG} = 0.6nmA_bF_{ub}$$

where m is the number of shear planes, A_b is the cross-sectional area of the bolt shank, F_{ub} is the tensile capacity of the bolt, and the 0.6 reduction is used to approximate shear capacity. Because of the reduction in cross-sectional area, if the bolt's threads are within the shear plane a factor of 0.7 is applied to the capacity given by Equation 2-17 (CSA 2009).

However, when the connection is eccentrically loaded, the bolt group is subjected to a moment and the bolts do not share equally in resisting the load. The capacity of the bolt group is found using the instantaneous centre of rotation method (Crawford and Kulak 1971). This is an iterative procedure that assumes the bolts rotate about an instantaneous centre of rotation, and bolt deformation is proportional to the distance between this point of rotation and the bolt. Figure 2-5

shows the variables and coordinate system for a general case using this method, where the origin is taken as the bolt group centroid.

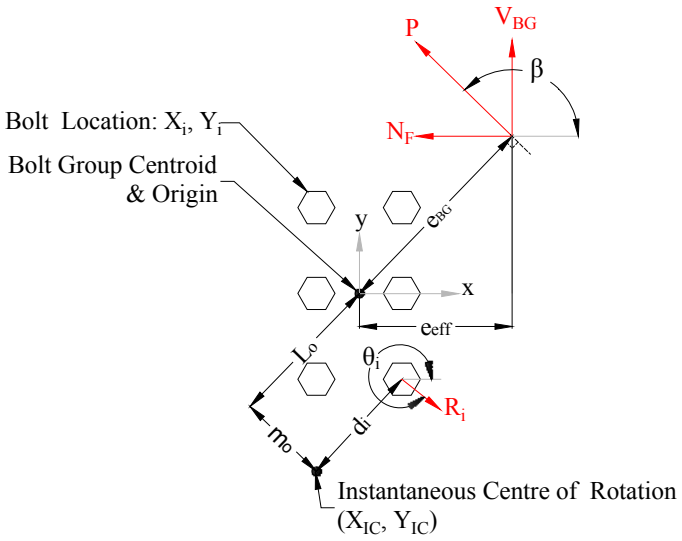

Figure 2-5: Instantaneous centre of rotation variables

The first step is to determine the loads acting on the bolt group and the eccentricity of these loads. Because it is initially unknown, the vertical load capacity of the bolt group, V_{BG}, must be assumed. The resultant load, P, can be calculated as follows:

2-18
$$P = \sqrt{N_F^2 + V_{BG}^2}$$

where N_F is the factored applied horizontal load. The angle with respect to the horizontal axis at which this resultant load acts, β, must also be calculated and is positive in the counter-clockwise direction. For a load case in which the horizontal load passes through the centroid of the bolt group, which is a reasonable assumption for an axially loaded shear tab, the moment about the centroid of the bolt group, M_{BG}, is:

2-19
$$M_{BG} = V_{BG} e_{eff}$$

where e_{eff} is the effective horizontal eccentricity of the vertical load. The eccentricity of the resultant force that would cause this moment, e_{BG}, is then determined as follows:

2-20 $$e_{BG} = \frac{M_{BG}}{P}$$

Next, the forces acting on each bolt, R_i, are determined. These forces depend on the location of the instantaneous centre of rotation, which is initially unknown. Therefore, a location is assumed for the first iteration that is defined from the origin by the dimensions L_o, perpendicular to the resultant applied load, and m_o, parallel to the resultant load. The coordinates of the instantaneous centre of rotation, X_{IC} and Y_{IC}, are then found:

2-21 $$X_{IC} = - L_o \sin\beta - m_o \cos\beta$$

2-22 $$Y_{IC} = L_o \cos\beta - m_o \sin\beta$$

The distance, d_i, from each bolt to the instantaneous centre of rotation and the angle of the bolt's force, θ_i, from the horizontal axis are calculated using the coordinates of the bolts, X_i and Y_i, measured from the origin using Equations 2-23 and 2-24, respectively.

2-23 $$d_i = \sqrt{(Y_i - Y_{IC})^2 + (X_i - X_{IC})^2}$$

2-24 $$\theta_i = \tan^{-1}\left(\frac{Y_i - Y_{IC}}{X_i - X_{IC}}\right) - \frac{\pi}{2}$$

The bolt with the maximum distance from the instantaneous centre of rotation, d_{max}, will be the first to fail and will therefore undergo the maximum theoretical bolt deformation, Δ_{max}, assumed to be 8.64 mm (Crawford and Kulak 1971). The remaining bolt deformations, Δ_i, are:

2-25 $$\Delta_i = \frac{\Delta_{max} d_i}{d_{max}}$$

The force in each bolt, R_i, is then calculated using Equation 2-26, where R_n is the nominal shear capacity of an individual bolt:

2-26 $$R_i = R_n(1 - e^{-0.4\Delta_i})^{0.55}$$

The final step in this procedure is to ensure equilibrium of the forces is achieved. The sum of the bolt force components in the vertical and horizontal directions are equated to the applied shear and axial loads, respectively, as shown in Equations 2-27 and 2-28. Equation 2-29 equates the moment created by the bolt forces about the instantaneous centre of rotation to the moment due to the applied loads. If Equations 2-28 to 2-30 are not all satisfied, the shear capacity, V_{BG}, and the location of the instantaneous centre of rotation, defined by L_o and m_o, are adjusted until equilibrium is achieved.

2-27 $$\sum R_i \sin\theta_i + P\sin\beta = 0$$

2-28 $$\sum R_i \cos\theta_i + P\cos\beta = 0$$

2-29 $$\sum R_i d_i + P(e_{BG}+L_o) = 0$$

2.3.7 Bolt Bearing

The connected material, the shear tab and the beam web, may fail due to excessive deformation from bolt bearing or by bolt tear out. The bearing capacity is directly related to the strength of the material that surrounds the bolts. Equation 2-1 gives the bearing equation applicable to tearing out of bolts loaded toward a plate edge, a failure mode that can be avoided by checking block shear failure (see Section 2.3.8). Equation 2-30 is used to avoid large deformations around the bolt group and is checked for the connected plates:

2-30 $$B_{BB}=3t_p d n F_u$$

where d is the bolt diameter. The bolts must also satisfy minimum end and edge distances to reduce the probability of bolt tear out.

2.3.8 Block Shear

Block shear failure occurs due to a combination of shear and tension on a block of material. Although both shear and tension contribute to the failure, rupture begins on the tension face, at which time the gross shear area normally carries a stress greater than the yield strength. Equation 2-31 is used in S16 (CSA 2009) for block shear failure, where A_{nt} and A_{gv} are the net area in tension and gross area in shear, respectively. However, the equation varies between codes.

2-31
$$T_{BS} = U_t A_{nt} F_u + 0.6 A_{gv} \frac{(F_y + F_u)}{2}$$

The efficiency factor, U_t, is used to account for any non-uniform stress distribution on the tension face. If both tension and shear are present, Tamboli (2010) suggests either treating the resultant force on the connection as a shear force or using Equation 2-32:

2-32
$$\left(\frac{V_F}{T_{BS\text{-}shear}}\right)^2 + \left(\frac{N_F}{T_{BS\text{-}tension}}\right)^2 \leq 1$$

which is an interaction equation that involves calculating the block shear capacities in both shear, $T_{BS\text{-}shear}$, and tension, $T_{BS\text{-}tension}$, separately. Using the interaction equation will produce less-conservative results than treating the resultant force as a shear load (Tamboli 2010).

2.4 Design Standards and Industry Handbooks

2.4.1 CISC Handbook

A design table for shear tabs is given in the Canadian Institute of Steel Construction (CISC) handbook (CISC 2010). This table is based on the work done by Astaneh et al. (1989) and includes resistances for connections with one vertical bolt line located 75 mm from the weld line. Depending on the number of horizontal bolt lines, ranging from two to seven, the connection resistance, plate length, plate thickness, and weld size are given for 19 mm (3/4 in) and M20 bolts as well as 22 mm (7/8 in) and M22 bolts. Although tables are given for both

flexible and rigid supports to account for variation in the effective eccentricity for different support conditions, the geometric eccentricity is restricted to 75 mm and, therefore, does not include provisions for extended shear tab design.

2.4.2 AISC Manual, 13th Edition

The AISC introduced a new prescriptive design procedure for single-plate connections in the 13th edition of the Steel Construction Manual (AISC 2005). The new procedure separated the design of shear tabs into two categories based on geometry: the conventional configuration and the extended configuration. The conventional configuration design procedure was an updated version of the method given in the previous editions for shear tabs. The new, extended configuration method expanded the design recommendations to include connections with larger eccentricities and an unlimited number of vertical and horizontal bolt lines.

There are some requirements that both configurations have in common. The connections must be made with ASTM A325, F1852, or A490 bolts that are snug-tight, pretensioned or slip critical. Either 248 MPa (36 ksi) or 345 MPa (50 ksi) steel is accepted for both methods. A standard fillet weld size of five-eighths of the plate thickness is required on both sides of the plate to assure the plate yields before the weld fractures. It was reduced from three-quarters of the plate thickness in the previous edition of the manual to reflect a change in the assumed critical limit state from weld yielding to weld fracture (Hewitt 2006). A derivation of the limit is given by Muir and Hewitt (2009). Experimental work done by Metzger (2006) verified that the reduction in weld size produces conservative designs.

The conventional configuration design method provides a simplified design procedure for shear tabs with 2 to 12 bolts in one vertical line that is a maximum of 88.9 mm (3.5 in) from the weld line. When these limitations are met and the remaining variables, such as plate thickness and edge distance, are chosen, the connection is checked for bolt shear, block shear, bolt bearing, shear yielding, and

shear rupture. The eccentricity is only required to be considered during the design of 10 to 12 bolt connections with standard holes. (AISC 2005)

The extended configuration design method was developed for situations in which the conventional configuration's limitations are not met. In other words, the number of bolts, number of vertical bolt lines, and plate length are not restricted. However, the design procedure is much more involved and is based on designing the plate to yield prior to other, more brittle failure modes.

First, the bolt group is designed for bolt shear and bolt bearing. The bolts must be able to resist the shear force, and the moment developed due to the eccentricity of this force. The eccentricity is taken as the distance from the support to the first vertical line of bolts. The maximum plate thickness, t_{max}, is then calculated such that gross section yielding will occur before bolt fracture, as follows:

2-33
$$t_{max} = \frac{6M_{0BG}}{F_y d_p^2}$$

The maximum plate thickness is found using the moment-only capacity of the bolt group, M_{0BG}, plate depth and nominal plate yield stress. This equation is derived using the elastic section modulus of the plate and assumes the plate will begin to redistribute stress as soon as it begins yielding. Equation 2-33 need not be satisfied for a single vertical line of bolts if either the beam web or plate thickness is less than half the bolt diameter plus one-sixteenth of an inch and the horizontal edge distances are greater than twice the bolt diameter. If two vertical bolt lines are used, both the beam web and plate must meet this thickness requirement in order for Equation 2-33 to be ignored.

The AISC Steel Construction Manual (2005) requires checks for shear yielding, shear rupture, and block shear of the plate, as well as a flexure check using the von Mises yield criterion to account for shear-moment interaction. Due to the larger eccentricity of extended shear tabs, the stability check for double-coped beams without any specific geometric limitations is also required, which is based on the classical buckling equation for a plate with one free and three simply-

supported edges under a uniform compressive stress. Muir and Thornton (2004) proposed a simplified equation to determine the plate buckling coefficient, k (see Equation 2-14), needed to determine the critical stress, F_{cr}, based on plate buckling curves presented by Gerard and Becker (1957). The procedure is outlined in Equations 2-34 to 2-36:

2-34 $$F_{cr} = QF_y$$

2-35 $$Q = 1 \text{ for } \lambda \leq 0.7$$

$$= 1.34 - 0.486\lambda \text{ for } 0.7 < \lambda \leq 1.41$$

$$= \frac{1.30}{\lambda^2} \text{ for } \lambda > 1.41$$

2-36 $$\lambda = \frac{d_p\sqrt{F_y}}{t_p\sqrt{47500+112000\left(\frac{d_p}{2L}\right)^2}}$$

where the yield stress is in kips per square inch, L is the unbraced length of the plate parallel to the compressive force, and λ is:

2-37 $$\lambda = \sqrt{\frac{F_y}{F_e}}$$

where F_e is the classic plate buckling stress.

Finally, the designer must ensure that the beam is braced laterally at the support. Using the foregoing procedures, the column can be designed for the transferred shear only, ignoring eccentricity. The AISC Steel Construction Manual (2005) also recommends a minimum depth of the plate equal to half the T-dimension of the beam to provide lateral stability for the beam and for stability during construction. A design example using the requirements given in the manual was completed by Muir and Hewitt (2009).

2.4.3 AISC Manual, 14th Edition

In the 14th edition of the AISC Steel Construction Manual (2011), the design guidelines for both conventional and extended single-plate connection configurations were updated. The conventional configuration procedure was updated to incorporate increased bolt shear capacity values given by AISC's 2010 Specification for Structural Steel Buildings (Muir and Thornton 2011). In previous editions, the load eccentricity was ignored because the bolt shear values included a 20% reduction to account for end-loaded connections and, because shear tabs are not end loaded, ignoring the eccentricity was still conservative. To account for the bolt strength increase, guidelines for determining the effective eccentricity and limits on plate thickness were developed and are given in Table 10-9 of the Steel Construction Manual (AISC 2011). Table 2-1 is a reproduction of these guidelines, where e_g is the geometric eccentricity and d is the bolt diameter.

Table 2-1: AISC 14th edition conventional configuration guidelines

Number of Bolts	Hole Type	Eccentricity	Max. Plate or Web Thickness
2 to 5	Short Slotted	$e_g/2$	None
	Standard	$e_g/2$	d/2 + 1/16
6 to 12	Short Slotted	$e_g/2$	d/2 + 1/16
	Standard	e_g	d/2 – 1/16

Table 2-1 was developed using results from 22 shear tab tests conducted by several researchers that failed due to bolt fracture. To determine the effective eccentricity for each test, the shear capacity of the bolt group was calculated, ignoring load eccentricity. The ratio of the tested capacity to the shear capacity of the bolt group was then calculated and, using the instantaneous centre of rotation method, the effective eccentricity causing this strength reduction was then calculated and expressed as a proportion of the geometric eccentricity. Figure 2-6 shows the effective eccentricities of the 22 tests with the Table 2-1 values ($e_g/2$ and e_g) shown as horizontal lines. The black data points correspond to the black line and the grey data points the grey line. Although the effective eccentricities for

many of the tests exceed the design values, Muir and Thornton (2011) have given a detailed rationalization for using the values in Table 2-1, including limiting the shear tab or beam web thickness to ensure ductility.

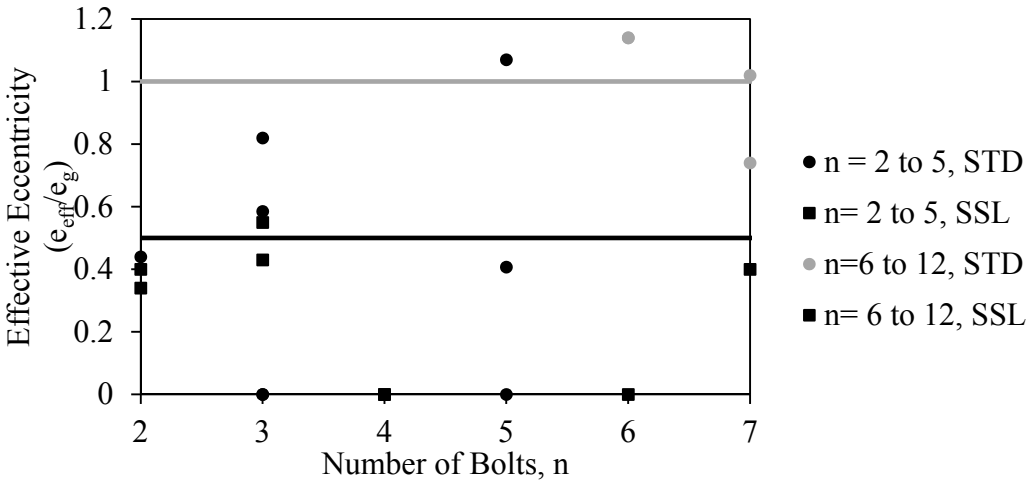

Figure 2-6: Effective eccentricities of the tests used for AISC Table 10-9

The conventional configuration design guidelines also address plate buckling in the 14th edition (AISC 2011). However, because the geometric eccentricity is limited to 89 mm (3.5 in), Equations 2-34 to 2-36 can be used to show that buckling of the plate will not occur (Muir and Thornton 2011).

Few changes were made to the extended configuration design method and most of them were minor. The calculation of the bolt group moment capacity was updated to reflect the changes to specified bolt strengths and the use of short slotted holes was addressed and became explicitly permitted. An interaction equation for shear and moment acting simultaneously on the plate was implemented that requires shear yielding and shear buckling be checked as per Equation 2-38, in lieu of the flexural check in the 13th edition that just accounts for the reduction in yield stress according to the von Mises yield criterion (AISC 2011):

2-38
$$\left(\frac{V_F}{V_r}\right)^2 + \left(\frac{M_F}{M_r}\right)^2 \leq 1.0$$

where V_F is the factored applied shear force, V_r is the factored shear resistance, M_F is the factored applied moment, and M_r is the factored moment capacity.

Guidelines for the use of the optional stiffeners shown in the previous edition of the manual were included in the 14th edition (AISC 2011). The new criteria for determining whether or not stabilizer plates (stiffeners) are required is based on the work by Cheng et al. (1984) on coped beams. Thornton and Fortney (2011) adapted the design method for unbraced double-coped beams to extended shear tabs by assuming that the beam itself acts as a rigid body between the shear tabs. Because the rigid beam was considered unbraced, two times the geometric eccentricity of the shear tab was used as the member length. Although the plates are not subjected to a constant moment over their length, applying the double-coped beam equation, which makes this assumption, was considered a conservative approach. While inconsistent with the constant moment, a constant shear was assumed over the length of the plate and, solving for the reaction force that would cause the plate to fail by lateral–torsional buckling:

2-39
$$V_{LTB}=1500\pi\frac{d_p t_p^{\,3}}{L^2}$$

If this resisting force is less than the applied shear, stiffeners are required.

Finally, the torsional capacity of the connection is calculated according to equations developed by Thornton and Fortney (2011) to account for the effect of the lap splice between the plate and the beam web. They proposed a resistance equal to the torsional capacity of the plate in addition to the resistance provided by the beam bearing against the concrete, if a slab if present. This resistance must be greater than the torsional moment caused by the lap splice. However, in the examples presented by Thornton and Fortney (2011), the capacities of the connection were much higher than required and, therefore, they suggest that the effect of the lap splice can be neglected in most cases.

2.4.4 Eurocode

The design requirements for the components of shear connections are covered by Eurocode 3: Design of Steel Structures – Part 1-8: Design of Joints (2005). However, design guidelines for specific types of connections are not given in this code. The British Constructional Steelwork Association (BCSA) and the Steel Construction Institute (SCI) jointly published detailed design procedures for connections, including shear tabs, that meet the requirements of Eurocode 3. When shear tabs are designed using this procedure, they can be classified as pinned, without additional analysis or experimental evidence to demonstrate their simple connection behaviour. (BCSA and SCI 2002)

The BCSA/SCI design guidelines (2002) define fin plates, or shear tabs, as either short (conventional) or long (extended) based on the plate's thickness and the distance from the weld line to the first vertical bolt line. The limit for conventional shear tabs is shown in Equation 2-40 and Equation 2-41 describes extended configurations.

2-40 $$t_p/_L \geq 0.15$$

2-41 $$t_p/_L < 0.15$$

The 15 design checks include provisions for both types; however, extended shear tabs are only allowed if the beam is laterally restrained because when unrestrained the behaviour is complex and the connections are more likely to twist, as observed by Moore and Owens (1992).

The BCSA/SCI design philosophy is to design the bolt group to resist the eccentric shear force, while the weld is designed to be stronger than the plate. The first design step is to detail the connection according to the recommended geometry. These recommendations were made to ensure the connection will have the required rotational capacity and, for conventional shear tabs, to provide

sufficient lateral strength when the beam is not laterally supported. In addition to the recommended geometry, standard dimensions are also given for the plate thickness (10 mm), plate width, gap distance, bolt size (20 mm), end distance, edge distance, minimum plate depth (60% of beam depth), and weld size (8 mm).

After the connection has been detailed accordingly, the bolt group is designed to resist the eccentric load. Bolt bearing on both the plate and beam web is then checked. The gross and net shear capacities, as well as block shear capacity of the plate, are verified. Although shear–moment interaction is not directly taken into account, the gross shear capacity is reduced by dividing it by 1.27 to account for moment in the plate. However, moment is not accounted for when calculating net or block shear failure. The lateral stability of the plate and its bending capacity are verified by dividing the plastic moment capacity of the plate by the geometric eccentricity to get the critical shear load. This critical shear value is then reduced to account for lateral–torsional buckling. Finally, the weld capacity is calculated. Although a weld size of 8 mm is recommended, the required size changes based on plate thickness and the material strength (BCSA and SCI 2002).

Additional design guidelines are outlined for the beam strength and stability, especially if it is coped. If an extended shear tab is used, the ability of the beam web to resist moment at the connection is verified. The shear strength of the supporting member, either a girder or column, is checked, as well as its resistance to web tearing if the connection is made on one side of the web of a W-section or to an HSS section (BCSA and SCI 2002).

The British Standard BS EN 1991-1-7 requires a tying force to be resisted by the connection to help mitigate possible progressive or disproportionate collapse. In this design procedure, the plate, bolts, beam web, supporting member, and weld must resist this tensile force. The tying force is considered independently of the design shear (BCSA and SCI 2002).

This design procedure was verified by tests completed by Moore and Owens (1992), as discussed in Section 2.2.3. These tests verified the procedure for beams

with a depth up to and including 610 mm. Larger beams are not recommended because the margin of safety between the design and tested capacities of the specimens decreased with increasing beam depth (BCSA and SCI 2002).

2.5 Summary

Conventional and extended shear tabs are common types of shear connections used for beam-to-girder and beam-to-column connections. Although there has been extensive research into the design of conventional shear tabs, few testing programs have concentrated on the behaviour of extended shear tabs. Research programs by Sherman and Ghorbanpor (2002), Goodrich (2005), and Metzger (2006) have been used to develop the AISC design procedures (2005; 2011), whereas the BCSA and SCI have verified design guidelines with research by Moore and Owens (1992). However, these design procedures do not address the presence of horizontal load or the increase in strength of the connection when stiffeners are present.

Failure modes for extended shear tabs are similar to those identified for conventional shear tabs: gross area yielding, net section fracture, bolt tear out, bolt bearing, bolt fracture, and weld rupture. However, additional failure modes have been observed and should be included in design procedures for extended shear tabs. These additional limit states are column web yielding and out-of-plane deformation. Several of the failure modes cited above are influenced by the presence of axial force and, if present, this force needs to be accounted for explicitly in design.

CHAPTER 3: EXPERIMENTAL PROGRAM

3.1 Introduction

In order to gain a better understanding of the behaviour of extended shear tabs, 23 full-scale tests were completed. A key aspect of this test program is the presence of axial load because, although the stability of this type of connection has always been a design concern, no prior tests had been done considering the effect of compression or tension. In addition to varying the magnitude of tension or compression, the program also investigates the influence of plate thickness, the number of horizontal bolt lines, and the presence of stiffeners (stabilizer plates).

In the following sections, a summary of specimen geometry and design is given, followed by an overview of the material properties, test set-up, instrumentation, and test procedures. A summary of the test results is presented by giving the peak vertical load and observed failure modes for each specimen.

3.2 Test Specimens

As no widely-accepted method currently exists for designing extended shear tab connections subjected to axial load, 12 specimen geometries were designed for the experimental program based on the design procedures used at Waiward Steel Fabricators Ltd. of Edmonton, Alberta, referred to as "the Fabricator" in the remainder of this document. The specimens, shown in Figure 3-1, differ in the number of horizontal bolt lines, the plate thickness, and the use of stiffeners. These three variables are used to identify specimen groups with the same geometry using an alphanumeric I.D. that begins with 2B, 3B, or 5B, depending on the number of horizontal bolt lines. The plate thickness to the nearest millimeter, either 10 or 13, follows. Finally, if the specimen is unstiffened, a "U" follows the plate thickness or, if stiffeners are present, an "S" is used to complete the group I.D. For example, the stiffened specimens with two horizontal bolt lines and a 10 mm plate are identified as specimen group 2B-10-S.

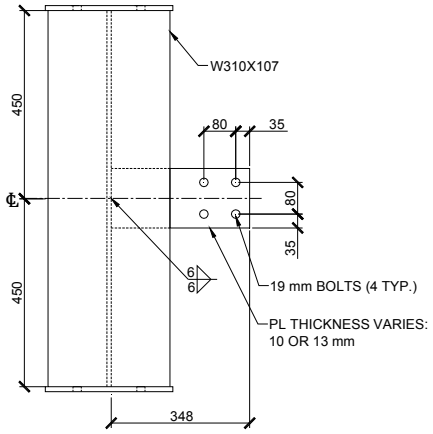

2B-10-U, 2B-13-U

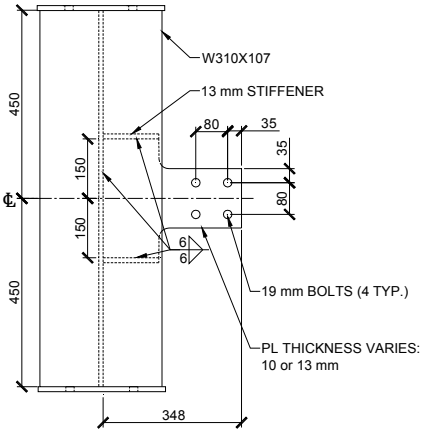

2B-10-S, 2B-13-S

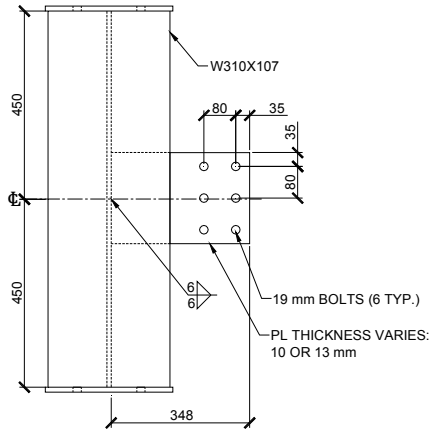

3B-10-U, 3B-13-U

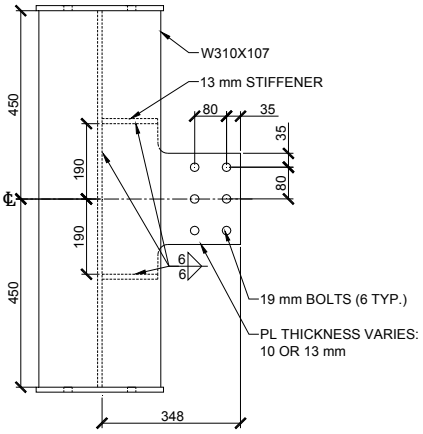

3B-10-S, 3B-13-S

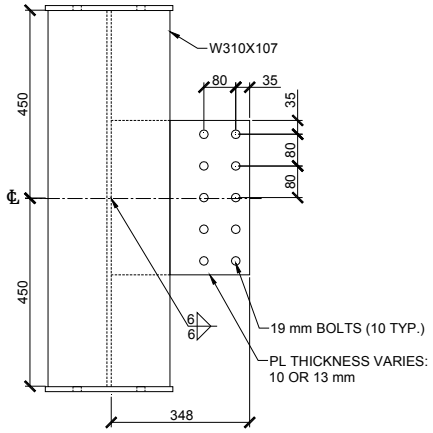

5B-10-U, 5B-13-U

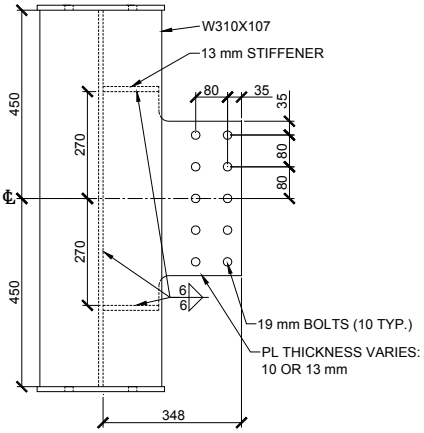

5B-10-S, 5B-13-S

Figure 3-1: Specimen geometries

The magnitude of the horizontal load applied to the specimen, in kilonewtons, is added to the end of the specimen group I.D. to differentiate among test results of specimens with the same geometry. This force is followed by a "C" if it was tested under compression, a "T" if tension was applied, or nothing if the horizontal load was 0 kN. While a small beam rotation was generally applied at the beginning of the test (see Section 3.6), one test was carried out with the beam at zero radians to investigate the influence of beam rotation on the connection capacity. This test is identified by adding an additional zero (there was no horizontal force) to the end of the I.D. (2B-10-U-00).

To determine how the variables described above influence the behaviour of extended shear tabs, typical sizes and dimensions were chosen for the remaining parameters. These constants include a W310x107 column stub, a 348 mm long connection plate, 19 mm (3/4 in) diameter ASTM A325 bolts, two vertical bolt lines, a 6 mm fillet weld, and a constant stiffener configuration, as shown in Figure 3-1. These parameters were used with the Fabricator's design procedure to determine the governing unfactored shear capacities shown in Table 3-1. This design procedure examines the bolt group capacity, bolt tear out, gross section yielding, net section fracture, plate stability, block shear capacity under axial loads, and weld capacity. Additional calculations for stiffener strength and stiffener weld capacity are included if required. Calculations are also completed to determine the maximum and minimum plate thicknesses that ensure a ductile mode of failure. The predicted failure mode for all specimens was shear yielding of the gross cross-section of the shear tab plate. Appendix A provides detailed calculations for a sample specimen.

Because it is commonly used in the design of extended shear tabs, the specimens in this program have two vertical bolt lines. The number of horizontal bolt lines was varied to determine not only the influence of this variable on the capacity, but also to test different plate depth-to-length ratios. Two, three, and five horizontal bolt lines were selected to cover a reasonable range commonly used in buildings.

The shear capacity of the bolt group was determined using the instantaneous centre of rotation method, with the eccentricity taken equal to the geometric eccentricity, i.e., the distance from the weld line to the centroid of the bolt group. Standard bolt holes were used in all specimens, 2 mm (1/16 in) greater than the nominal bolt diameter.

Table 3-1: Unfactored capacities (kN) using Fabricator's design procedure

	Horizontal Load (kN)					
Specimen Group	200T	0	200C	300C	400C	500C
2B-10-U	-	66	55	-	-	-
2B-13-U	-		81	-	-	-
2B-10-S	-	66	55	-	-	-
2B-13-S	-		81	-	-	-
3B-10-U	142	151	142	125	-	-
3B-13-U	-	-	194		-	-
3B-10-S	-	151	142	125	-	-
3B-13-S	-	-	194		-	-
5B-10-U	385	395	-	374	-	-
5B-13-U	-	-	-	467	-	-
5B-10-S	-	-	-	374	334	-
5B-13-S	-	-	-	-	-	420

The extended shear tab plates, fabricated from CAN/CSA-G40.20/G40.21-04 grade 350W steel, vary in both depth and thickness. As the number of bolts increases, the plate depth also increases in order to keep a consistent 80 mm spacing between both the vertical and horizontal bolt lines and 35 mm end and edge distances. The two plate thicknesses chosen, 9.5 mm (3/8 in) and 12.7 mm (1/2 in), are commonly used for extended shear tabs.

The plate length is constant for all specimens. In reality, there is no typical value for this dimension because it depends on the column size, the required gap between the beam and column flanges (with or without clearance for fire-proofing material), the number of vertical bolt lines, the vertical bolt line spacing, and the edge distance. Therefore, typical sizes and dimensions were specified for these parameters and, with the exception of the gap distance, are shown in Figure 3-1. A

gap distance of 50 mm was selected to represent a "worst case" scenario: when fireproofing must be accommodated between the column and beam. As a result, a 348 mm plate was used with a geometric eccentricity of 273 mm.

Due to the large load eccentricity, which was used without any reduction to design the connection, the interaction of shear, moment, and axial load had to be taken into consideration to calculate the gross and net section capacities of the plate. These capacities were estimated using a von Mises stress equation, modified to include the presence of some strain hardening.

Because the specimens were subjected to axial load, the possibility of block shear failure was checked according to standard S16 (CSA 2009), given in Chapter 2. The torsional moment caused by the lap of the plate and beam web was ignored because the beam was laterally and torsionally braced next to the connection.

For the unstiffened extended shear tab connections, the plate-to-column-web weld was designed by neglecting the eccentricity of the load and using the equation for a concentrically loaded weld (see Chapter 2). The weld was sized for the shear capacity of the connection, taken as the minimum of the bolt group and plate capacities. As a result, a 6 mm fillet weld was used on both sides of the plate, for both plate thicknesses.

For stiffened extended shear tab connections, the stiffeners were designed for the shear capacity of the plate and the horizontal load. Because the distance between stiffeners, their thickness, and the weld sizes depend not only on the loads transferred from the weak-axis connection(s) to the column, but also on the forces acting on the column's strong-axis connection(s), the stiffener configuration was chosen to represent typical dimensions used in practice. The stiffeners had a thickness of 12.7 mm (1/2 in) and were offset from the top and bottom of the shear tabs by a clear distance of 75 mm. The radius of the interior corner where the plate depth changes was 25 mm and the stiffener plate extended 115 mm from the column web before changing depth. Double-sided, 6 mm fillet welds were

specified to connect the stiffener plate to the extended shear tab, the column web, and the column flanges.

Each extended shear tab plate was supported by a 900 mm long, W310×107 column stub. A 12.7 mm (1/2 in) column cap plate was welded onto the top and bottom of the column stub for installation of the specimen into the set-up, as described and shown in Section 3.4. The shear tabs were centred vertically on the column web and offset horizontally by one-half of the total beam web plus shear tab thickness to keep the beam and column axes aligned.

The beam was reused for all the specimens tested with the same number of horizontal bolt lines, with the exception of the 5B-10-S-300C and 5B-13-S-500C tests. A new beam was installed for these specimens due to excessive deformation of the web that occurred during the 5B-10-S-400C test. For the two and three bolt line specimens, a W310x129 beam was used, whereas for the deeper, five bolt line specimens, a W530x165 beam was used. These were chosen for three reasons: compatibility with the test set-up, similar web thicknesses, and to preclude beam web failure. The beams had the same edge distance as the extended shear tabs: 35 mm.

As-built dimensions were measured for all of the specimens to ensure they were fabricated as specified. However, because the actual dimensions only varied slightly from those given in Figure 3-1, the specified specimen geometries are used for the remainder of the document.

3.3 Material Properties

3.3.1 Plate Coupon Tests

Tension coupons were fabricated from 500 mm × 500 mm plates that were cut from the same source plate as was used for the extended shear tab specimens. For each plate thickness, four material samples were taken. The coupons were oriented as shown in Figure 3-2, with two samples taken from one direction and the remaining pair taken at 90 degrees from the first. The pairs were cut at

90 degrees to assess the material properties from two orthogonal directions, but the observed differences are not considered to be significant.

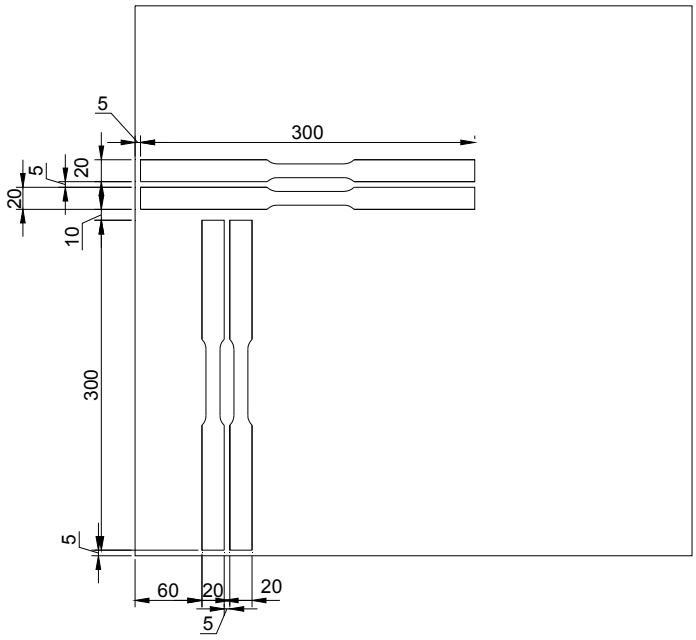

Figure 3-2: Shear tab tension coupons cut from 500 mm × 500 mm plate

The dog-bone shaped material samples were tested according to ASTM standard A370-12a (ASTM 2012). The stress was calculated by dividing the force, recorded by the testing apparatus, by the initial area of the "reduced" section. The strain was measured by an extensometer with a gauge length of 50 mm. Three static points were taken on the yield plateau and averaged in order to calculate the static yield strength, and one static point was taken at the ultimate tensile load. The yield and tensile strengths of each coupon are shown in Table 3-2. These values were averaged to find the material properties of both plate thicknesses.

The elastic modulus, final elongation, and area reduction are also reported in Table 3-2. The elastic modulus was found by performing a linear regression on the elastic portion of the stress–strain curve. The final percent elongation was calculated by dividing the final change in length between two punch marks by the

undeformed distance measured before testing. Finally, the initial and minimum final cross-sectional areas were used to calculate the area reduction.

Table 3-2: Material properties

Plate Size (mm)	Coupon Number	Yield Strength (MPa)	Tensile Strength (MPa)	Elastic Modulus (MPa)	Final Elongation (%)	Area Reduction (%)
10	i	458	500	202000	23.2	68.3
	ii	464	505	206520	23.0	73.0
	iii	451	529	177510	24.8	71.9
	iv	448	495	171500	26.1	73.7
	Average	**455**	**507**	**189383**	**24.3**	**71.8**
13	i	424	473	196250	21.4	59.9
	ii	431	467	200590	25.8	62.7
	iii	404	442	172650	26.0	65.2
	iv	413	496	186540	24.1	65.3
	Average	**418**	**470**	**189008**	**24.3**	**63.3**

For both plate thicknesses, the minimum strength and ductility given by CSA G40.21-04 for this grade were met. The standard deviations of the yield and tensile stresses are within 5% of the mean values for both thicknesses.

3.3.2 Bolt Shear Tests

To determine the shear capacity of the bolts used to connect the shear tab to the beam web, six bolt shear tests were completed on bolts from the same lot. These bolt tests were conducted in single shear to mimic the test conditions. To ensure the shear plane was in the same location as it was during the tests, three tests were completed for each plate thickness. In both cases the shear plane was in the thread run-out region of the bolt, but for the thicker plate it was near the minimum diameter and for the thinner plate it was on the boundary between the thread run-out and the unthreaded shank. The results of the bolt tests are summarized in Table 3-3.

Table 3-3: Bolt shear strength

Test Number	Plate Thickness	
	13 mm	10 mm
1	159 kN	180 kN
2	159 kN	176 kN
3	158	176 kN
Average	**159 kN**	**177 kN**

3.4 Test Set-up

The test set-up was designed to allow any combination of vertical load, horizontal load, and rotation to be applied to the connection. As shown in Figure 3-3, the set-up consisted of an interchangeable column stub specimen (including the shear tab), a beam, and three actuators. This set-up is a modified version of that used by Oosterhof and Driver (2012) for progressive collapse research.

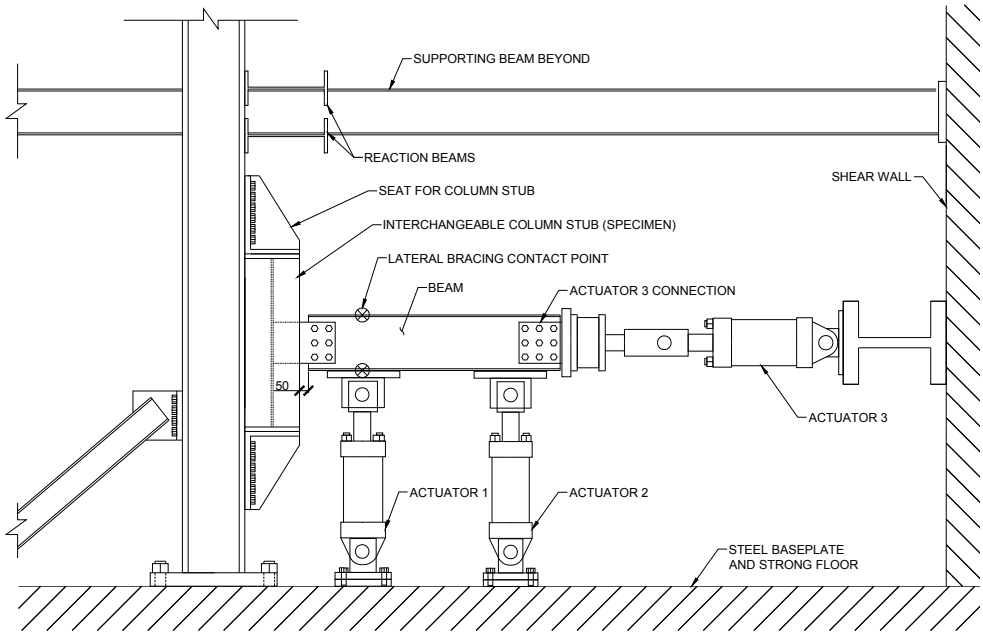

Figure 3-3: Test set-up

Actuator 1 was used to apply vertical load near the connection, while Actuator 2 primarily controlled the rotation of the beam. The specified horizontal load for each test was applied using Actuator 3. The beams were bolted to Actuators 1 and 2 using four 22 mm (7/8 in) diameter pretensioned bolts. Actuator 3 was

connected to the beam using 12.7 mm (1/2 in) lap plates on both sides of the beam web. The plates were connected to the beam web by nine 22 mm (7/8 in) pretensioned bolts in double shear. The other end of the plates were welded to a thick load transfer plate that was in turn bolted to the actuator using eight 25.4 mm (1 in) pretensioned bolts. Actuators 1 and 2 were anchored to the lab's strong floor, while Actuator 3 was connected to a stiff shear wall.

Before testing, the specimen was bolted to seats at the top and bottom of the column stub using the column cap plates. On both ends, the connection was made using four 25.4 mm (1 in) pretensioned bolts to prevent the column stub from slipping. The seats were designed to minimize the possibility of vertical or horizontal deformation during the tests, and were each mounted on a strong column using two vertical lines of nine 25.4 mm (1 in) pretensioned bolts. The column was anchored to the strong floor and braced diagonally to the floor and also back to the shear wall.

Two types of lateral bracing were used in the set-up. First, facing pairs of steel-backed Teflon® slide plates were provided on each side of the beam to serve as bracing near the connection, and their location is shown in Figure 3-3. These slide plates braced both the top and bottom flanges and were shimmed snug between a support column and the beam flanges before each test. In order to apply compressive horizontal loads greater than 300 kN safely, a second set of lateral braces that utilised end rollers against a stiff steel running surface was provided for Actuator 3. The bracing was the same on both sides of the actuator and is shown in Figure 3-4.

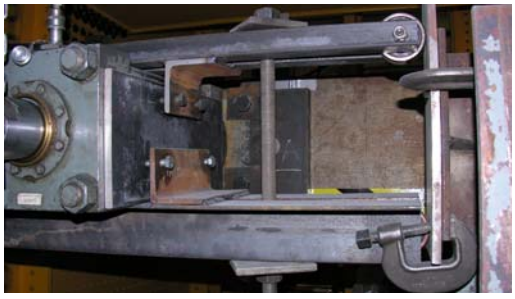

Figure 3-4: Actuator 3 lateral bracing system

3.5 Instrumentation

Loads cells, clinometers, cable transducers, pressure transducers and linear variable differential transformers (LVDTs) were used to monitor the behaviour of the extended shear tab connections throughout the tests and were located on the set-up as shown in Figure 3-5. The instruments were connected to an HBM MGCplus® data acquisition system, and a data point from each instrument was recorded every two seconds using HBM's catman®Easy data acquisition software. In addition to the instruments listed above, a digital image correlation camera system, by Correlated Solutions, was used to map the three-dimensional displacements and strains of the connection specimens.

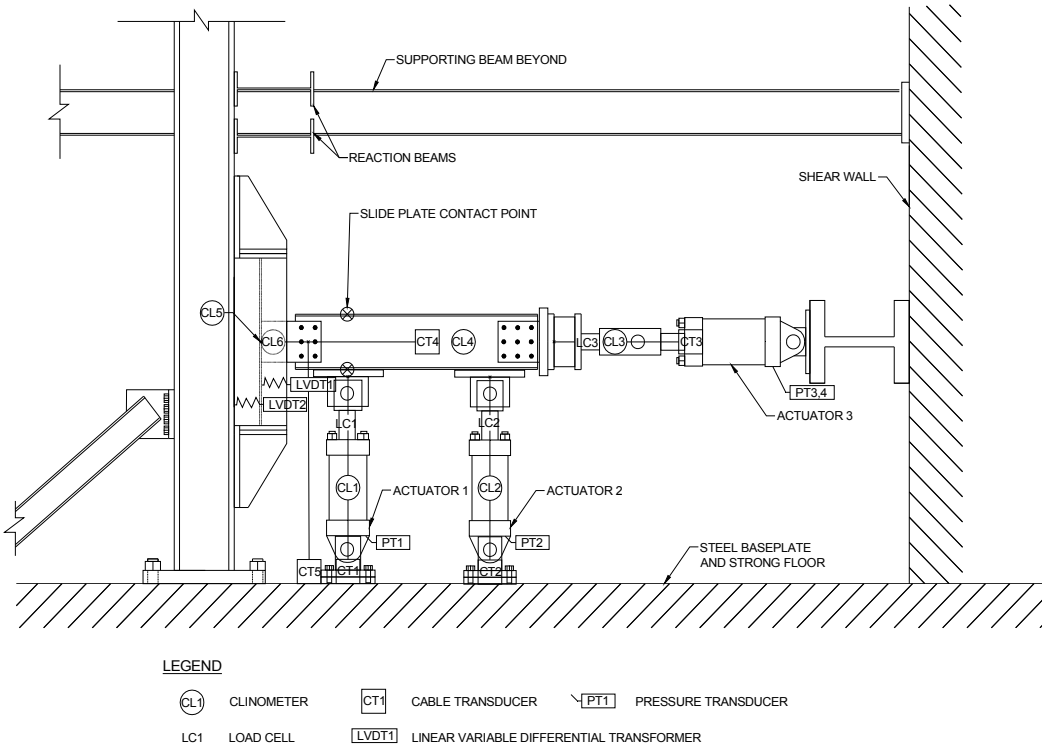

Figure 3-5: Instrumentation plan

A load cell and clinometer were mounted on each actuator. The clinometers were installed using a plumb line so that when vertical, they read zero radians. This allowed the forces from the load cells to be separated into vertical and horizontal

components. By adding the three vertical and three horizontal load components, the total load on the connection in each principal directions was calculated. Redundant load measurements were taken by pressure transducers connected to the hoses of the hydraulic actuators. The ratio of the force in each load cell to that measured by the corresponding pressure transducer was monitored during the tests to ensure the instruments were functioning properly. For several of the tests, the values read by Actuator 3's pressure transducer were used for the force calculations because the load cell was unable to read the load, likely due to bending causing slightly eccentric forces in the load cell.

In addition to the total load, the moment acting on the connection was calculated using the horizontal and vertical forces from each actuator and their respective moment arms. The moment arms were calculated using cable transducers, clinometers, and the dimensions of the set-up components measured prior to testing.

Beam rotation was measured both directly, using a clinometer, and indirectly using cable transducers and the clinometers on Actuators 1 and 2. The ratio of the direct and indirect measurements was monitored during the tests to confirm that the instruments were functioning properly.

Clinometers were also mounted on the flange of the column stub and on the extended shear tab plate. The former was used to monitor global column stub rotation; however, it did not record a rotation higher than 0.00325 radians (0.19 degrees) during the first 12 tests, so the use of this clinometer was discontinued. The clinometer on the connection plate was located as close to the weld line as possible to get an indication of the column web rotation.

Two additional cable transducers were used to measure the extended shear tab deformations. One measured the vertical deformation of the connection at the centroid of the bolt group, while the other measured axial deformation along the centreline of the beam, between the beam and the column web. Any elastic axial beam deformation captured was assumed negligible compared to the connection

deformation. The horizontal displacement of the column stub web and the overall horizontal movement of the column stub in relation to the strong-column support were measured by LVDTs.

In order to use the strain cameras, the areas of interest—the extended shear tab plate and beam web—were painted white with black speckles. The cameras were positioned to capture as much information on the plate as possible, without sacrificing the accuracy of the measurements. However, a large portion of the extended shear tab plate was not visible because it was obstructed by the column flanges.

3.6 Test Procedure

Once the specimen was bolted to the beam using the required number of 19 mm (3/4 in) diameter snug-tight bolts, the beam was rotated by 0.03 radians. This angle was chosen to reflect the expected end rotations of a typical-length simply supported beam when the middle of the beam reaches its plastic moment, as discussed in Section 2.2.1. While rotating the beam, the total horizontal and vertical loads were kept at or near zero. When 0.03 radians was reached, the horizontal load for that test was applied while the rotation was held constant and the vertical load was kept at or near zero. Once the desired horizontal load had been applied, both it and the beam rotation were held constant for the remainder of the test. Finally, upward vertical load was applied to the connection until failure occurred and the vertical load had decreased substantially from its peak value. After the load was removed, the specimen was examined and any visible failure modes were recorded.

3.7 Safety

In accordance with the university's health and safety act, precautions had to be implemented to prevent injury and loss of equipment during testing. The risks associated with the tests were evaluated and the necessary safeguards were put into place. One of the major safety concerns was bolt failure in a projectile-like

manner, and, therefore, a barrier was required between the specimen and researchers at all times while the tests were in progress. This safeguard, though necessary, caused the specimens to be inaccessible during testing. Although inaccessible directly, equipment was put into place to allow visual monitoring of the specimens. On one side of the set-up, a Plexiglas® shield was installed as a viewport and, although access to the other side was not permitted, the strain cameras were set-up on this side, allowing deformations to be monitored. A live video stream of the area in which failure was expected to begin was also used for viewing the specimens during the tests.

3.8 Test Results

Results from the 23 tests are shown in Table 3-4. The peak vertical load and observed failure modes are given according to each specimen's I.D. Of the possible failure modes discussed in Chapter 2, only those that were observed are listed. The manner in which these modes contributed to failure and the order in which they occurred are discussed in Chapters 4 and 5 for unstiffened and stiffened specimens, respectively.

Bolt fracture, in the threaded region, was commonly observed during these tests. A number was assigned to each bolt to describe bolt failure, as shown in Figure 3-6. The numbers corresponding to the failed bolts from each test are listed in Table 3-4, although the specific sequence of failure could not be determined reliably. Nearly all of the unstiffened specimens experienced some degree of weld fracture, but the severity varied considerably; however, they were grouped into two categories to facilitate discussion. The less severe, dubbed a "tip fracture", describes weld fracture at the tension tip of the weld only, as shown in Figure 3-7(a). This occurred due to the high stress concentration at this location, but the crack was then quickly arrested and the weld is considered to have performed acceptably. If fracture extended beyond the weld tip, it is categorized as "rupture", indicating that the weld capacity diminished significantly due to tearing and the weld is considered to have failed. As shown in Figure 3-7(b) and Figure 3-7(c),

the extent of weld rupture in this category varies. If out-of-plane deformation was visible after testing, Table 3-4 contains a "Y", indicating it was present. Otherwise, an "N" is used to indicate that out-of-plane deformation was not evident. In general, it was present for stiffened specimens and not for unstiffened ones. The presence of column web yielding is given by a yes (Y) or no (N) indicator based on whether or not the column web underwent plastic deformation. In general, it was present for unstiffened specimens and not for stiffened ones.

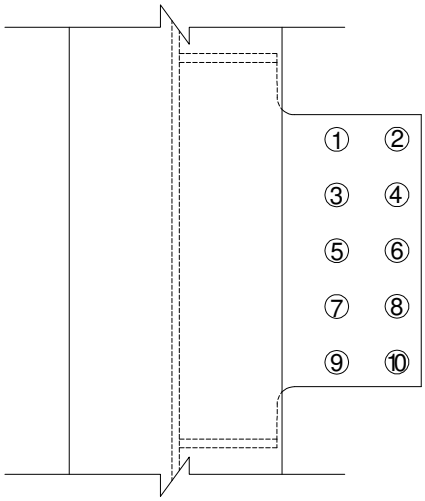

Figure 3-6: Bolt numbering system

(a) (b) (c)

Figure 3-7: Weld fracture (a) tip fracture, (b) and (c) rupture

Table 3-4: Test results

Specimen ID	Peak Load (kN)	Bolt Failure(s)	Weld Failure	Out-of-plane Deformation (Y/N)	Column Web Yielding (Y/N)
2B-10-U-0	188	3,4	Rupture	N	Y
2B-10-U-00	197	3	Rupture	N	Y
2B-10-U-200C	159	3,4	Tip Fracture	N	Y
2B-13-U-200C	138	3,4	Tip Fracture	N	Y
2B-10-S-0	317	1,3	-	Y	N
2B-10-S-200C	258	1,3	-	Y	N
2B-13-S-200C	323	1,3	-	Y	N
3B-10-U-0	330	5,6	Rupture	N	Y
3B-10-U-200C	339	5,6	Rupture	N	Y
3B-10-U-300C	278	5,6	Tip Fracture	N	Y
3B-10-U-200T	270	-	Rupture	N	N
3B-13-U-200C	263	5,6	Tip Fracture	N	Y
3B-10-S-0	511	1,2,3,5	-	Y	N
3B-10-S-200C	382	-	-	Y	N
3B-10-S-300C	279	-	-	Y	N
3B-13-S-200C	562	1,2,3,4,5,6	-	Y	N
5B-10-U-0*	762	1,2,7,9,10	-	N	Y**
5B-10-U-300C	732	5,7,8,9,10	Tip Fracture	Y	Y
5B-10-U-200T	612	9,10	Rupture	N	Y
5B-13-U-300C	613	5,7,8,9,10	Tip Fracture	N	Y
5B-10-S-300C*	798	-	-	Y	N
5B-10-S-400C	586	-	-	Y	N
5B-13-S-500C*	861	7,9,10	-	Y	N

*Actuator 1 capacity reached
**Column web tear

As discussed previously, the only difference between tests 2B-10-U-0 and 2B-10-U-00 is the angle of the beam during the test. Although 0.03 radians was chosen as a constant beam rotation for all tests, to determine the sensitivity of the connection capacity to the beam rotation at the beginning of the program, a second test with the same specimen geometry as 2B-10-U-0 was conducted, keeping the rotation at zero radians. Because these tests resulted in capacities

within 10 kN (5%) of one another, and the rotated beam capacity was the lower of the two, the 0.03 radian rotation was used for the remaining tests.

The vertical load reported in Table 3-4 is the maximum value recorded during testing. When comparing these values with the design capacities in Table 3-1, it is evident that the specimens were much stronger. In fact, the actual capacities of the larger, five-bolt-line extended shear tabs approached or exceeded the capacity of the set-up, which was governed by the maximum force that could be applied by Actuator 1. Although the capacity of Actuator 1 was reached during three of the tests (denoted in Table 3-4 by *), the maximum vertical load recorded is still considered representative of the connection capacity in each case. First, although no horizontal load was to be applied to specimen 5B-10-U-0, 146 kN of tension had to be applied to reach failure, and this is not considered to have influenced the vertical load capacity greatly. For the two stiffened specimen tests in which the actuator capacity was reached, 5B-10-S-300C and 5B-13-S-500C, the vertical load versus deformation curve had reached an extended plateau, suggesting that the capacity of the connection had been closely approached.

3.9 Summary

A total of 23 extended shear tab connections were tested. The connections varied in the number of horizontal bolt lines, plate thickness and presence of stiffeners. As such, the following extended shear tab test groups are identified:

- 7 two-bolt-line, 9 three-bolt-line, and 7 five-bolt-line
- 17 with a 10 mm plate and 6 with a 13 mm plate
- 13 unstiffened and 10 stiffened.

An existing set-up was modified to meet the requirements for these tests and a variety of instruments were used to monitor and record the behaviour of the specimens. The tests were conducted by rotating the beam to 0.03 radians, applying a predetermined horizontal load, and then failing the connection in shear. The peak vertical load and observed failure modes for each test were recorded.

The tests have revealed that the Fabricator's procedure used for specimen design appears to underestimate the capacities of extended shear tab connections considerably.

CHAPTER 4: UNSTIFFENED EXTENDED SHEAR TABS

4.1 Introduction

A discussion of the 13 unstiffened extended shear tabs that were tested is presented in this chapter. The key variables, peak shear load, and observed failure modes are discussed in detail and used to describe typical connection behaviour. Following this, existing design procedures are examined and compared to the test results. The ability of each design procedure to predict ultimate shear capacities, as well as critical failure modes, is discussed. Finally, design recommendations for unstiffened extended shear tab connections are proposed and compared to the test data.

4.2 Observed Behaviour

4.2.1 Failure Modes

The commonly observed failure modes for the unstiffened extended shear tabs tested were bolt fracture, weld rupture, and column web yielding. In some cases, the extended shear tab plates underwent permanent plastic deformations due to gross section yielding and/or deformations of the bolt holes due to bolt bearing. However, the critical failure mode—considered to be that which caused the initial post-peak decrease in vertical load—tended to be bolt fracture or weld rupture. In one case, specimen 5B-10-U-0, the weld did not rupture but column web tearing began on the tension side of the weld. Significant out-of-plane deformation of the shear tab plate was only observed on specimen 5B-10-U-300C.

A summary of the observed failure modes was given in Chapter 3; however, a more detailed list including all of the failure modes described in Chapter 2 is given in Table 4-1. These failure modes include weld rupture (WR), bolt fracture (BF), column web yielding (CWY), gross section yielding (GSY), net section fracture (NSF), bolt bearing (BB), and out-of-plane deformation (OPD). In this table, the critical failure mode is marked as CFM. Each of these modes is discussed in the following sections. Whether or not gross section yielding

occurred during test 3B-13-U-200C is unknown due to a problem with data collection from the camera system.

Table 4-1: Critical and other observed failure modes

	Failure Modes						
Specimen I.D.	WR	BF	CWY	GSY	NSF	BB	OPD
2B-10-U-0	✓	CFM	✓	✓	-	-	-
2B-10-U-00	✓	CFM	✓	✓	-	-	-
2B-10-U-200C	-	CFM	✓	✓	-	-	-
2B-13-U-200C	-	CFM	✓	✓	-	-	-
3B-10-U-0	CFM	✓	✓	✓	-	-	-
3B-10-U-200C	CFM	✓	✓	✓	-	-	-
3B-10-U-300C	-	CFM	✓	✓	-	-	-
3B-10-U-200T	CFM	-	-	-	-	-	-
3B-13-U-200C	-	CFM	✓	N/A	-	-	-
5B-10-U-0*	-	✓	CFM**	✓	-	-	-
5B-10-U-300C	-	CFM	✓	✓	-	-	✓
5B-10-U-200T	CFM	✓	✓	✓	-	-	-
5B-13-U-300C	-	CFM	✓	✓	-	-	-

* Actuator 1 Capacity Reached
** Column Web Tearing (CWT)

4.2.1.1 Weld Rupture

Even if it did not cause the drop in vertical load, some extent of weld rupture was observed in every test specimen, except for the specimen that experienced column web tearing instead: 5B-10-U-0. The rupture would begin at the tension tip of the weld and in some cases propagate towards the compression side, while in others it was arrested quickly (see Table 3-3). If the tip fracture did not propagate, it was considered a local effect and the weld performance was deemed acceptable. Weld rupture tended to occur when the specimens were tested without axial load or with axial tension. In both cases where tension was applied, weld rupture was the critical failure mode. It is unclear why the critical failure mode of specimen 3B-10-U-200C, with a large compressive force, was also weld rupture, but this mode may have been triggered by a weld flaw that went undetected.

4.2.1.2 Bolt Fracture

In many cases, the decrease in vertical load was attributed to the fracture of one or more bolts. With the exception of test 3B-10-U-200T, during which no bolts fractured, this failure mode occurred during every test. In some cases, bolt fracture was a secondary failure mode. In these tests, after the primary decrease in vertical load, the forces were redistributed in order for the connection to reach a new equilibrium state. This redistribution of forces eventually led to an increased bolt shear that caused failure, either very quickly after the initial load dropped or after a plateau at a lower vertical force.

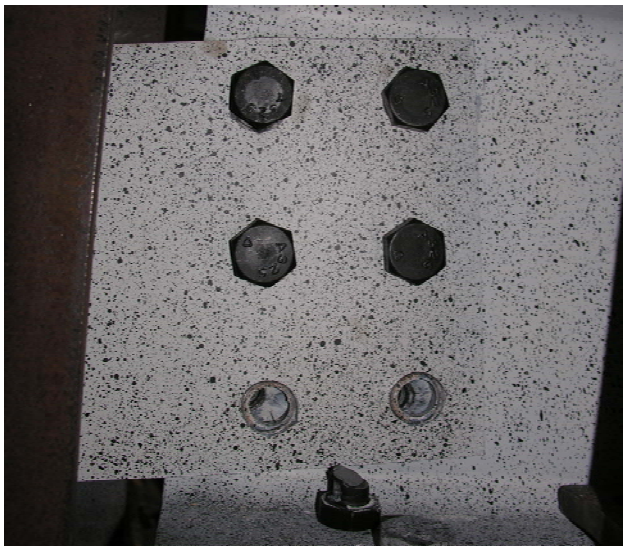

Figure 4-1: Bolt fracture of Specimen 3B-10-U-0

4.2.1.3 Column Web Yielding

Column web yielding was observed during all 13 unstiffened extended shear tab tests and in one case, specimen 5B-10-U-0, the column web tore, as shown in Figure 4-2. The column webs were whitewashed prior to testing to determine the column web yield pattern. The whitewash revealed Lüders' lines extending radially on the column web from top and bottom of the plate, as shown in Figure 4-3 for a typical case at the conclusion of the test. Specimen 3B-10-U-200T,

which did not exhibit signs of column web yielding prior to the weld rupturing, was the only exception.

Figure 4-2: Column web tearing in specimen 5B-10-U-0

Figure 4-3: Lüders' lines at the compression edge of plate

With the exception of specimen 3B-10-U-200T, the column webs underwent significant permanent deformation consistent with the failure geometry presented by Sherman and Ghorbanpoor (2002) based on a yield line analysis and discussed in Chapter 2.

4.2.1.4 Gross Section Yielding/Net Section Fracture of Plate

Although evidence of localized plate yielding was observed on all specimens, it was not responsible for a decrease in vertical load. Plate yielding occurred along the vertical bolt line closest to the weld, such that the plate was bending around bolt number 1 (see Chapter 3 for bolt numbering system) and causing a discrete kink in the plate at this location. This plate deformation was most visible on the connections tested without axial load and those with a 10 mm plate thickness. An example of the deformation due to plate yielding in specimen 2B-10-U-0 is shown in Figure 4-4. Transverse necking of the plate was evident where it bent around the bolt hole in this specimen and four others: 2B-10-U-00, 3B-10-U-0, 5B-10-U-0, and 5B-10-U-200T, indicating that net section fracture would have occurred along this line had it not been pre-empted by another mode. Because the necking deformation occurred in the region of the plate that was primarily subjected to tension, these deformations were not observed when the connection was subjected to horizontal compressive loads. Necking was not observed on specimen 3B-10-U-200T due to the high tensile force on the weld during this test; the only failure mode observed was weld rupture.

Figure 4-4: Plate deformation in specimen 2B-10-U-0

Gross section yielding is one mechanism that can be used in design to ensure that the connection has sufficient ductility. The vertical load at which the plate yielded through its full depth is given in Table 4-2 for each specimen, other than 3B-10-U-200T, which experienced only localized yielding. This point was determined by analyzing the strain field on the surface of the plate, found using the strain cameras. The yield line was always in the same location: along the vertical bolt line closest to the weld. Data could not be extracted for test 3B-13-U-200C as the image files were not recorded properly and could not be analyzed.

Table 4-2: Vertical load (kN) causing yielding through the plate depth

	Axial Load (kN)			
Specimen Group	200T	0	200C	300C
2B-10-U	-	160	127	-
2B-13-U	-	-	124	-
3B-10-U	N/A	311	302	273
3B-13-U	-	-	N/A	-
5B-10-U	569	670*	-	615
5B-13-U	-	-	-	595*

*Occurred after peak load

4.2.1.5 Bolt Bearing

Varying degrees of bolt bearing deformation were observed on all unstiffened specimens. This was not a critical failure mode for any specimen, but rather contributed to the overall ductility of the connections. In Figure 4-4, permanent bearing deformations around the bolt holes can be seen, especially around bolt number 1 which had the maximum deformation of all specimens, 8.6 mm. The other specimens tested without axial load also exhibited higher than average maximum bolt hole deformations. In contrast, the specimens with a 13 mm plate experienced less than one millimeter of deformation.

4.2.1.6 Out-of-Plane Deformation

Out-of-plane deformation was not a common failure mode for the unstiffened extended shear tabs tested. In previous testing programs, Moore and Owens (1992) and Sherman and Ghorbanpoor (2002) observed plate twisting. However, because the beams were braced next to the connection, plate twisting did not occur in this testing program. Specimen 5B-10-U-300C exhibited plastic out-of-plane deformation, indicative of the onset of plate buckling failure, not twisting.

4.2.2 Vertical Load–Deformation Curves

The behaviour of the 13 unstiffened extended shear tabs can be explained by breaking the vertical load–vertical deformation graphs into three zones, A, B, and C, delineated by the critical and secondary failure modes. A typical vertical load–deformation curve for specimen 3B-10-U-0 is given in Figure 4-5. The displacement is that of the bolt group centroid on the beam.

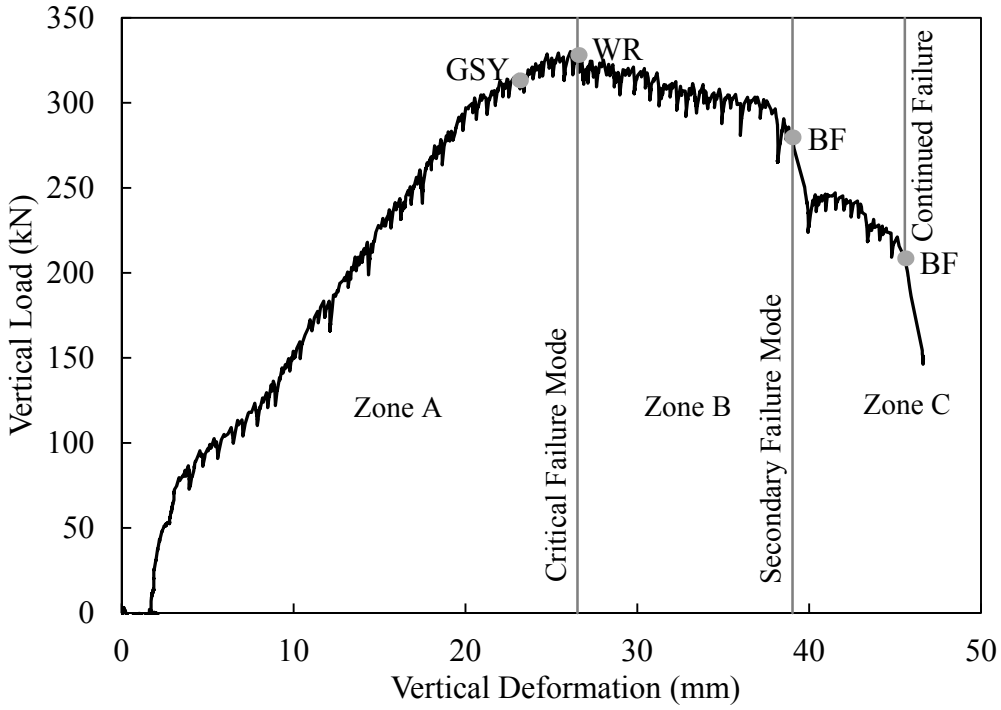

Figure 4-5: Load–deformation behaviour of specimen 3B-10-U-0

In zone A, the 0.03 radian beam rotation is imposed, horizontal load is then applied (if required), and the vertical load is applied subsequently. During the beam rotation and application of horizontal load, a small amount of deformation was recorded, approximately 2 mm in Figure 4-5. In this zone, stiffness changes occurred as the connection elements began to yield, primarily the column web. The deformation continued while the vertical load increased until, in most cases, the plate yielded through its depth causing the linear portion of the graph to end. Zone A finishes at the critical failure mode, where the vertical load begins to decrease after the peak value. When weld rupture was the critical failure mode, the load decreased gradually, as shown in Figure 4-5. The vertical load tended to drop more suddenly when bolts fractured.

After initial failure occurred, load redistribution began in Zone B. The vertical load either continued to decrease gradually as the weld rupture propagated, as shown in Figure 4-5, or remained relatively constant until secondary failure occurred. The deformation between the critical and secondary failure modes varied considerably.

In zone C, the vertical load continued to drop while the bolts progressively failed and/or weld rupture propagated. Again, the number and extent of the load drops in this zone varied. During the 3B-10-U-0 test, two bolts failed, shown as the secondary failure mode and continued failure points in Figure 4-5. The vertical load–deformation graph for each unstiffened extended shear tab is given in Appendix B.

4.2.3 Effects of Key Variables

Of the 13 unstiffened shear tab specimens, four had two horizontal bolt lines, five specimens had three, and four specimens had five. In each of these groups, one of the specimens had a 13 mm plate, while the rest were 10 mm thick. The specimens were also tested under a variety of horizontal loads, as discussed in Chapter 3. General observations about the effects of these three key variables are discussed below. It must be kept in mind that these results are influenced by the

hierarchy of failure modes experienced by the specimens, so any design changes that alter the failure sequence, such as a thicker column web or a larger weld or bolts, may affect these observations.

4.2.3.1 Number of horizontal bolt lines

As the number of horizontal bolt lines and, therefore, the plate depth increased, the strength of the connection also increased, as expected. However, as Figure 4-6 shows, the load plateau occurs at similar deformations. This is consistent for all specimens that varied only by connection depth. The critical failure mode also correlates with plate depth. All the two bolt line tests failed due to bolt fracture, whereas weld tearing was critical in some of the deeper connections.

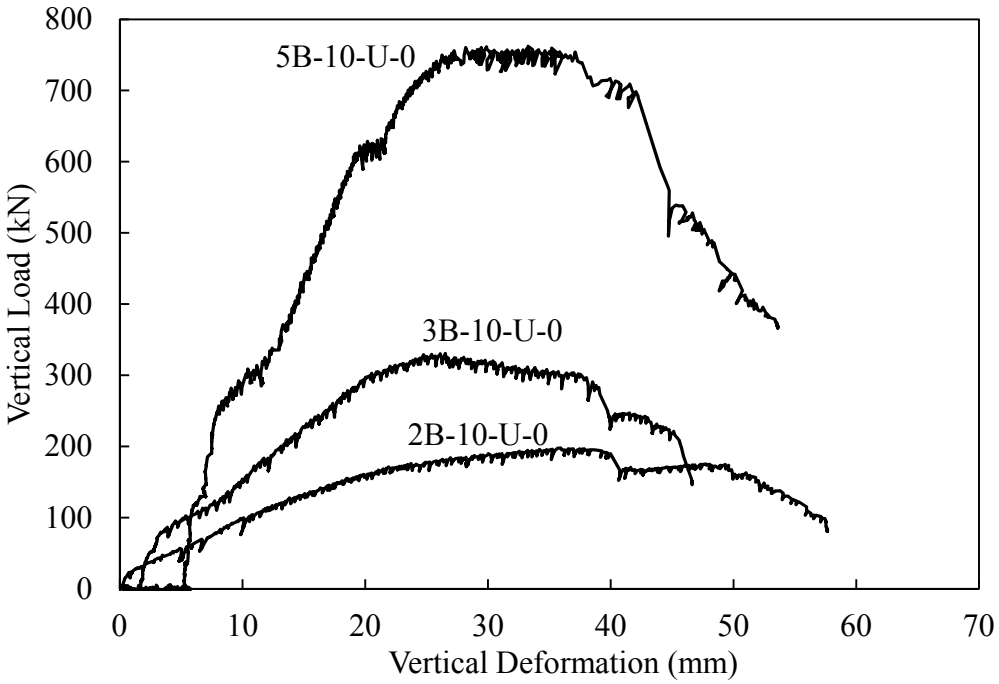

Figure 4-6: Effect of number of horizontal bolt lines on connection behaviour

4.2.3.2 Plate Thickness

The test matrix permits a comparison of three pairs of specimens wherein only the plate thickness is varied. Increasing the thickness of the plate caused a decrease in the peak vertical load observed during testing in all cases. The peak vertical loads

were lower for the thicker plate by 13%, 22%, and 16% for the two, three, and five horizontal bolt line connections, respectively. Although these results may seem counter-intuitive, the connection's stiffness was increased by increasing the plate thickness, in turn reducing plate deformation and increasing the demands on the weld and the bolt group. In addition to the increased demand on the bolt group, the shear plane through the bolts of specimens with the thicker plate was closer to the minimum diameter in the threads, resulting in a 10% lower bolt strength (see Chapter 3). Because bolt fracture was the critical failure mode for these three pairs of connections, failure occurred at lower loads when the 13 mm plate was used in lieu of the 10 mm plate. While the increased demand from the 13 mm plates did not result in weld failure in any of these cases, the specimens were all subjected to significant compressive load. Weld failure instead of bolt failure may be critical for cases with a smaller compressive or a tensile load.

4.2.3.3 Horizontal Load

Figure 4-7 shows the results of the 5B-10-U, 3B-10-U, and 2B-10-U tests. A negative horizontal load indicates the specimen was subjected to compression. As this figure shows, adding horizontal load tended to reduce the shear capacity of the connections; the reduction was more pronounced for deeper connections and for tensile loads.

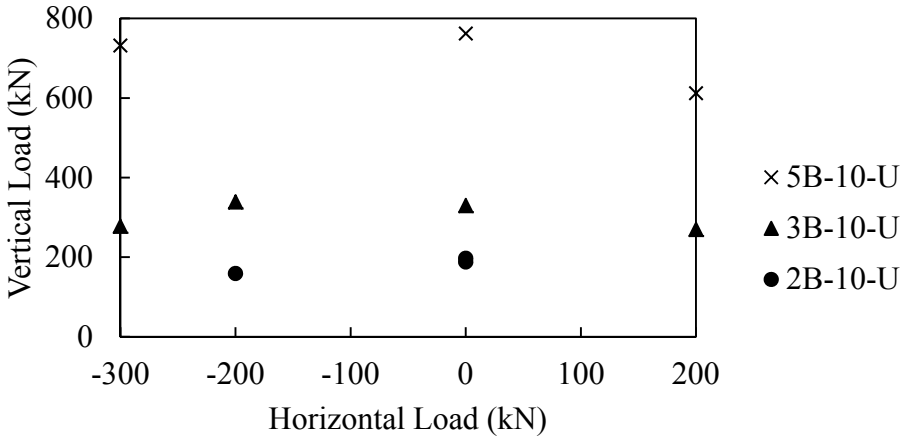

Figure 4-7: Effect of horizontal load on connection capacity

The capacities of the unstiffened connections, shown in Figure 4-7, were reduced due to the addition of horizontal load by a maximum of 29 kN (15%), 60 kN (18%), and 150 kN (20%) for the two, three and five horizontal bolt line connections, respectively. In the case of the 3B-10-U specimens, the addition of 200 kN of compression actually increased the shear capacity of the connection by 9 kN, but when 300 kN was applied the capacity was reduced. This result indicates that there may be a limiting value of compression below which the shear capacity of the connection is not affected. In contrast, the addition of tension caused the largest decreases in peak vertical load because more demand was placed on the tension side of the weld.

4.3 Current Design Procedures

Four design procedures have been used to calculate the shear strengths of the unstiffened extended shear tab specimens. In all cases, the resistance factor was omitted and measured material strengths were used. The design procedures given by SCI/BCSA (2002) and AISC (2011), as discussed in Chapter 2, were used to calculate strengths of the unstiffened specimens tested without horizontal load, since these two procedures do not include provisions for axial load. The strengths of the specimens, including those tested under horizontal tension or compression, were also calculated using the guidelines presented by Tamboli (2010). Finally, the measured material properties and bolt strengths were used to recalculate specimen capacities using the Fabricator's procedure. The resulting strengths from these four design procedures are compared to the peak vertical loads observed during testing in Table 4-3.

The specimens did not meet all of the requirements given by SCI/BCSA (2002). First, the 6 mm weld does not meet the basic requirement of 80% of the plate thickness. This would require the welds to be 8 mm and 10 mm for the 10 mm and 13 mm plates respectively. SCI/BCSA also limits the plate thickness to 42% of the bolt diameter, and both plate sizes exceed the 8 mm maximum thickness for

19 mm bolts. Finally, the end distance must be at least double the bolt diameter, or 38 mm, rather than the 35 mm specified for the test specimens.

Table 4-3: Comparison of design procedures and experimental capacities

Specimen ID	Test Capacity (kN)	SCI/BCSA Capacity* (kN)	AISC Capacity (kN)	Tamboli Capacity (kN)	Fabricator Capacity (kN)
2B-10-U-0	188	70	60	105	87
2B-10-U-00	197	70	60	105	87
2B-10-U-200C	159	-	-	66	72
2B-13-U-200C	138	-	-	94	95
3B-10-U-0	330	149	119	239	197
3B-10-U-200C	339	-	-	180	182
3B-10-U-300C	278	-	-	149	163
3B-10-U-200T	270	-	-	186	182
3B-13-U-200C	263	-	-	211	222
5B-10-U-0	762	394	202	493	513
5B-10-U-300C	732	-	-	431	496
5B-10-U-200T	612	-	-	475	505
5B-13-U-300C	613	-	-	505	534

*Minimum weld size not met and plate thickness limit exceeded

Although all of the peak shears are under-predicted substantially by all four design procedures, the trends observed during testing are mimicked. That is, the strength increases with the number of horizontal bolt lines and, for those that include horizontal load, the strength decreases as the horizontal load increases. However, the reduction in load capacity due to an increase in plate thickness observed in the tests is not reflected, even though the difference in the bolt shear capacities is accounted for, as the design procedures are predicated on preventing weld and bolt failure from occurring, and it is the increased demand on these elements from the thicker plates that caused this phenomenon.

In Table 4-4, the calculated strengths given in Table 4-3 are presented as a fraction of the peak vertical load obtained from the test to evaluate the ability of the design procedures to predict the connection capacity. As the table shows, the Fabricator's procedure and that proposed by Tamboli (2010) are the most accurate overall. However, even these methods significantly underestimated the capacities.

Though less accurate, the ability of the method proposed by the SCI/BSCA (2002) to predict the strength also increases slightly with connection depth. The extended configuration design procedure given by AISC (2011) predicts a capacity of less than 40% of the peak shear observed during testing in all cases.

Table 4-4: Predicted/test strength ratios

Specimen I.D.	SCI/BCSA Capacity	AISC Capacity	Tamboli Capacity	Fabricator Capacity
2B-10-U-0	0.37	0.32	0.56	0.46
2B-10-U-00	0.36	0.30	0.53	0.44
2B-10-U-200C	-	-	0.42	0.45
2B-13-U-200C	-	-	0.68	0.69
3B-10-U-0	0.45	0.36	0.72	0.60
3B-10-U-200C	-	-	0.53	0.54
3B-10-U-300C	-	-	0.54	0.59
3B-10-U-200T	-	-	0.69	0.67
3B-13-U-200C	-	-	0.80	0.84
5B-10-U-0	0.52	0.26	0.65	0.67
5B-10-U-300C	-	-	0.59	0.68
5B-10-U-200T	-	-	0.78	0.83
5B-13-U-300C	-	-	0.82	0.87
Average	0.43	0.31	0.64	0.64

The design procedures not only under-predict connection capacity, but also incorrectly identify the failure mode in most cases. Table 4-5 gives the governing failure modes predicted for each specimen by each design method, as well as the critical failure mode observed from testing. If the failure mode is properly identified, it is shown in bold text. While gross section yielding is not considered to be the critical failure mode in the tests because it did not cause the vertical load to decrease, it did occur prior to the critical mode in most cases. Therefore, if this is correctly reflected by the design procedure, the failure mode is indicated in the table as being properly identified. However, when gross section yielding is the predicted failure mode, the capacities are always significantly underestimated suggesting that, though widely accepted, this failure mode may not be an appropriate ultimate limit state for extended shear tab design. From Tables 4-4

and 4-5, it is apparent that the calculated capacities have often been restricted by failure modes that did not ultimately cause the specimens to fail.

Table 4-5: Comparison of observed and predicted critical failure modes

Specimen I.D.	Critical Failure Mode	SCI/BCSA Failure Mode	AISC Failure Mode	Tamboli Failure Mode	Fabricator's Failure Mode
2B-10-U-0	BF	**GSY**	OPD	**GSY**	**GSY**
2B-10-U-00	BF	**GSY**	OPD	**GSY**	**GSY**
2B-10-U-200C	BF	-	-	NSF	NSF
2B-13-U-200C	BF	-	-	NSF	NSF
3B-10-U-0	WR	**GSY**	OPD	NSF	**GSY**
3B-10-U-200C	WR	-	-	NSF	NSF
3B-10-U-300C	BF	-	-	NSF	NSF
3B-10-U-200T	WR	-	-	NSF	NSF
3B-13-U-200C	BF	-	-	**BF**	**BF**
5B-10-U-0	CWT	OPD	OPD	NSF	GSY
5B-10-U-300C	BF	-	-	NSF	NSF
5B-10-U-200T	WR	-	-	NSF	**GSY**
5B-13-U-300C	BF	-	-	**BF**	**BF**

The SCI/BCSA method and the AISC extended configuration method can only be applied to connections without horizontal load. For these four cases, gross section yielding was identified by the SCI/BCSA method as the failure mode for three, and out-of-plane deformation due to lateral-torsional buckling was predicted for the five horizontal bolt line specimen. The AISC method predicts out-of-plane deformation as the critical failure mode for all four specimens. For the two horizontal bolt line specimen, plate buckling limited the predicted capacity, whereas lateral-torsional buckling was critical (based on the check of the need for stiffeners) for the specimens with three and five horizontal bolt lines. Neither mode was observed in these tests.

The Tamboli (2010) method identified the failure mode correctly in four cases, two of which were bolt fracture and matched the critical mode observed at the peak load. To design the bolts, this procedure uses the eccentrically loaded bolt

group tables given in Part 7 of the AISC Manual (2011). The horizontal and vertical loads are combined into an inclined resultant force with an eccentricity equal to the geometric eccentricity. This method does not take advantage of the full bolt group capacity and is highly dependent on the angle of the inclined load. The strengths of other specimens determined by this design procedure were limited by the plate net section fracture check, which was not observed in the tests.

The Fabricator's procedure correctly identified the failure mode for six specimens, including two that failed due to bolt fracture. To determine the capacity of the bolt group, the full geometric eccentricity is used with the instantaneous centre of rotation method described in Chapter 2. However, the calculated strength is considerably lower than the tested capacity, implying that only a portion of the eccentricity need be considered. In several other cases the calculated strengths were limited by net section fracture.

4.4 Design Recommendations

New design recommendations for unstiffened extended shear tabs under loading conditions that can include axial force are proposed in this section. These recommendations are based on both the current AISC guidelines for single plate connections with an extended configuration (AISC 2011) and the design procedure used by the Fabricator. The procedure addresses both strength and ductility considerations. The strengths of the bolt group, column web, and plate are considered, whereas ductility is ensured by specifying a minimum weld size and both minimum and maximum plate thicknesses. Axial compression or tension, if present, is addressed explicitly in each section. Methods for determining block shear and bolt bearing capacities are not included in the discussions that follow as failures of these types were not observed during testing. However, these limit states must be checked during design.

4.4.1 Bolt Group Capacity

4.4.1.1 Instantaneous Centre of Rotation Method

The first step in the design of unstiffened extended shear tabs is to size the bolt group to resist the applied shear and axial loads. Because the load is eccentrically applied, the instantaneous centre of rotation method is used to calculate the bolt group shear capacity, V_{BG}. A detailed description of this method is given in Chapter 2.

In the AISC Manual's design procedure for extended single plate connections, the use of Tables 7-6 to 7-13 (AISC 2011), which give coefficients, C, for specific joint configurations, is recommended; these tables also have the instantaneous centre of rotation method as their basis. For configurations not covered by these tables, an iterative procedure is needed that can be facilitated by the use of a spreadsheet. Therefore, the proposed method is consistent with the AISC design procedures and is also used by the Fabricator.

4.4.1.2 Effective Eccentricity

The effective eccentricity, e_{eff}, used to determine the bolt group capacity has a substantial impact on the resulting strength. Both the AISC and Fabricator's procedures use the geometric eccentricity, but when this value is used the predicted shear capacity of the bolt group is lower than the capacities of the specimens tested. However, ignoring the eccentricity over-predicts the capacity significantly. Therefore, only a fraction of the total eccentricity need be considered for this calculation, implying the existence of an inflection point in the plate somewhere between the weld line and the centroid of the bolt group.

Using the tested capacities, the effective eccentricity was determined by calculating the eccentricity that would cause bolt group failure at the peak shear recorded during testing for each specimen that failed due to bolt fracture. To provide accurate input for the instantaneous centre of rotation calculations, the experimentally-determined shear strengths of bolts from the same lot as those

used in the connection tests, described in Chapter 3, are used rather than nominal values. However, the maximum bolt deformation, 8.64 mm, given by Crawford and Kulak (1971) was used to define the individual bolt response. Table 4-6 gives the effective eccentricities as a proportion of the geometric eccentricity. The average effective eccentricity is 75.9% of the geometric eccentricity, with a standard deviation of 6.2%.

Unless a more accurate value can be determined, an effective eccentricity equal to 75% of the geometric eccentricity is recommended for design, and this value is used in Section 4.4.6 to determine the capacities of the bolt groups in all specimens. Because the column web was thin, this effective eccentricity is considered conservative for bolt group design since the observed column web rotations where higher than what should typically be permitted in practice.

Table 4-6: Effective eccentricities of test specimens failing in bolt fracture

	Axial Load (kN)			
Specimen Group	0	00	200C	300C
2B-10-U	0.695	0.658	0.734	-
2B-13-U	-	-	0.745	-
3B-10-U	-	-	-	0.823
3B-13-U	-	-	0.812	-
5B-10-U	-	-	-	0.772
5B-13-U	-	-	-	0.832

4.4.2 Plate Thickness

For an extended shear tab connection, the desired failure mode is plate yielding. In other words, the plate must be strong enough to resist the applied loads, but also have proportions that ensure a ductile failure mode. This involves creating a fuse that precludes any potential for failure of the bolt group or the weld, or lateral buckling of the plate itself. Assuming an efficient connection design, it is recommended that the ductility checks be satisfied even if all components of the connection have sufficient strength to resist the applied loads. This allows for variations of the load-carrying mechanism from that assumed in the design

procedure, while still ensuring ductile behaviour and the ability of the joint to rotate in a way consistent with the assumption of a simple beam support. For that reason, design provisions for both a maximum and a minimum plate thickness are proposed. The maximum plate thickness defined in the next section is to prevent premature failure of the bolt group; design of the weld for both strength and connection ductility is discussed in Section 4.4.4. The minimum plate thickness is to ensure that lateral–torsional buckling of the plate is not the governing failure mode.

4.4.2.1 Maximum Plate Thickness

To ensure the connection has sufficient ductility, plate yielding must occur prior to bolt failure. Using this requirement, the maximum plate thickness, t_{max}, is determined by equating the yield moment of the plate, reduced to account for the effects of any coexisting axial force, with the moment capacity of the bolt group and solving for plate thickness:

4-1
$$t_{max} = \frac{6\phi_b M_{BG}}{R_y F_y d_p^{\,2}} + \frac{N}{R_y F_y d_p}$$

where ϕ_b is the bolt resistance factor, F_y is the nominal yield stress, d_p is the depth of the plate, N is the nominal axial load, taken as positive for both tension and compression, and R_y is discussed below. The moment capacity of the bolt group, M_{BG}, is found by multiplying the shear capacity of the bolt group by the effective eccentricity of the load, taken equal to 75% of the geometric eccentricity, as follows:

4-2
$$M_{BG} = V_{BG} e_{eff}$$

The first term in Equation 4-1 is similar to the maximum plate thickness equation given by AISC (2011) and used by the Fabricator. However, in those design procedures, the moment-only capacity of the bolt group is used. In other words, eccentricity of the shear load is not taken into account and the bolt group moment capacity is therefore over-estimated, resulting in a non-conservative maximum

plate thickness. These methods also use the nominal bolt group moment capacity in calculating t_{max}. However, because bolt fracture is an undesirable failure mode leading to non-ductile connection behaviour, it should be calculated based on the reliable bolt capacity and, therefore, the factored moment capacity of the bolt group is utilized in Equation 4-1.

The second term in Equation 4-1 has been added to allow for an increase in maximum plate thickness if axial load is present because the plate will yield when subjected to a lower shear force. However, this increase should only be taken into account if the axial load is a constant load, such as that due to permanent equipment, or is a load fundamentally linked to the applied shear load, as would be the case for an inclined design load that imposes both axial and shear forces on the connection concurrently. In other words, a transient or cyclical axial load should be neglected when applying Equation 4-1 to ensure a ductile failure mode. In general, the inclusion or exclusion of axial load should be consistent in the determination of M_{BG} and the use or omission of the second term in Equation 4-1.

The yield stress used in Equation 4-1 significantly impacts the maximum plate thickness obtained. If the nominal value is used, the actual maximum plate thickness required to ensure ductile failure may be less than that calculated, since actual yield strengths are nearly always greater than the nominal. This is especially important for connection plates designed with a nominal yield strength of 300 MPa or lower because in many cases plate material will be used that is dual-certified and has an actual yield strength exceeding 350 MPa. To account for this in seismic design, the nominal yield stress is increased by the factor R_y to obtain a probable yield stress whenever design loads are defined in accordance with capacity design principles (CSA 2009). For structural plate, R_y is typically taken as 1.1, but with a minimum value of 385 MPa for R_yF_y. This design philosophy has been adopted for calculating the maximum thickness to ensure ductile connection behaviour, as shown in Equation 4-1.

It is worth noting that while shear is present in the plate in addition to moment and, potentially, axial force, its influence on the onset of yielding is neglected in Equation 4-1. This is a reasonable and conservative approximation to the true behaviour, although yielding is expected to be somewhat more extensive on the critical section of the plate than at the extreme fibre only, as is implied by Equation 4-1.

As discussed in Chapter 2, the AISC Manual (AISC 2011) allows the connection plate to exceed the maximum thickness requirement if certain geometric conditions are met by the plate and/or beam web, depending on the number of vertical bolt lines. Because the test specimens did not meet these conditions, they are not included as an exception for Equation 4-1.

4.4.2.2 Minimum Plate Thickness

Because extended shear tab plates are slender, out-of-plane deformation, or buckling, could occur. To preclude this type of failure and ensure a ductile failure mode, a minimum plate thickness is established. A minimum plate thickness required to ensure a ductile failure mode is not given by AISC (2011); rather, a check for plate lateral–torsional buckling under the design loads is carried out to determine the need for stabilizer plates. However, by meeting the proposed ductility limit, stability of the plate need not be considered under the design loads and stabilizer plates are not required. Implementing a minimum plate thickness requirement could increase the required plate thickness compared to that required by AISC in some cases. However, the improved connection behaviour in the event of an overload—or a variation in the load-carrying mechanism—achieved by forcing a ductile failure mode outweighs the nominal increase in cost of using a thicker plate. The Fabricator uses a method similar to that proposed below.

As discussed in Chapter 2, the critical moment causing lateral–torsional buckling of an extended shear tab, M_{cr}, can be approximated as:

4-3 $$M_{cr} = \frac{\omega_2 \pi}{L} \sqrt{EI_y GJ}$$

in which ω_2 is a coefficient to account for the moment gradient along the length of the plate, L is the clear span of the plate, from the weld to the first vertical bolt line, and E is the modulus of elasticity. The moment of inertia of the plate for out-of-plane bending, I_y, is:

4-4 $$I_y = \frac{d_p t_p^3}{12}$$

where t_p is the plate thickness. The elastic shear modulus, G, is:

4-5 $$G = \frac{E}{2.6}$$

and J is the St. Venant torsional constant of the plate:

4-6 $$J = \frac{d_p t_p^3}{3} = 4I_y$$

By substituting Equations 4-4 through 4-6 into Equation 4-3, the equation for the critical moment becomes:

4-7 $$M_{cr} = \frac{0.325\omega_2 E d_p t_p^3}{L}$$

Equating Equation 4-7 with the plastic moment capacity of the plate, M_p, given in Equation 4-8, a relationship for the minimum plate thickness, t_{min}, is found:

4-8 $$M_p = \frac{F_y t_p d_p^2}{4}$$

4-9 $$t_{min} = 0.877 \sqrt{\frac{F_y d_p L}{\omega_2 E}}$$

Although the yield moment was used to derive the maximum plate thickness ductility requirement, the plastic moment capacity has been used to derive Equation 4-9 for two reasons: consistency and simplicity. First, an actual yield

stress higher than the nominal value would cause the plate to yield at a higher load, and variability in the buckling capacity of the plate could cause the critical moment to be lower than calculated. The use of the plastic moment instead of the yield moment conservatively takes the net effect of these probabilistic issues into account without the need to introduce the probable yield stress or a resistance factor. Second, although the presence of shear was ignored in the derivation of Equation 4-9 for simplicity, the shear force would accelerate not only plate yielding, but also lateral–torsional buckling. However, accounting for the shear–moment interaction on both sides of the equation would result in a much more complex equation for minimum thickness. Therefore, any potential increase in minimum thickness due to the presence of shear is accounted for indirectly by using the plastic moment capacity. A similar argument can be made for the presence of axial load, if any. However, if a large axial load is applied compared to the shear force, engineering judgement should be exercised in determining the minimum plate thickness and a column-type strength check may be appropriate.

To apply Equation 4-9, the moment distribution along the plate must be estimated. For linear moment distributions, the coefficient, ω_2, is:

4-10 $$\omega_2 = 1.75 + 1.05\kappa + 0.3\kappa^2 \leq 2.5$$

according to S16 (CSA 2009), in which κ is the ratio of the smaller end moment to the larger, taken positive for double curvature and negative for single curvature. Thornton and Fortney (2011) conservatively assumed a constant moment along the length of the plate to derive the stabilizer plate requirement in the AISC Manual (2011), resulting in a value of ω_2 equal to 1.0. However, due to the deformed shape of the test specimens, it is apparent that the plates are in double curvature. Although a moment gradient consistent with the actual location of the inflection point, given approximately in Table 4-6, might seem appropriate for consistency, because the actual gradient is uncertain, the moment at the column web is conservatively assumed to be zero for this check, resulting in an ω_2 value of 1.75. Equation 4-9 then becomes:

4-11

$$t_{min} = 0.663\sqrt{\frac{F_y d_p L}{E}}$$

4.4.3 Column Web Capacity

The column web capacity is checked against the applied axial and shear loads separately using classical yield line theory. For the axial capacity, the web capacity equation is based on the failure geometry proposed by Kapp (1974), as discussed in Chapter 2. However, the thickness of the plate is conservatively neglected to simplify the equation:

4-12

$$N_{CW} = 2F_{yc}w^2\left(\frac{d_p}{T}+2\right)$$

where the yield stress, F_{yc}, is that of the column web, w is the thickness of the column web, and T is the clear distance between column web-to-flange fillets, as tabulated for W-shapes in the CISC Handbook (CISC 2010). The assumed failure geometry defined by this equation is shown in Figure 4-8. Note that the direction of the web deformation depends on whether axial tension or compression is applied.

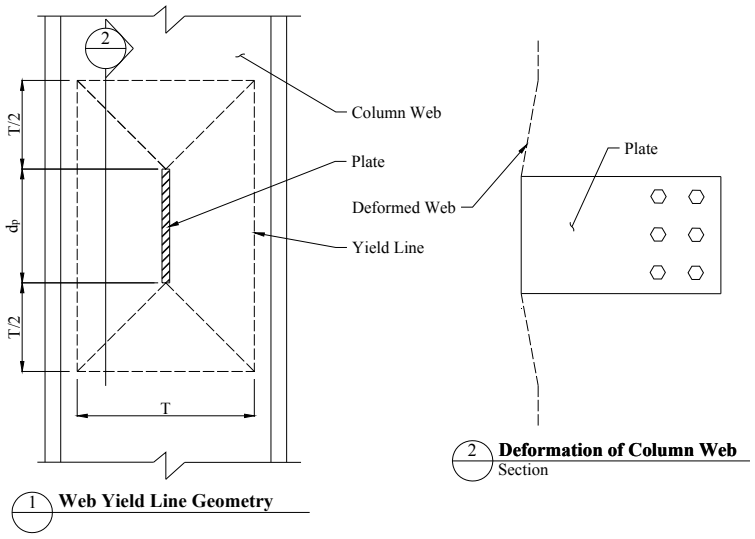

Figure 4-8: Column web yield line geometry under axial load

The proposed capacity equation for yielding of the column web under an eccentric shear load originates from a yield line analysis by Abolitz and Warner (1965), as suggested by Sherman and Ghorbanpoor (2002) and discussed in Chapter 2. Assuming the column web capacity is limited by the formation of a flexural yield mechanism, the shear capacity of the column web, V_{CW}, is:

4-13
$$V_{CW}=\frac{F_{yc}w^2d_p}{0.5e_g}\left[\frac{T}{2d_p}+\frac{d_p}{T}+\sqrt{3}\right]$$

where the eccentricity is half of the geometric eccentricity. This eccentricity has been chosen rather than that corresponding to the effective eccentricity discussed in Section 4.4.1.2 to represent the likely location of inflection prior to any deformation of the column web. Once the column web begins to deform and, therefore, its stiffness decreases, the inflection point begins to migrate toward the column web, which resulted in an eccentricity from the column web of 25% of the geometric eccentricity at the ultimate load during the tests. Because this deformation should be minimized, the approximate initial condition is used. The assumed failure geometry is shown in Figure 4-9, where u is:

4-14
$$u=\frac{T}{6}\sqrt{3}$$

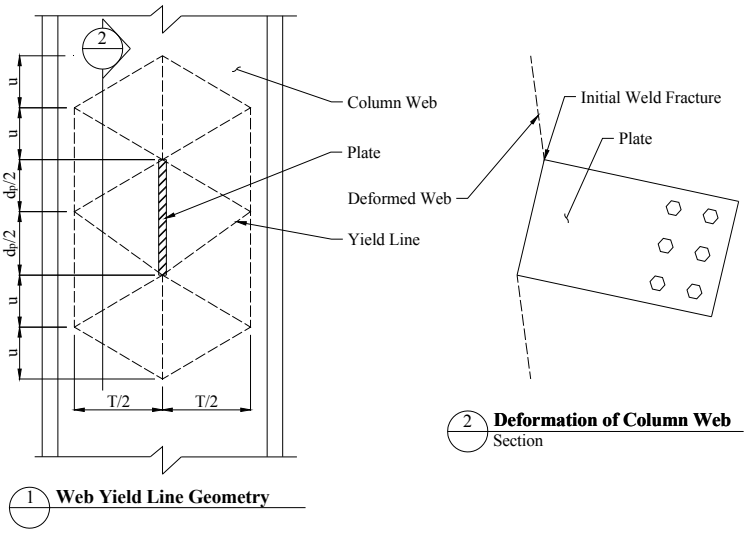

Figure 4-9: Column web yield line geometry under eccentric shear

Although Equation 4-13 results in a strength that is lower than the ultimate strength of the column web, as the potential for the development of membrane action is neglected, it is included as a limit state to avoid excessive rotation of the flexible support. During the tests, deformation of the column web likely contributed to some degree of weld rupture, even if only at the weld tip, in 12 of the 13 specimens. However, the tested unstiffened extended shear tabs were supported by a 10.9 mm web and as the column web thickness increases this limit state becomes less of a concern. Figure 4-10 shows the effect of increasing the column web thickness on the column web shear capacity for the shear tab depths tested. Especially for the deeper shear tabs, increasing the column web thickness results in a rapid increase in capacity. While the same result could be accomplished by adding stiffeners, selecting an appropriate column section to avoid excessive web distortion would in most cases be a more economical solution unless stiffeners are already required for another purpose.

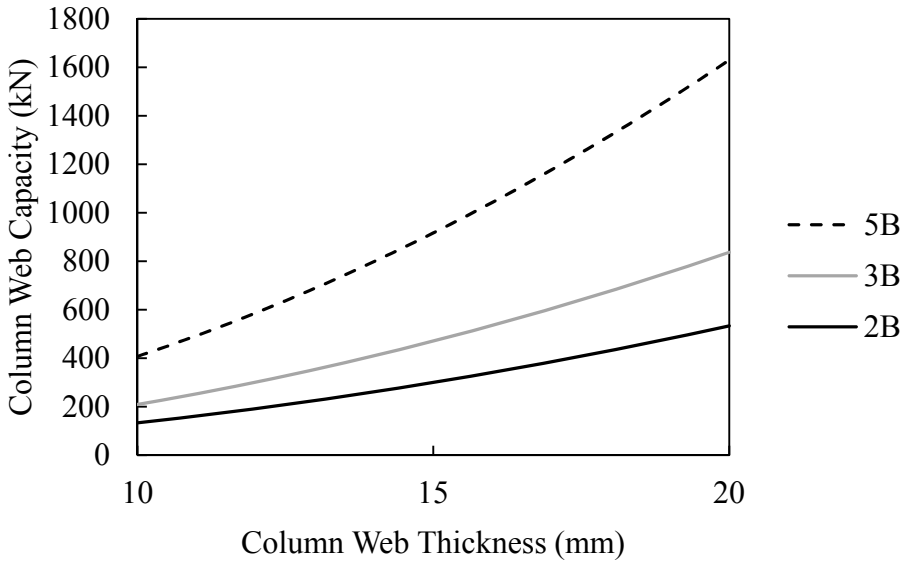

Figure 4-10: Effect of column web thickness on flexural yield mechanism capacity

Although column web rotation has been identified as a failure mode in previous research programs (Sherman and Ghorbanpoor 2002; Moore and Owens 1992)

and excessive yielding and deformation of the column web was noted when the column web was flexible (Moore and Owens 1992), column web yielding has not been incorporated as a limit state in any current design guidelines. However, basing the axial and eccentric shear capacities of the column web on Equations 4-12 and 4-13, respectively, is recommended not only to limit the deformation, but also to avoid initiating rupture at the tip of the weld. Nevertheless, the nominal material strength is used in these equations for design to reflect the fact that small column web deformations do not represent an ultimate limit state for the connection.

4.4.4 Weld Design

To ensure ductile failure, the column-to-plate weld should be sized such that the plate will yield prior to rupture of the weld. To determine the weld size, D, that is required to develop the capacity of the plate, the weld capacity equation, given in Chapter 2, is equated to the plate capacity. Because extended shear tabs can be subjected to shear, moment, and/or axial load, three load cases were investigated. For shear, the plate capacity was taken as:

4-15 $$V_{GS} = 0.66 R_y F_y t_p d_p$$

resulting in a minimum weld size of:

4-16 $$D \geq \frac{0.697 R_y F_y t_p}{\phi_w X_u}$$

where X_u is the ultimate strength of the weld, ϕ_w is the weld's resistance factor and R_y is included for the same reasons as those described in Section 4.4.2.1 for the maximum plate thickness. Solving for the weld size based on the gross tensile and plastic moment capacity of the plate both result in the limit:

4-17 $$D \geq \frac{0.704 R_y F_y t_p}{\phi_w X_u}$$

Because Equations 4-16 and 4-17 differ by only 1%, that derived for axial/moment is conservatively adopted for all cases. Substituting 0.67 into

Equation 4-17 for the weld's resistance factor (CSA 2009) and 1.1 for R_y, the minimum weld size becomes:

4-18 $$D \geq 1.155 \frac{F_y}{X_u} t_p$$

The AISC Manual (2011) follows a similar approach as that outlined above, resulting in a minimum weld size of five-eighths of the plate thickness. However, rather than consider the forces individually, the interaction of moment and shear is taken into consideration. Muir and Hewitt (2009) derived this limit assuming the weld's rupture strength to be $\sqrt{2/3}\,X_u$ and its shear strength to be $\sqrt{2}X_u/3$. The resulting equation for weld size is simplified by assuming a yield stress of 50 ksi and an ultimate weld strength of 70 ksi. Because the resistance factor has been included to account for the large variability in weld strength and the probable yield stress has been included in lieu of the nominal, Equation 4-18 results in a larger weld size than the AISC method. Nevertheless, these factors are needed to ensure that the intended connection ductility is achieved. It should be noted that the resistance factor used to obtain Equation 4-18 has been shown in previous research to provide reliability indices for fillet welds in lap joints that are well in excess of 4.0 (Ng et al. 2002; Deng et al. 2006). If reliability studies justify the use of a larger resistance factor for this application, it should be incorporated into the equation.

The approach of sizing the weld so that it will not rupture before the plate yields is different from that used by the Fabricator and, therefore, the method used to design the test specimens. The welds were designed to resist the shear force only, neglecting the eccentricity, since the full geometric eccentricity was used to design the bolt group. However, some degree of weld rupture was evident on all unstiffened extended shear tab specimens. For this reason, the design philosophy that forms the basis of Equation 4-18 is adopted.

4.4.5 Plate Design

The extended shear tab plate must meet not only the maximum and minimum thickness requirements, but also the strength requirements for the applied factored axial force, shear force and moment. As long as the plate thickness is greater than the minimum value, the lateral stability of the plate need not be considered.

The shear resistance is taken as the lesser of the gross section shear capacity:

4-19 $$\phi V_{GS} = 0.66\phi F_y t_p d_p$$

and the net section shear capacity:

4-20 $$\phi V_{NS} = 0.6\phi_u F_u t_p \left(d_p - n_h d_{bh}\right)$$

in which n is the number of bolts per vertical line and d_{bh} is the bolt hole diameter.

If the shear stress, τ, exceeds 50% of the factored yield strength, ϕF_y, the interaction of shear and normal stress needs to be taken into consideration, and the maximum permissible factored normal stress, $\phi\sigma_n$, can conservatively be approximated as (CSA 2014):

4-21 $$\phi\sigma_n = \min\left[\phi F_y, 6.25\left(0.66\phi F_y - \tau\right)\right]$$

where the shear stress, τ, is the factored applied shear force divided by the gross cross-sectional area of the plate.

The flexural capacity of the plate is expressed as the shear force that would cause the plate to reach its plastic moment capacity in the presence of the axial force, if any. Using the factored normal stress capacity from Equation 4-21, the factored shear capacity, ϕV_{MN}, is calculated based on the clear span effective eccentricity, $e_{eff\text{-}cs}$. This eccentricity is found by subtracting the distance from the bolt group centroid to the first vertical line of bolts from the effective eccentricity given in Section 4.4.1.2:

4-22 $$\phi V_{MN} = \frac{\phi \sigma_n t_p d_p^2}{4 e_{eff\text{-}cs}} - \frac{N_F^2}{4 \sigma_n t_p e_{eff\text{-}cs}}$$

Although the AISC Manual (2011) requires that the plate be checked for torsion—due to the small out-of-plane eccentricity arising from the lapped connection with the beam web—and block shear, these failure modes were not observed in the tests and, therefore, are not included in these design recommendations. However, there may be situations in which these failure modes govern.

4.4.6 Comparison of Test Results to Design Recommendations

The design recommendations made in the previous sections have been applied to the unstiffened test specimens. A summary of the ductility requirements is given in Table 4-7 and the shear strength calculations are located in Table 4-8. The axial capacities of the column web for the two, three, and five horizontal bolt line specimens were 242 kN, 273 kN, and 336 kN, respectively. Although the 273 kN value was exceeded in the 3B-10-U-300C test and the column web did not fail, this limit is still required to preclude excessive column web deformation.

The maximum plate thickness recommendation was met for all 13 specimens, and the minimum thickness requirement was met with the exception of the 5B-10-U specimen group, where the limit was violated by only 0.3 mm. As out-of-plane deformation was not the critical failure mode for any of the unstiffened specimens, the actual plate thicknesses of the six unstiffened specimen geometries should meet or exceed the minimum thickness. Because a small amount of out-of-plane deformation was observed after testing the 5B-10-U-300C specimen and the limit is only exceeded by 0.3 mm, the test results appear consistent with the proposed limit.

Because the procedure used to design the test specimens ignores the shear force eccentricity and tensile forces when calculating the weld capacity, the weld size required by the proposed equation exceeds the actual weld size in all cases.

According to the proposed criteria, the welds are undersized by 3.3 mm and 5.4 mm for the 9.5 mm and 12.7 mm plates, respectively, although the ten specimens with a 9.5 mm thick plate had welds equal to the AISC (2011) minimum permissible size. Because the welds were undersized, it is not surprising that some degree of weld rupture was evident on all but one specimen.

The connection shear capacities, calculated using measured strengths for the bolts and shear tab plates given in Chapter 3, for the various limit states are given in Table 4-8. As this table shows, the capacities of the three and five horizontal bolt line specimens would have been limited by the column web capacity. However, this requirement is included to prevent excessive support deformation and does not reflect the actual connection strength. Also, if a larger column had been used, the column web capacity would not limit the overall connection capacity. Therefore, this limit state has been ignored when evaluating the test-to-predicted capacity ratios in Table 4-8. Based on the recommended design equations, the predicted critical failure mode was bolt fracture for all of the specimens excluding the 2B-10-U specimen group. This correlates well with the test results, since bolt fracture occurred during all but one test in which the weld ruptured entirely and, if the welds hadn't been undersized, would have likely been the critical failure mode for each specimen. The 2B-10-U group of specimens underwent the most plate deformation; therefore, predicting plate failure due to the combination of flexure and axial force for this specimen group mimics the observed behaviour.

The average test-to-predicted capacity ratio is 1.02, with a coefficient of variation equal to 0.154. The ratio for the 2B-10-U specimen group is high because the calculated capacities are limited by the plate strength, not the bolt group as was observed during testing. Because the average effective eccentricity was used to determine the bolt group capacities, some of the calculated specimen capacities differ from the corresponding test values even though bolt failure was predicted to be the governing limit state. However, the test-to-predicted ratios for these specimens are within 8% of unity, other than those tested with a tensile force.

Specimens 3B-10-U-200T and 5B-10-U-200T have the smallest test-to-predicted ratios at 0.85 and 0.80, respectively. These specimens failed due to weld rupture resulting from an undersized weld, as well as a stress concentration at the tension tip of the weld. Given that the welds were undersized, if they had been proportioned as proposed in Section 4.4.4, bolt fracture would have likely been the critical failure mode, as was the case for most of the specimens, and the test-to-predicted ratios would be increased. These specimens were also more sensitive to column web deformation, because the applied tension increased the tensile stress concentration at the tip of the weld resulting from bending of the column web. As a result of the small weld size and increased tensile stress, specimen 3B-10-U-200T did not experience gross section yielding at all.

All connections with 13 mm plates exhibited lower test-to-predicted ratios than their thinner counterparts with the same depth and axial force, as well as less ductile behaviour, and specimens 3B-13-U-200C and 5B-13-U-300C both had ratios lower than unity. The ductility was not only limited by negligible bolt bearing deformation, but also by gross section yielding, which occurred after the peak load for specimen 5B-13-U-300C (for 3B-13-U-200C this point could not be determined). Although the maximum plate thickness requirement is based on the plate reaching its yield moment, rather than its full plastic moment, these observations imply that more a more stringent limit may be warranted. However, since significant rotations at the column web occurred, which increases the effective eccentricity of the shear force on the bolt group and would have been prevented had the associated proposed design requirement been met, changes to the maximum thickness equation could not be justified without more information.

The only other specimen with a low test-to-predicted strength ratio was 3B-10-U-300C. The calculated effective eccentricity of this connection given in Table 4-6 was high, likely because both the recommended axial and shear column web capacities were exceeded. It is believed that had the recommended weld size

and column web thickness requirements been met, the test-to-predicted ratios would have been acceptable for all of the specimens.

The test-to-predicted ratios are shown graphically in Figure 4-11. If the data point is above the diagonal line, the design recommendations are conservative. The connections subjected to tension are identified by the grey data points and are the farthest from the diagonal line.

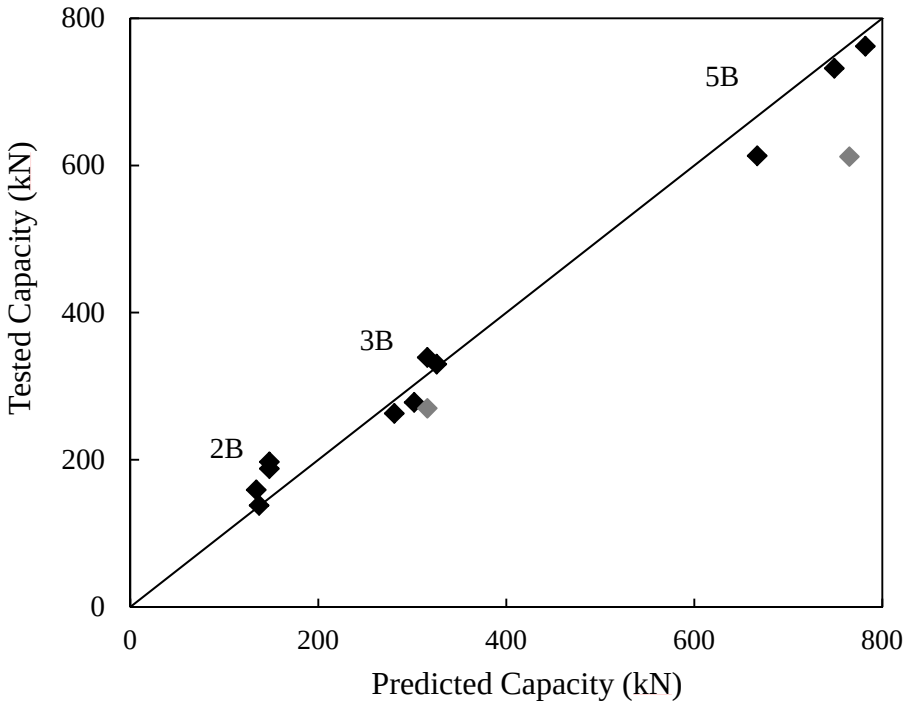

Figure 4-11: Test-to-predicted ratios for unstiffened connections

Table 4-7: Comparison of proposed ductility requirements with test specimens

Specimen ID	Plate thickness (mm)			Min. Weld Size (mm)	Weld Size (mm)
	t_{max}	t_p	t_{min}		
2B-10-U-0	21.1	9.5	6.1	9.3	6.0
2B-10-U-00	21.1	9.5	6.1	9.3	6.0
2B-10-U-200C	21.7	9.5	6.1	9.3	6.0
2B-13-U-200C	21.1	12.7	5.8	11.4	6.0
3B-10-U-0	16.6	9.5	7.5	9.3	6.0
3B-10-U-200C	18.0	9.5	7.5	9.3	6.0
3B-10-U-300C	18.3	9.5	7.5	9.3	6.0
3B-10-U-200T	18.0	9.5	7.5	9.3	6.0
3B-13-U-200C	17.7	12.7	7.2	11.4	6.0
5B-10-U-0	13.9	9.5	9.8	9.3	6.0
5B-10-U-300C	15.0	9.5	9.8	9.3	6.0
5B-10-U-200T	14.7	9.5	9.8	9.3	6.0
5B-13-U-300C	14.7	12.7	9.4	11.4	6.0

Table 4-8: Comparison of proposed shear capacity equations with test specimen capacities

Specimen ID	Column Web Capacity (kN)	Bolt Group Capacity (kN)	Gross Shear Capacity (kN)	Net Shear Capacity (kN)	Flexural/ Axial Capacity (kN)	Minimum Shear Capacity (kN)	Shear Capacity w/o CWY (kN)	Measured Peak Shear (kN)	Test-to-Predicted Ratio[1] (kN)
2B-10-U-0	158	176	429	315	148	148	148	188	1.27
2B-10-U-00	158	176	429	315	148	148	148	197	1.33
2B-10-U-200C	158	156	429	315	134	134	134	159	1.19
2B-13-U-200C	158	137	526	389	170	137	137	138	1.01
3B-10-U-0	249	326	658	487	348	249	326	330	1.01
3B-10-U-200C	249	316	658	487	334	249	316	339	1.07
3B-10-U-300C	249	302	658	487	316	249	302	278	0.92
3B-10-U-200T	249	316	658	487	334	249	316	270	0.85
3B-13-U-200C	249	281	806	602	415	249	281	263	0.94
5B-10-U-0	484	782	1116	831	1000	484	782	762	0.97
5B-10-U-300C	484	749	1116	831	969	484	749	732	0.98
5B-10-U-200T	484	765	1116	831	986	484	765	612	0.80
5B-13-U-300C	484	667	1366	1027	1200	484	667	613	0.92
								Mean:	1.02
							Coefficient of Variation:		0.154

[1]Shear capacity w/o column web yielding used in comparison

4.5 Summary

The unstiffened extended shear tab specimens failed due to either bolt shear or weld rupture, with the exception of one specimen that failed due to column web tearing. In most cases, the plate yielded through its depth prior to failure. The behaviour of the specimens can be described using a graph of the vertical load-vertical deformation, located in Appendix B for all unstiffened extended shear tab specimens. As expected, the strength of the connection increased with plate depth. However, the capacity decreased when a thicker plate was used, due in part to a lower bolt strength, but also to the increased demand on the bolt group resulting from the stiffer plate behaviour. When horizontal tension was applied to the connections, the failure mode was weld rupture, whereas the addition of compression tended to cause bolt fracture. Because current design procedures under-predict the connection capacity significantly, new design recommendations are proposed. These recommendations are based on the test results, AISC's extended configuration design method, and the design procedure used by the Fabricator. Maximum and minimum plate thickness requirements are included to ensure the plate yields prior to bolt fracture and to prevent lateral–torsional buckling. The weld and adjacent column web are also sized to ensure ductile behaviour, and strength requirements are outlined for both the bolt group and plate. The proposed recommendations result in a mean test-to-predicted capacity ratio of 1.02 when compared to the peak vertical load observed during testing.

CHAPTER 5: STIFFENED EXTENDED SHEAR TABS

5.1 Introduction

A discussion of the ten stiffened extended shear tab connections that were tested is presented in this chapter. The key variables, peak shear load, and observed failure modes are discussed and used to describe typical connection behaviour. Finally, the design recommendations made in Chapter 4 for unstiffened shear tabs are adapted for stiffened extended shear tabs. An additional design recommendation to address out-of-plane deformation is presented to reflect the observed behaviour.

5.2 Observed Behaviour

5.2.1 Failure Modes

Using stiffeners increased the connection strength compared to the unstiffened extended shear tabs with geometry that was otherwise identical. With the addition of stiffeners, the plate-to-column web connection becomes much more stable and the possibility of column web yielding or weld fracture occurring—two commonly observed failure modes for unstiffened extended shear tab tests—is greatly reduced. Out-of-plane deformation was the critical failure mode for each of the ten stiffened specimens. Six of the specimens also had bolt shear as a secondary failure mode. A summary of the failure modes is given in Chapter 3; however, a detailed list of all of the observed failure modes is presented in Table 5-1 for each stiffened extended shear tab specimen. These failure modes include weld rupture (WR), bolt fracture (BF), column web yielding (CWY), gross section yielding (GSY), bolt bearing (BB), and out-of-plane deformation (OPD). No indication of net section fracture was observed on any specimen, but plate rupture (PR) was observed in the radius of two specimens. In this table the critical failure mode is marked as CFM.

Table 5-1: Critical and other observed failure modes

	Failure Mode						
Specimen I.D.	WR	BF	CWY	PR	GSY	BB	OPD
2B-10-S-0	-	✓	-	✓	✓	-	CFM
2B-10-S-200C	-	✓	-	-	✓	-	CFM
2B-13-S-200C	-	✓	-	-	✓	-	CFM
3B-10-S-0	-	✓	-	✓	✓	-	CFM
3B-10-S-200C	-	-	-	-	✓	-	CFM
3B-10-S-300C	-	-	-	-	✓	-	CFM
3B-13-S-200C	-	✓	-	-	✓	-	CFM
5B-10-S-300C*	-	-	-	-	✓	-	CFM
5B-10-S-400C**	-	-	-	-	✓	-	CFM
5B-13-S-500C*	-	✓	-	-	✓	-	CFM

*Actuator 1 Capacity Reached
**Beam Web Deformation

During the 5B-10-S-300C and 5B-13-S-500C tests, the capacity of Actuator 1 was reached. However, in both cases the load had reached the plateau and additional actuator capacity was only required to maintain the beam rotation during plate deformation. Once the actuator capacity was reached, the 5B-10-S-300C test was stopped, whereas an additional 50 kN of horizontal compression was applied to the 5B-13-S-500C specimen to accelerate plate deformation. Due to the high loads and plate depth, out-of-plane deformation of the beam web was visible after testing specimen 5B-10-S-400C. Therefore, the beam was replaced for the remaining tests.

5.2.1.1 Weld Rupture

Weld rupture was not an issue during the stiffened extended shear tab tests, as the stress concentration seen in the unstiffened specimens was prevented by the stiffeners. This suggests that the column-end of the connection behaves similarly to a moment-resisting beam-to-column connection, in that the shear force is transferred to the column primarily through the vertical weld and the moment is transferred through the horizontal stiffeners.

5.2.1.2 Bolt Fracture

In six of the ten tests, bolt fracture was a secondary failure mode. As the plates deformed out-of-plane, the bolts were subjected to an increasing tensile force in addition to the horizontal and vertical loads. Therefore, with the exception of the three and five bolt line specimens with 10 mm plates and high axial load, the bolts failed. The bolts in the vertical line closest to the support typically failed as they were subjected to a higher proportion of the tensile load. However, the severity of bolt fracture varied. For example, the 3B-13-S-200C test ended abruptly, with the entire bolt group rupturing at once, whereas during the 5B-13-S-500C test the bolts failed progressively.

5.2.1.3 Column Web Yielding

Significant column web yielding was not observed during any of the unstiffened extended shear tab tests. However, when high compressive loads were applied to the connections, some Lüders' lines were observed on the face of the column web opposite the plate, as seen in Figure 5-1 for specimen 5B-13-S-500C. Similar to weld rupture, the large column web deformation seen during unstiffened extended shear tab tests was prevented by the stiffeners.

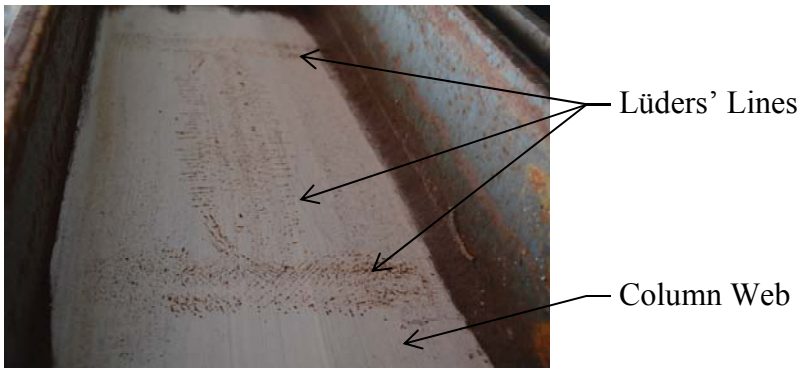

Figure 5-1: Lüders' lines on the column web opposite stiffened specimens

5.2.1.4 Gross Section Yielding

Although not the critical failure mode, gross section yielding was observed in all cases. The specimens with two horizontal bolt lines yielded through their depth

prior to the plate deforming out-of-plane, but the vertical load continued to increase until the plate began to bend out-of-plane. At this point, the load plateaued while the plate continued to fold and, ultimately, the load began to decrease.

5.2.1.5 Out-of-plane Deformation

Out-of-plane deformation was the critical failure mode in all of the specimens. The plates began to move out-of-plane prior to reaching the peak shear and continued until either the plate could not sustain half the peak vertical load or bolt fracture caused a decrease in the vertical load. The amount of deformation varied, but was more severe for specimens with 10 mm plates. Figure 5-2 shows the final deformation of specimen 3B-10-S-200C.

Figure 5-2: Out-of-plane deformation of specimen 3B-10-S-200C

5.2.1.6 Plate Rupture

The specimens tested without horizontal compression, specimens 2B-10-S-0 and 3B-10-S-0, both tore at the radius of the plate on the flexural tension side, as shown in Figure 5-3. Cheng (1993) identified radius cuts as potential fatigue crack initiation sites in coped beams. The tears result from a combination of the stress

concentration induced under loading due to the cross-sectional discontinuity and tensile residual stresses if flame-cutting is used. A similar stress concentration exists in these stiffened extended shear tabs and produces a location of potential tearing, even under non-cyclic loading. However, the tears in both specimens began after peak load and significant deformation had already occurred. Compression in the connection mitigates the potential for tearing.

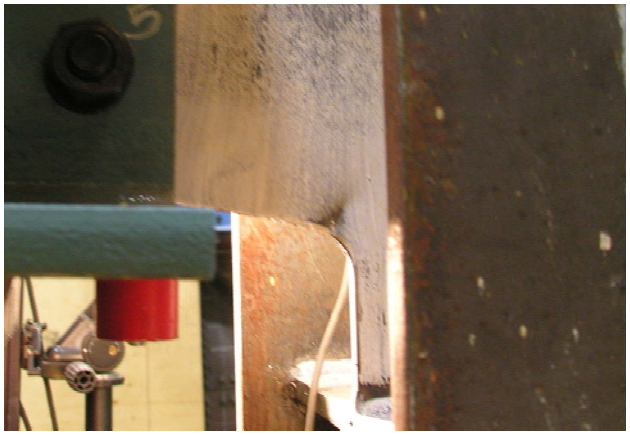

Figure 5-3: Tear in the radius of specimen 3B-10-S-0

5.2.1.7 Bolt Bearing

Varying degrees of bolt bearing were observed on the stiffened extended shear tab plates. Many of the maximum deformations were less than or equal to approximately one millimeter; the largest deformation, 5.7 mm, occurred around bolt number 1 on specimen 3B-10-S-0. Because the deformations were small, they are contributing to the overall ductility of the connection, rather than causing failure.

5.2.2 Vertical Load–Deformation Curves

The behaviour of the ten stiffened extended shear tabs can be explained by breaking the vertical load-vertical deformation graph into three zones: A, B, and C, delineated by the beginning and end of the load carrying capacity plateau. A typical vertical load-deformation curve, for specimen 2B-10-S-0, is given in Figure 5-4. The deformation is that of the bolt group centroid on the beam.

Zone A contains the beginning of the test, when the beam was rotated to 0.03 radians and horizontal load was applied, if required. Vertical load was then gradually applied and the plate began to yield, typically in the area around the radius in compression. As the plate continued to yield, it began to deform out-of-plane until the vertical load no longer increased. For some tests, the plate yielded along its full depth prior to deforming out-of-plane. The point of maximum vertical load, marks the end of Zone A.

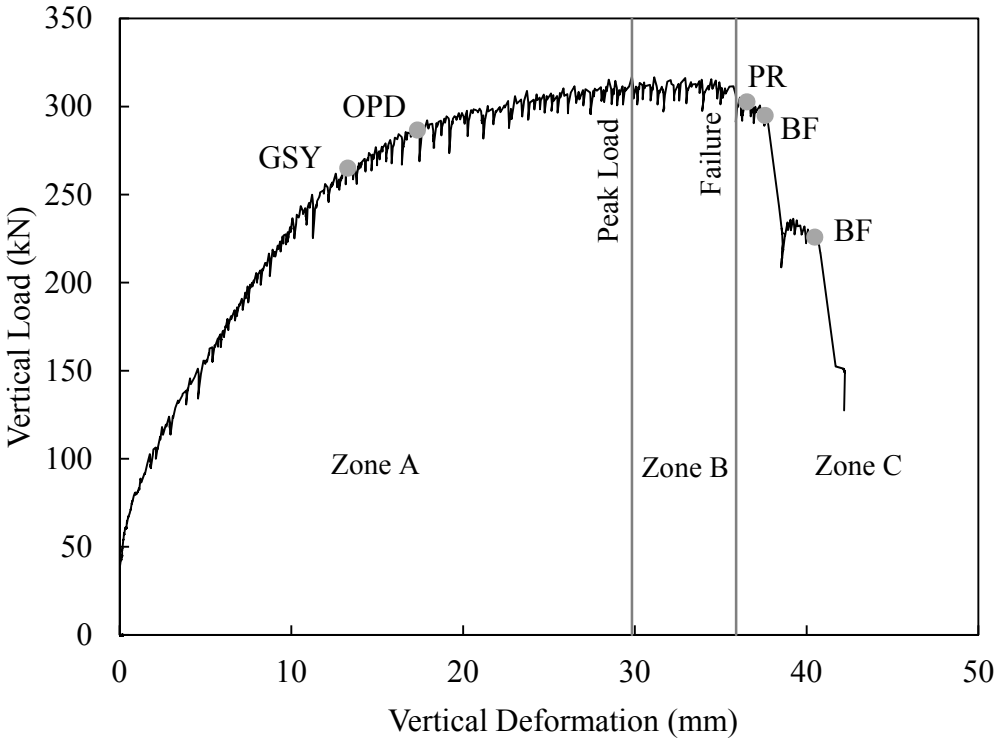

Figure 5-4: Load-Deformation behaviour of specimen 2B-10-S-0

After the peak vertical load was reached, the plate continued to deform out-of-plane while remaining at or near the peak load. The length of this load plateau varied but the vertical load eventually began to decrease, marking the end of Zone B. For the 5B-10-S-300C and 5B-13-S-500C tests, the beginning of Zone B was reached prior to reaching the actuator capacity. However, because the force in Actuator 1 needed to be increased to maintain the 0.03 radians while the specimen deformed (even though the net shear force on the connection was not

increasing), specimen 5B-10-S-300C had not reached the end of this zone when the actuator reached its capacity and the test was terminated. A similar situation arose with specimen 5B-13-S-500C, but additional horizontal load was applied to complete the test.

Zone C begins when the vertical load starts to decline steadily. The decrease in vertical load either continued to be gradual until half of the peak vertical load was reached, or began to gradually decrease until bolt fracture occurred, which caused a more abrupt load decline. Zone C in Figure 5-4 is an example of the latter; the load begins to decrease gradually until two bolts progressively fail. Vertical load–deformation graphs for each stiffened extended shear tab are given in Appendix C.

5.2.3 Effect of Key Variables

Of the ten specimens, three had two horizontal bolt lines, four specimens had three, and three specimens had five. In each of these groups, one of the specimens had a 13 mm plate, while the rest were 10 mm thick. The specimens were also tested under a variety of horizontal loads, as discussed in Chapter 3. General observations about the effects of these three key variables are discussed below. It must be kept in mind that these results are influenced by the hierarchy of failure modes experienced by the specimens, so any design changes that alter the failure sequence, such as a thicker plate or smaller bolts, may affect these observations.

5.2.3.1 Presence of Stiffeners

The influence of stiffeners on connection strength is examined by comparing specimens that differed only by the presence of stiffeners. Table 5-2 shows both the unstiffened and stiffened peak vertical load, as well as the increase in capacity due to the addition of stiffeners. The “U” or “S” has been removed from the specimen I.D. in the table for ease of comparison.

Table 5-2: Effect of stiffeners on connection capacity

Specimen I.D.	Peak Shear (kN)		Percent Increase
	Unstiffened	Stiffened	
2B-10-0	188	317	68.6%
2B-10-200C	159	258	62.3%
2B-13-200C	138	323	134.1%
3B-10-0	330	511	54.8%
3B-10-200C	339	382	12.7%
3B-10-300C	278	279	0.4%
3B-13-200C	263	562	113.7%
5B-10-300C	732	798	9.0%

This comparison shows that stiffeners increased the capacities of the connections, especially for specimens with two horizontal bolt lines and/or the 13 mm plate. However, the increase in capacity decreases with the addition of horizontal compression. For example, when the 3B-10-S geometry was tested with a horizontal compression of 300 kN, the extra strength expected due to the addition of stiffeners was no longer present.

5.2.3.2 Number of horizontal bolt lines

While deforming, the stiffened extended shear tab plate moved away from the beam web, causing the bolts to be loaded in combined shear and tension. Because more bolts were used, deeper plates sustained larger deformations after out-of-plane deformation began. Therefore, the shear carried by the smaller connections dropped more quickly than for the deeper specimens, leading to a more ductile failure, as shown in Figure 5-5.

The sequence of failure modes was also dependent on plate depth. The two horizontal bolt line connections met or exceeded their plastic moment capacity prior to deforming out-of-plane. In the deeper connections, the plate began to deform out-of-plane prior to reaching its full moment capacity.

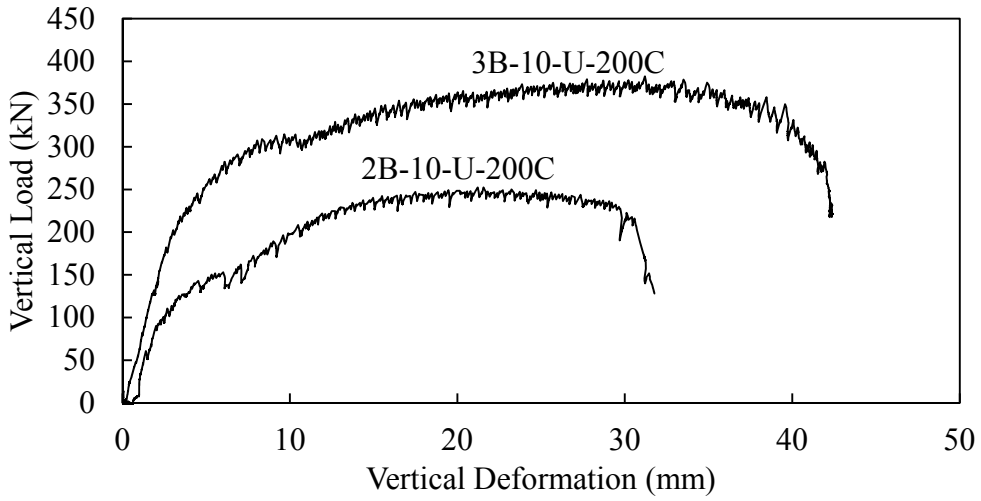

Figure 5-5: Effect of number of horizontal bolt lines on connection ductility

5.2.3.3 Plate Thickness

In contrast to the unstiffened specimens, stiffened extended shear tabs obtained higher peak loads when the thicker plate was used. This higher capacity was achieved because the thicker connection plate was less susceptible to out-of-plane deformation. The connections with thicker plates exhibited more brittle failures because more force was required to deform the plates, and the out-of-plane movement exposed the bolts to higher tensile forces and caused a more sudden bolt fracture, as shown in Figure 5-6.

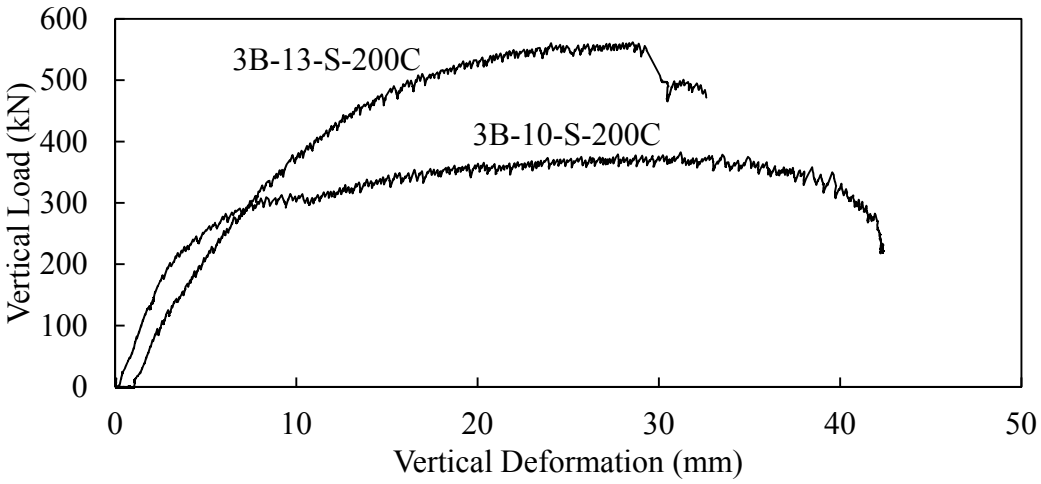

Figure 5-6: Effect of plate thickness on connection behaviour

5.2.3.4 Horizontal Load

The peak vertical load reached by the stiffened extended shear tab specimens decreased significantly with the addition of compression, as shown in Figure 5-7. With the application of 200 kN of compression, the capacity of the 2B-10-S specimen group decreased by 59 kN (19%), and the 3B-10-S group by 129 kN (25%). Increasing the horizontal load from 300 kN to 400 kN in compression resulted in a decrease of 212 kN (27%) for the 5B-10-S specimen group. Because the stiffened specimens typically deformed out-of-plane, applying axial compression accelerated the movement and decreased the shear capacity of the connections.

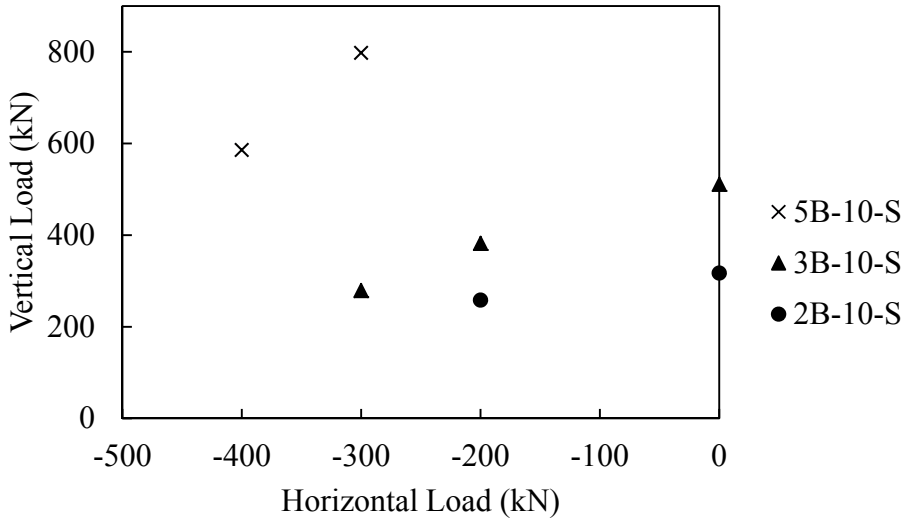

Figure 5-7: Effect of horizontal compression on connection capacity

5.3 Current Design Procedures

Not all of the design procedures discussed in Chapter 4 address the presence of stiffeners. AISC (2011) and the Fabricator include provisions for stiffeners to improve the connection's behaviour, but do not allow for an increase in capacity with the addition of stiffeners. The test data shows that using stiffeners increases the strength of the extended shear tabs with geometry that is otherwise identical to an unstiffened specimen, unless high compressive forces are applied. Because the

design procedures examined in Chapter 4 significantly underestimated the capacity of unstiffened extended shear tabs, comparing the stiffened specimens' test results to these procedures would not provide any insight into their ability to describe specimen behaviour.

5.4 Design Recommendations

The design recommendations in Chapter 4 have been modified as required for the design of stiffened extended shear tabs. The recommendations made for bolt group capacity and maximum plate thickness differ only by the definition of eccentricity, whereas the weld design philosophy has changed. The latter is now based on transferring the shear force to the support, rather than sizing the weld to ensure ductile failure. Design recommendations for column web yielding are not included because it was not an observed failure mode, but an additional maximum depth-to-thickness ratio, instead of the minimum thickness ratio used in Chapter 4, has been included to prevent the out-of-plane failure of the stiffened extended shear tabs seen during testing. Again, not all failure modes that must be addressed during design are included in these recommendations.

5.4.1 Bolt Group Capacity

The bolt group capacity of stiffened extended shear tabs is calculated using the instantaneous centre of rotation method, similar to the unstiffened configuration. However, because the stiffeners act as a support on the column side of the plate, the shear force eccentricity is not based on the geometric eccentricity from the weld line; rather, it is the clear distance from the stiffeners to the centroid of the bolt group. In other words, the eccentricity becomes the geometric eccentricity minus the stiffener depth. For the test specimens, this eccentricity is 158 mm.

Because bolt fracture was not a critical failure mode for any of the stiffened specimens, the method used in Chapter 4 to quantify the eccentricity causing bolt fracture could not be used. Therefore, the effective eccentricity is assumed to be 50% of the design eccentricity (i.e., 50% of 158 mm for the stiffened test

specimens). Because the stiffeners reduce the rotation at the column-end of the plate seen during the unstiffened extended shear tabs, using 75% underestimates the bolt group capacities when comparing with the test results. An effective eccentricity of 50% of the design eccentricity is a reasonable approximation of the true inflection location. However, judgement is required to evaluate whether a larger eccentricity should be used to account for the possibility of a rotationally flexible supporting member.

5.4.2 Plate Thickness

The maximum plate thickness equation in Chapter 4 is also valid for extended shear tabs with stiffeners. The calculation differs only in the definition of the effective eccentricity, as discussed in the previous section.

The minimum plate thickness requirement has been redefined from that used for unstiffened extended shear tabs. Because the stiffeners decreased the length of the shear tab plate significantly, their capacities increased and out-of-plane deformation became the critical failure mode for all test specimens. Moreover, the short length makes the formulation based on flexural lateral–torsional buckling inaccurate. Out-of-plane deformation occurred prior to gross section yielding for specimens with larger depth-to-thickness ratios. Therefore, to mitigate buckling-like failure, stiffened extended shear tabs should meet a maximum depth-to-thickness ratio. The limit given in S16 (CSA 2009) for elements in uniform compression supported along one edge that must reach the yield strain without buckling is $200/\sqrt{F_y}$ and for the same element at the extreme fibre of a flexural member that is capable of achieving a fully plastic cross-section (i.e., the strain is uniform and greatly exceeds the yield value), the limit is $170/\sqrt{F_y}$. Considering the point at which the stress changes from compression to tension along the depth of the plate as the supported edge, the actual strain state on the part of the plate in compression is between these two cases. That is, the strain increases from zero at the neutral axis to a value much greater than the yield strain

at the free edge when the plate becomes fully plastic. Therefore, an average value is proposed for the maximum depth-to-thickness ratio:

5-1 $$\frac{d_c}{t_p} \leq \frac{185}{\sqrt{F_y}}$$

where F_y is the nominal yield stress. The depth of the plate in compression, d_c, is given by:

5-2 $$d_c = \frac{d_p}{2} - \frac{N_F}{2F_y t_p}$$

where the factored axial load, N_F, is taken as positive for tension. Rearranging Equations 5-1 and 5-2 results in an equation for the minimum plate thickness:

5-3 $$t_{min} = \frac{\sqrt{F_y}}{370}\left(d_p - \frac{N_F}{F_y t_p}\right)$$

5.4.3 Weld Design

For stiffened extended shear tabs, the weld is designed to transfer shear force to the column, with no eccentricity. As discussed in Chapter 2, the factored weld capacity, $\phi_w V_W$, can be calculated as follows when the force is parallel to the weld axis:

5-4 $$\phi_w V_W = 0.67 \phi_w A_w X_u$$

where X_u is the ultimate tensile strength of the filler metal and ϕ_w is the resistance factor for welds. The area of the weld throat, A_w, is:

5-5 $$A_w = 0.707 D L_w$$

where D is the leg size of the fillet weld and L_w is the length of the weld. The weld that connects the stiffener to the connection plate can also be designed using Equations 5-4 and 5-5. These welds should be designed to transfer the horizontal load and moment.

5.4.4 Plate Design

Similar to the unstiffened case, the plate must be designed to resist the applied shear on both the net and gross sections. In addition, the flexural capacity of the plate can be calculated using the same relationship as for unstiffened extended shear tabs, but with a modified eccentricity. During the unstiffened specimen tests, the high stress region in the plate was at the first vertical bolt line; therefore, the distance from the inflection point to the first vertical bolt line was used to calculate its flexural capacity. Conversely, in the stiffened extended shear tab tests high stress regions were present at both ends of the plate span. Therefore, the clear span, L, from the edge of the stiffeners to the first vertical bolt line, is conservatively used to calculate the eccentric shear force that would result in flexural failure.

5.4.5 Comparison of Test Results to Design Recommendations

The design recommendations made in previous sections have been applied to the stiffened test specimens. A summary of the plate thickness requirements is given in Table 5-3 and the shear strength calculations are located in Table 5-4.

The maximum plate thickness recommendation was met for all specimens with the exception of specimen 5B-13-S-500C. This result was expected because all of the specimens exhibited ductile failure and this maximum thickness requirement is used to ensure plate yielding occurs prior to bolt fracture. Specimen 5B-13-S-500C exceeded the limit by 1.3 mm and was the least ductile of the stiffened extended shear tab specimens because bolt fracture occurred quickly after peak load, as would be expected when the maximum thickness is exceeded.

The minimum thickness requirement was only met by two specimens: 2B-10-S-0, and 2B-13-S-200C. This requirement is in place to ensure the plate will reach its plastic moment prior to deforming out-of-plane and was calculated for comparison to the test specimens using the measured yield stress to determine the depth of the plate in compression, but the nominal yield stress (350 MPa) was

used to calculate the limiting ratio. The tested capacities of the specimens that met the limit exceeded the capacities calculated using the equation for plate flexure. Moreover, two (2B-10-S-200C and 3B-13-S-200C) that violated the limit by no more than 0.8 mm either closely approximated or exceeded the calculated capacities. In all but one of the remaining cases the test capacity was significantly lower. Therefore, the depth-to-thickness ratio appears to be a good indicator of when the fully plastic plate capacity can be achieved. However, restricting the plate size to prevent out-of-plane deformation in this way has resulted in minimum plate thicknesses that are larger than the maximum for all of the specimens with five horizontal bolt lines and one with three. This indicates that for these connection geometries, the combinations of bolt diameter and axial load used for these tests would not be permitted because adequate ductility cannot be assured.

The shear requirements are given in Table 5-4 and, as this table shows, these design recommendations are conservative when predicting plate flexure as the failure mode, but otherwise non-conservative. Although the mean test-to-predicted ratio is equal to 1.04, the coefficient of variation is high (0.30). The specimens with the highest test-to-predicted ratio are those with two horizontal bolt lines. The capacity of these connections is limited by the flexural capacity of the plate which, as shown in Figure 5-4, underestimates the peak load. Plate flexure is also the predicted failure mode for specimen 3B-10-S-0; however, because the plate actually failed due to out-of-plane deformation, the ratio is closer to unity. All of the specimens with very low test-to-predicted ratios, 3B-10-S-200C, 3B-10-S-300C, 5B-10-S-400C, and 5B-13-S-500C, had plate thicknesses well below the minimum requirement.

The test-to-predicted ratios are shown graphically in Figure 5-8. If the data point is above the diagonal line, the design recommendations are conservative. The points shown in grey meet the minimum thickness requirement.

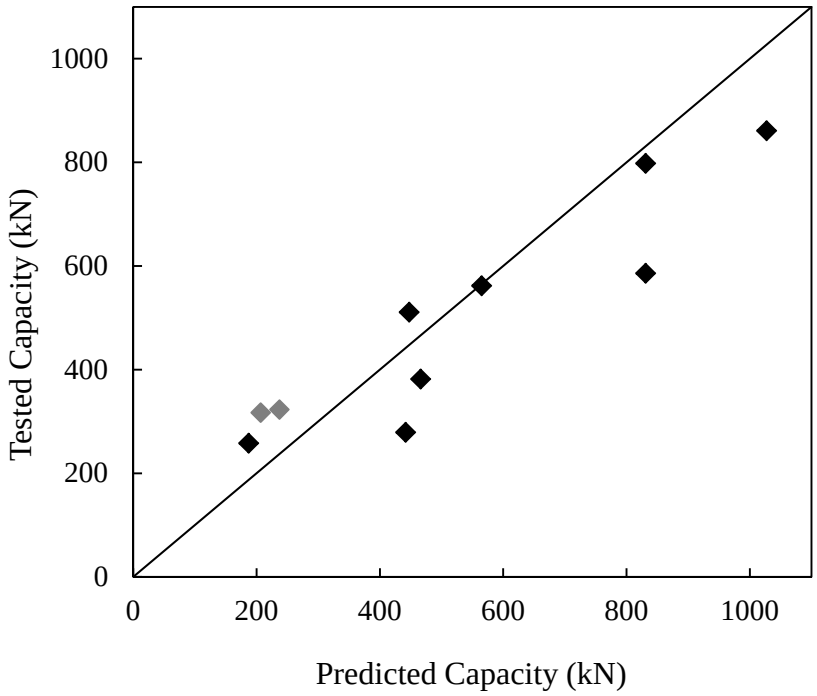

Figure 5-8: Test-to-predicted ratios for stiffened connections

Although bolt fracture was not a critical failure mode in any of the tests, the calculated capacity of specimen 3B-13-S-200C is limited by bolt fracture. However, the plate flexure capacity exceeds the bolt group capacity by only 14 kN (2.5%). The bolt fracture, experienced quickly after reaching the load plateau, supports reducing the effective eccentricity to 50% of the design eccentricity as it mimics the tested behaviour.

Table 5-3: Comparison of proposed plate thickness requirements with specimens

Specimen ID	Plate thickness (mm)		
	t_{max}	t_p	t_{min}*
2B-10-S-0	16.8	9.5	7.6
2B-10-S-200C	17.9	9.5	9.9
2B-13-S-200C	17.5	12.7	9.5
3B-10-S-0	12.9	9.5	11.6
3B-10-S-200C	14.4	9.5	14.0
3B-10-S-300C	14.8	9.5	15.1
3B-13-S-200C	14.2	12.7	13.5
5B-10-S-300C	10.9	9.5	23.2
5B-10-S-400C	11.2	9.5	24.4
5B-13-S-500C	11.4	12.7	24.5

*Limit calculated using the nominal yield stress (350 MPa)

Table 5-4: Comparison of proposed shear capacity equations with test specimen capacities

Specimen ID	Bolt Group Capacity (kN)	Weld Capacity (kN)	Gross Shear Capacity (kN)	Net Shear Capacity (kN)	Flexural/ Axial Capacity (kN)	Minimum Shear Capacity (kN)	Measured Peak Shear (kN)	Test-to-Predicted Ratio (kN)
2B-10-S-0	363	418	429	315	207	207	317	1.53
2B-10-S-200C	324	418	429	315	187	187	258	1.38
2B-13-S-200C	284	418	526	389	237	237	323	1.36
3B-10-S-0	657	641	658	487	447	447	511	1.14
3B-10-S-200C	634	641	658	487	466	466	382	0.82
3B-10-S-300C	607	641	658	487	442	442	279	0.63
3B-13-S-200C	565	641	806	602	579	565	562	0.99
5B-10-S-300C	1338	1086	1116	831	1353	831	798	0.96
5B-10-S-400C	1310	1086	1116	831	1318	831	586	0.71
5B-13-S-500C	1124	1086	1366	1027	1611	1027	861	0.84
							Mean:	1.04
							Coefficient of Variation:	0.297

5.5 Summary

The stiffened extended shear tab specimens failed due to out of plane deformation. In some cases, the plates deformed until bolts fractured as a secondary failure mode. The behaviour of the specimens can be described on a vertical load vertical deformation graph. These graphs are located in Appendix C for all stiffened extended shear tab specimens. As expected, the peak shears of the stiffened extended shear tabs were higher than those for analogous specimens without stiffeners. The capacity of the stiffened specimens also increased with plate depth and thickness, but was sensitive to the application of horizontal compression. If a large enough compressive force was applied, the increase in strength observed due to the presence of stiffeners was no longer evident. Because current design procedures do not allow for an increase in strength when extended shear tabs are stiffened, the test results could not be compared to any current design guidelines. The design recommendations made in Chapter 4 were modified for application to stiffened extended shear tab connections and a new maximum plate depth to thickness ratio was proposed. These recommendations result in a test to predicted strength ratio of 1.04 when compared to the peak vertical loads observed during testing; however, the coefficient of variation is high and several test-to-predicted ratios are quite low because many of the specimens exceeded the maximum plate depth to thickness ratio.

CHAPTER 6: CONCLUSIONS AND RECOMMENDATIONS

6.1 Summary

Conventional and extended shear tabs are common types of shear connections used for beam-to-girder and beam-to-column connections. Although there has been extensive research into the design of conventional shear tabs, few testing programs have concentrated on the behaviour of extended shear tabs. Research programs by Sherman and Ghorbanpoor (2002), Goodrich (2005), and Metzger (2006) have been used to develop the AISC design procedures (2005; 2011), whereas the BCSA and SCI have verified design guidelines with research by Moore and Owens (1992). However, these design procedures do not address the presence of horizontal load or the increase in strength of the connection when stiffeners are present.

To address these issues, 23 extended shear tab connections, both with and without stiffeners, were tested under various combinations of vertical and horizontal loads. The beam was braced laterally near its end to isolate the connection behaviour. The tests were completed by rotating the beam to 0.03 radians, applying horizontal load (if required), and failing the connections by applying vertical load while holding the horizontal load and beam rotation constant. An existing set-up was modified to meet the requirements for these tests and a variety of instruments were used to monitor and record the behaviour of the specimens. Additional tests were completed to determine the material properties of the connection plates and the shear capacity of the bolts used to make the connection to the beam.

The critical failure mode was identified for each specimen, as well as any other failure modes that were present. The unstiffened extended shear tabs tended to fail due to bolt fracture or weld rupture, whereas out-of-plane deformation governed the capacities of the stiffened specimens. Current design procedures were examined to determine their ability to predict the capacity and failure mode of the specimens.

Using the test results, design recommendations are made based on procedures currently used by the Fabricator and those recommended by AISC (2005; 2011). Design equations to ensure both strength and ductility are proposed. The predicted capacities and failure modes of the 23 specimens have been evaluated using these recommendations and compared to the test results. The recommended design procedures produce a mean test-to-predicted ratio of 1.02 for unstiffened and 1.04 for stiffened extended shear tabs when compared to the peak vertical loads observed during testing.

6.2 Conclusions and Design Recommendations

The capacity of an extended shear tab connection can, in general, be increased by using stiffeners. If stiffeners are not used, the capacity can be increased by using a deeper plate with more bolts. However, increasing the plate thickness does not necessarily strengthen unstiffened extended shear tabs, as it may reduce ductility and thereby trigger another failure mode. When stiffeners are used, additional shear capacity can be added by increasing the plate depth and number of bolts, or the plate thickness. The reduction in shear strength of stiffened extended shear tabs was observed to be more rapid with the addition of horizontal load when compared to the unstiffened configuration, whose capacity may not decrease at all under small horizontal compressive loads. Also, small beam rotations do not have a large impact on the connection capacity. Ten failure modes have been identified that need to be considered during design:

1. Gross Section Yielding
2. Bolt Fracture
3. Weld Rupture
4. Net-Section Fracture
5. Column Web Yielding
6. Out-Of-Plane Deformation
7. Bolt Bearing
8. Plate Rupture

9. Block Shear
10. Plate Twisting

Failure modes one through eight were observed during testing and are addressed in the design recommendations. While bolt bearing deformations played a role in several of the tests, in no case was bearing failure observed.

To ensure a ductile failure mode, the connection should be designed to undergo plate yielding prior to more brittle failure modes, like weld rupture and bolt fracture. The design recommendations for extended shear tabs made in Chapters 4 and 5 were derived to achieve this failure mode hierarchy:

1. The bolt group is designed using the instantaneous centre of rotation method with an effective eccentricity equal to 75% of the design eccentricity for unstiffened specimens. For the stiffened specimens, this value can be reduced to 50% to account for the increased fixity of the support opposite the bolt group.
2. A maximum plate thickness is calculated such that the plate will yield prior to bolt fracture occurring. Axial load can be used to reduce the yield capacity of the plate; however, transient axial loads cannot be included in this calculation.
3. A minimum plate thickness is calculated to avoid out-of-plane deformation. For unstiffened specimens, this failure mode is precluded by equating the plastic moment capacity of the plate to the lateral-torsional buckling capacity. A linear moment distribution is used, conservatively assuming zero moment at the support and the maximum moment at the bolt group. This limit is replaced with a more stringent maximum depth-to-thickness ratio for stiffened extended shear tabs to prevent buckling-like failure. The ratio of the depth of the plate in compression to the plate thickness must not exceed $185/\sqrt{F_y}$.
4. The plate is designed to resist the applied shear, and buckling need not be considered. If the shear stress does not exceed half of the yield stress, the

full yield stress can be used to determine the flexural/axial capacity of the plate. Otherwise, the normal stress is reduced using a linear relationship based on the magnitude of the shear stress.

Additional design guidelines were developed exclusively for unstiffened extended shear tabs. After the tests, some degree of weld rupture was observed on 12 of the 13 specimens; similarly, column web yielding was noted on all specimens. Therefore, the following design recommendations were made:

5. The fillet welds are designed to develop the plate yield strength. Using the factors and equations given in S16 (CSA 2009), the weld leg size should be 1.155 times the plate thickness, multiplied by the ratio of the plate's nominal yield stress to the ultimate strength of the weld.
6. The ability of the column web to resist both axial load and eccentric shear force is determined using yield line analysis. Although these capacities are not consistent with the ultimate strength of the connection, they deter significant deformation of thin column webs.

Because weld rupture and column web yielding were not observed during the stiffened extended shear tab tests, the above recommendations (numbers 5 and 6) apply only to unstiffened connections. However, for stiffened extended shear tabs:

7. The weld is sized to transfer the shear force into the column web.

6.3 Recommendations for Further Research

The design equations developed are applicable for connections that resist eccentric shear only or a combination of eccentric shear and horizontal load. The connection depth is limited to that required for 2 to 5 horizontal bolt lines and the beam must be fully braced. To limit the number tests, not all potential variables were studied. Therefore, using the results of these tests, a parametric study is recommended to further validate or develop the design recommendations made in Chapters 4 and 5. Additional parameters worthy of study include the plate length,

column web thickness, stiffener configuration, and the presence of back-to-back extended shear tabs.

The column web thickness, stiffener configuration, and presence of back-to-back stiffeners may influence the effective eccentricity, found to be 75% of the design eccentricity for unstiffened extended shear tabs and 50% for the stiffened configurations. The design eccentricity is the geometric eccentricity for the former and the geometric eccentricity minus the stiffener depth for the latter. These values depend on the relative rotational stiffnesses at the ends of the plate. For example, thick column webs or back-to-back unstiffened extended shear tabs would result in a stiffer support condition than was present for the tested connections, and the point of inflection might be closer to the bolt group, reducing the effective eccentricity. The sensitivity of the location of the inflection to these changes should be studied.

The maximum plate thickness equation allows the use of thick plates, especially for the unstiffened case. Tests to verify that sufficient ductility is provided when using the maximum allowed plate thickness should be completed. Also, the weld size requirement given for unstiffened extended shear tabs uses the resistance factor given by S16 (CSA 2009), which results in a high reliability index for fillet welds. Therefore, the required weld size could be reduced, if justified by a reliability study.

Finally, good ductility was observed for many of the stiffened extended shear tab connections that violated the minimum thickness requirement and therefore exhibited out-of-plane deformation as the critical failure mode. In these cases, the stiffeners reduced the length of the connection plate and the shorter length allowed the plate to buckle in a controlled manner. As such, an equation predicting the capacity of these specimens for this mode should be developed that could be used when the maximum plate depth-to-thickness ratio cannot be met.

REFERENCES

AISC. (2011). *Steel Construction Manual, 14th Edition.* American Institute of Steel Construction, Chicago, IL.

AISC. (2005). *Steel Construction Manual, 13th Edition.* American Institute of Steel Construction, Chicago, IL.

Astaneh, A., Call, S. M., and McMullin, K. M. (1989). "Design of single plate shear connections." *Eng. J.*, 26(1), 21-32.

Astaneh, A., Liu, J., and McMullin, K. M. (2002). "Behavior and design of single plate shear connections." *J. Constr. Steel. Res.*, 58(5), 1121-1141.

Astaneh, A., McMullin, K. M., and Call, S. M. (1993). "Behavior and design of steel single plate shear connections." *J. Struct. Eng.*, 119(8), 2421-2440.

Astaneh, A. (1989). "Demand and supply of ductility in steel shear connections." *J. Constr. Steel. Res.*, 14(1), 1-19.

ASTM Standard A370-12a. (2012). *Standard Test Methods and Definitions for Mechanical Testing of Steel Products.* ASTM International, West Conshohocken, PA,

BCSA and SCI. (2002). *Joints in Steel Construction, Simple Connections, Revised 2005.* British Constructional Steelwork Association Limited and Steel Construction Institute, London, UK and Ascot, UK.

BSI. (2005). "Eurocode 3: Design of Steel Structures - Part 1-8: Design of Joints." *BS EN 1993-1-8:2005 Incorporating Corrigenda Nos. 1 and 2,* European Committee for Standardization, Brussels, Belgium.

Cheng, J. J. R. (1993). "Design of steel beams with end copes." *Journal of Constructional Steel Research,* 25(1–2), 3-22.

Cheng, J. J., Yura, J. A., and Johnson, C. P. (1984). “Design and behavior of coped beams”. Ph.D thesis. Univ. of Texas, Austin, Tex.

CISC. (2010). *Handbook of Steel Construction, 10th Edition, Second Revised Printing 2011.* Canadian Institute of Steel Construction, Markham, ON.

Crawford, S. F., and Kulak, G. L. (1971). "Eccentrically loaded bolted connections." *J. Struct. Div,* 97(ST3), 738-765.

Creech, D. D. (2005). "Behavior of single plate shear connections with rigid and flexible supports". M.Sc. thesis. North Carolina State Univ., Raleigh, NC.

CSA. (2014). *S16-14 Design of Steel Structures.* Canadian Standards Association, Mississauga, ON.

CSA. (2009). *S16-09 Design of Steel Structures with Update No.1*. Canadian Standards Association, Mississauga, ON.

Deng, K., Grondin, G. Y., and Driver, R. G. (2006). "Effect of loading angle on the behavior of fillet welds." *Eng.J.*, 43(1), 9-24.

Gerard, G., and Becker, H. (1957). *Handbook of Structural Stability Part 1 - Buckling of Flat Plates.* New York Univ., New York.

Goodrich, W. (2005). "Behavior of extended shear tabs in stiffened beam-to-column web connections". M.Sc. thesis. Vanderbilt Univ., Nashville, TN.

Guravich, S. J., and Dawe, J. L. (2006). "Simple beam connections in combined shear and tension." *Can. J. Civ. Eng.*, 33(4), 357-372.

Hewitt, C. (2006). "Simpler shear connections: design procedures for single-plate shear connections have been expanded in the new Manual to incorporate a wider variety of geometric parameters." *Mod Steel Constr*, 46(10), 51-53.

Kapp, R. H. (1974). "Yield line analysis of a web connection in direct tension." *Eng. J.*, 11(2), 38-41.

Lipson, S. (1968). "Single-angle and single-plate beam framing connections." *Canadian Structural Engineering Conference*, Canadian Steel Industries Construction Council, Toronto, ON, 141-162.

Marosi, M., D'Aronco, M., Tremblay, R., and Rogers, C. (2011a). "Multi-row bolted beam to column shear tab connections." *Eurosteel*, European Convention for Constructional Steelwork, Budapest, Hungary, 555-560.

Marosi, M., Tremblay, R., and Rogers, C. A. (2011b). "Behaviour of single and double row bolted shear tab connections and weld retrofits". Research Report. Deptartment of Civil Engineering & Applied Mechanics, McGill University, Montreal, QC.

Metzger, K. A. B. (2006). "Experimental verification of a new single plate shear connection design model". M.Sc. thesis. Virginia Polytechnic Institute and State Univ., Blacksburg, VA.

Mohr, B. A. (2005). "Investigation of ultimate bending strength of steel bracket plates". M.Sc. thesis. Virginia Polytechnic Institute and State Univ., Blacksburg, Virginia.

Moore, D. B., and Owens, G. W. (1992). "Verification of design methods for finplate connections." *Struct. Eng.,* 70(3), 46-53.

Muir, L. S., and Hewitt, C. M. (2009). "Design of unstiffened extended single-plate shear connections." *Eng.J.,* 46(2), 67-79.

Muir, L. S., and Thornton, W. A. (2004). "A technical note: a direct method for obtaining the plate buckling coefficient for double-coped beams." *Eng. J.,* 41(3), 133-134.

Muir, L. S., and Thornton, W. A. (2011). "The development of a new design procedure for conventional single-plate shear connections." *Eng.J.,* 48(2), 141-152.

Ng, K. F., Driver, R. G., and Grondin, G. Y. (2002). "Behaviour of transverse fillet welds." *Structural Engineering Report No. 245,* Department of Civil and Environmental Engineering, University of Alberta.

Oosterhof, S. A., and Driver, R. G. (2012). "Performance of steel shear connections under combined moment, shear, and tension." *Structures Congress,* American Society of Civil Engineers, Chicago, Il, 146-157.

Porter, K. A., and Astaneh, A. (1990). "Design of single plate shear connections with snug-tight bolts in short slotted holes." *Rep. No. UCB/SEMM-90/23,* Department of Civil Engineering, University of California, Berkeley, CA.

Richard, R. M., Kriegh, J. D., and Hormby, D. E. (1982). "Design of single plate framing connections with A307 bolts." *Eng. J.,* 19(4), 209-213.

Richard, R. M., Gillett, P. E., Kriegh, J. D., and Lewis, B. A. (1980). "The analysis and design of single plate framing connections." *Eng. J.,* 17(2), 38-52.

Salvadori, M. G., (1955). "Lateral buckling of I-beams." *T. Am. Soc. Civ. Eng.*, 120(1), 1165-1177.

Shaw, A. L., and Astaneh, A. (1992). "Experimental study of single-plate steel beam-to-girder connections." *Rep. No. UCB/SEMM-92/13,* Department of Civil Engineering, University of California, Berkeley, CA.

Sherman, D. R., and Ghorbanpoor, A. (2002). "Final report: design of extended shear tabs." American Institute of Steel Construction, University of Wisconsin-Milwaukee.

Tamboli, A. (2010). "Design of connections for axial, moment, and shear forces." *Handbook of Structural Steel Connection Design and Details, Second Edition*, McGraw Hill Professional, AccessEngineering.

Thornton, W. A. (1997). "Strength and ductility requirements for simple shear connections with shear and axial load." *National Steel Construction Conference*, American Institute of Steel Construction, Chicago, IL, 38-1-38-17.

Thornton, W. A., and Fortney, P. J. (2011). "On the need for stiffeners for and the effect of lap eccentricity on extended single-plate connections." *Eng. J.*, 48(2), 117-125.

APPENDIX A: SAMPLE CALCULATIONS

WAIWARD STEEL FABRICATORS LTD. DESIGN PROCEDURE

Sample calculation for specimen 3B-10-U-200C

Loads:

Shear Capacity: 182 kN

Axial Load: 200 kN C

Given:

Plate:

t_p = 9.52 mm

d_p = 230 mm

s = 80.0 mm

e_g = 273 mm

L = 233 mm

F_y = 455 MPa

F_u = 507 MPa

R_y = 1 (using actual yield stress)

E = 189383 MPa

Bolts:

R_n = 177 kN

d_{BH} = 20.6 mm

n = 6

n_h = 3

Weld:

D = 6.00 mm

Beam:

t_b = 13.0 mm

Calculations:

1. Check the bolt group using the instantaneous centre of rotation. From iterative analysis:
   a. $V_{BG} = 245$ kN
   b. $m_o = 0.0720$ mm

c. $L_o = 33.2$ mm

$$P = \sqrt{V_{BG}^2 + N_F^2}$$

$$P = \sqrt{(243\text{ kN})^2 + (200\text{ kN})^2} = 316\text{ kN}$$

$$\beta = \tan^{-1}\frac{V_{BG}}{N_F}$$

$$\beta = \tan^{-1}\frac{243\text{ kN}}{-200\text{ kN}} = -0.882\text{ radians}$$

$$M_{BG} = V_{BG}e_{eff}$$

$$M_{BG} = 243\text{ kN}(273\text{ mm}) = 66.3\text{ kNm}$$

$$e_{BG} = \frac{M_{BG}}{P}$$

$$e_{BG} = \frac{66.3\text{ kNm}}{314\text{ kN}} = 211\text{ mm}$$

$$X_{IC} = -L_o \sin\beta - m_o \cos\beta$$

$$X_{IC} = -(33.2\text{ mm})\sin(-0.882) - (0.0720\text{ mm})\cos(-0.882) = 25.7\text{ mm}$$

$$Y_{IC} = L_o \cos\beta - m_o \sin\beta$$

$$Y_{IC} = (33.2\text{ mm})\cos(-0.882) - (0.0720\text{ mm})\sin(-0.882) = 21.1\text{ mm}$$

Bolt Calculations:

Bolt	X_i (mm)	Y_i (mm)	θ_i (rad)	d_i (mm)	Δ_i (mm)	R_i (kN)	$R_i*\sin\theta_i$	$R_i*\cos\theta i$	R_i*d_i
1	-40.0	80.0	0.840	88.3	6.32	169	126	113	14926
2	40.0	80.0	-0.238	60.6	4.34	159	-38	155	9651
3	-40.0	0.0	-4.40	69.0	4.94	163	155	-50	11252
4	40.0	0.0	-2.55	25.5	1.82	123	-69	-102	3137
5	-40.0	-80.0	-3.72	121	8.64	174	95	-146	20963
6	40.0	-80.0	-3.00	102	7.31	172	-24	-170	17526
						Sum:	245	-200	77454

$$d_i = \sqrt{(Y_i - Y_{IC})^2 + (X_i - X_{IC})^2}$$

$$d_1 = \sqrt{(80\text{ mm} - 21.1\text{ mm})^2 + (-40\text{ mm} - 25.7\text{ mm})^2} = 88.3\text{ mm}$$

$$\theta_i = \tan^{-1}\left(\frac{Y_i - Y_{IC}}{X_i - X_{IC}}\right) - \frac{\pi}{2}$$

$$\theta_1 = \tan^{-1}\left(\frac{80\text{ mm} - 21.1\text{ mm}}{-40\text{ mm} - 25.7\text{ mm}}\right) - \frac{\pi}{2} = 0.840\text{ radians}$$

$$\Delta_i = \frac{\Delta_{max} d_i}{d_{max}}$$

$$\Delta_1 = \frac{8.34 \text{ mm}(88.3 \text{ mm})}{121 \text{ mm}} = 6.32 \text{ mm}$$

$$R_i = R_n(1 - e^{-0.4\Delta_i})^{0.55}$$

$$R_1 = 177 \text{ kN}\left(1 - e^{-0.4(6.32 \text{ mm})}\right)^{0.55} = 169 \text{ kN}$$

$$0 = \sum R_i \sin\theta_i + P \sin\beta$$

$$0 = 245 \text{ kN} + (316 \text{ kN}) \sin(-0.886) = 245 \text{ kN} - 241 \text{ kN} \sim 0 \text{ (rounding)}$$

$$0 = \sum R_i \cos\theta_i + P \cos\beta$$

$$0 = -200 \text{ kN} + (316 \text{ kN}) \cos(-0.866) = -200 \text{ kN} + 204 \text{ kN} \sim 0 \text{ (rounding)}$$

$$0 = \sum R_i d_i - P(e_{BG} + L_o)$$

$$0 = 77.5 \text{ kNm} - (316 \text{ kN})(211 \text{ mm} + 33.2 \text{ mm}) = 77.5 \text{ kNm} - 77.2 \text{ kNm} \sim 0 \text{ (rounding)}$$

2. Check the gross section capacity of the plate

$$\tau = \frac{V}{d_p t_p}$$

$$\tau = \frac{182 \text{ kN}}{(230 \text{ mm})(9.52 \text{ mm})} = 83.1 \text{ MPa}$$

$$\sigma_n = \sqrt{F_y^2 - 3\tau^2}$$

$$\sigma_n = \sqrt{(455 \text{ MPa})^2 - 3(83.1 \text{ MPa})^2} = 431 \text{ MPa}$$

$$M_p = \frac{\sigma_n t_p}{4}\left[(d_p)^2 - \left(\frac{N_F}{\sigma_n t_p}\right)^2\right]$$

$$M_p = \frac{(431 \text{ MPa})(9.52 \text{ mm})}{4}\left[(230 \text{ mm})^2 - \left(\frac{200 \text{ kN}}{(431 \text{ MPa})(9.52 \text{ mm})}\right)^2\right]$$

$$M_p = 51.9 \text{ kNm}$$

$$M = Ve_g = (182 \text{ kN})(273 \text{ mm}) = 49.7 \text{ kNm} \leq M_p$$

3. Check the net section capacity of the plate (neutral axis is 71.6 mm from the compression face of the plate determined by trial and error; all axial load is considered

tensile and bolt holes are ignored in tensile zone)

$$\sigma_n = \sqrt{\left[\frac{(F_y+F_u)}{2}\right]^2 - 2.8\tau^2}$$

$$\sigma_n = \sqrt{\left[\frac{(455\text{ MPa}+507\text{ MPa})}{2}\right]^2 - (83.1\text{ MPa})^2} = 459\text{ MPa}$$

$C = (71.6\text{ mm})(9.52\text{ mm})(459\text{ MPa}) = 313\text{ kN}$

$T_1 = (35\text{ mm} - 20.6\text{mm}/2)(9.52\text{ mm})(459\text{ MPa}) = 108\text{ kN}$

$T_2 = (80\text{ mm} - 20.6\text{mm})(9.52\text{ mm})(459\text{ MPa}) = 260\text{ kN}$

$T_3 = (230\text{ mm}/2 - 20.6\text{mm}/2 - 71.6\text{ mm})(9.52\text{ mm})(459\text{ MPa}) = 145\text{ kN}$

$M_p = 313\text{ kN}(79.2\text{ mm})/2 + 108\text{ kN}(102.7\text{ mm}) + 260\text{ kN}(40.0\text{ mm}) - 145\text{ kN}(26.7\text{ mm})$

$M_p = 42.4\text{ kNm}$

$M = VL = (182\text{ kN})(233\text{ mm}) = 42.4\text{ kNm} \leq M_p$

4. Block shear due to axial load: will not govern.
5. Check the weld capacity

$$V_W = 0.67X_uA_w(1.00+0.5(\sin\theta_w)^{1.5})$$

$$V_W = 0.67(490\text{ MPa})\frac{[(2)(6\text{ mm})(230\text{ mm})]}{\sqrt{2}}(0) = 641\text{ kN}$$

6. Check plate ductility
   a. Minimum plate thickness: can be ignored as the column web is thin

$$t_{min} = 0.877\sqrt{\frac{F_y d_p e_g}{E}}$$

$$t_{min} = 0.877\sqrt{\frac{(455\text{ MPa})(230\text{ mm})(273\text{ mm})}{189383\text{ MPa}}} = 10.8\text{ mm}$$

   b. Maximum plate thickness

$$M_{OBG} = R_n\sum\sqrt{X_i^2+Y_i^2}$$

$$M_{OBG} = 177\text{ kN}\left[4\left(\sqrt{(40\text{ mm})^2+(80\text{ mm})^2}\right)+2\left(\sqrt{(40\text{ mm})^2+0}\right)\right]$$

$$M_{OBG} = 77.5 \text{ KNm}$$

$$t_{max} = \frac{6M_{OBG}}{R_y F_y d_p^2}$$

$$t_{max} = \frac{6(75.7 \text{ kNm})}{1(455 \text{ MPa})(230 \text{ mm})^2} = 19.3 \text{ mm}$$

$$9.52 \text{ mm} < 19.3 \text{ mm}$$

THE AMERICAN INSTITUTE OF STEEL CONSTRUCTION EXTENDED CONFIGURATION DESIGN PROCEDURE (2011)

Sample calculation for specimen 3B-10-U-0

Loads:

Shear Capacity: 119 kN (Stiffener plate requirement)

Axial Load: 0 kN

Given:

Plate:

t_p = 9.52 mm

d_p = 230 mm

s = 80.0 mm

e_g = 273 mm

L = 233 mm

F_y = 455 MPa

F_u = 507 MPa

Bolts:

R_n = 177 kN

d_{BH} = 20.6 mm

n = 6

n_h = 3

Weld:

D = 6.00 mm

Beam:

t_b = 13.0 mm

Calculations:

1. Check weld size:

$$D \geq \frac{5}{8} t_p$$

$$D \geq \frac{5}{8}(9.52) = 5.95 \text{ mm} \leq 6 \text{ mm}$$

2. Check bolt group capacity:

$C = 1.46$ ($e_g = 254$ mm)

$C = 1.25$ ($e_g = 305$ mm)

$C = 1.46+(1.25-1.46)*(273-254)/(305-254)$

$C = 1.38$

$V_{BG} = CR_n$

$V_{BG} = 1.38(177 \text{ kN}) = 244 \text{ kN}$

3. Check plate thickness for ductility requirement:

$C' = 401$ (in mm)

$M_{OBG} = R_nC'$

$M_{OBG} = 177 \text{ kN } (401 \text{ mm}) = 71.0 \text{ kNm}$

$$t_{max} = \frac{6M_{OBG}}{F_y d_p^2}$$

$$t_{max} = \frac{6(71.0 \text{ kNm})}{455 \text{ MPa } (230 \text{ mm})^2} = 17.7 \text{ mm} > 9.52 \text{ mm}$$

4. Check the plate strength:

   a. Gross section yielding

$V_{GS} = 0.6F_y t_p d_p$

$V_{GS} = 0.6(455 \text{ MPa})(9.52 \text{ mm})(230 \text{ mm}) = 598 \text{ kN}$

   b. Net section fracture

$V_{NS} = 0.6F_u t_p(d_p - n_h d_{BH})$

$V_{NS} = 0.6(507 \text{ MPa})(9.52 \text{ mm})(230 \text{ mm} - 3(20.6 \text{ mm})) = 487 \text{ kN}$

   c. Block shear – will not govern

5. Check stabilizer plate requirement:

$$V_{LTB} = 10.3\pi\frac{d_p t_p^3}{L^2} \text{ (in metric)}$$

$$V_{LTB} = 10.3\pi\frac{(230\text{ mm})(9.52\text{ mm})^3}{(233)^2} = 119\text{ kN}$$

6. Check plate buckling (using "all other cases" double coped beam equations):

$$\lambda = \frac{d_p\sqrt{F_y}}{t_p\sqrt{47500 + 112000\left(\frac{d_p}{2L}\right)^2}}$$

$$\lambda = \frac{230\text{ mm}\sqrt{455\text{ MPa (0.145ksi/MPa)}}}{9.52\text{ mm}\sqrt{47500 + 112000\left(\frac{230\text{ mm}}{2(233\text{ mm})}\right)^2}} = 0.717$$

$$Q = 1.34 - 0.486\lambda \text{ (for } \lambda > 0.7)$$

$$Q = 1.34 - 0.486(0.717) = 0.992$$

$$F_{cr} = QF_y$$

$$F_{cr} = 0.992(455\text{ MPa}) = 451\text{ MPa}$$

$$V_{PB} = \frac{F_{cr} t_p d_p^2}{6e_g}$$

$$V_{PB} = \frac{451\text{ MPa}(9.52\text{ mm})(230\text{ mm})^2}{6(273\text{ mm})} = 139\text{ kN}$$

7. Determine capacity:

$$V = \min(205\text{ kN}, 598\text{ kN}, 487\text{ kN}, 119\text{ kN}, 139\text{ kN}) = 119\text{ kN}$$

8. Check plate flexure:

$$M_p = \frac{F_y t_p d_p^2}{4}$$

$$M_p = \frac{455\text{ MPa}(9.52\text{ mm})(230\text{ mm})^2}{4} = 57.3\text{ kNm}$$

$$1 \geq \left(\frac{V}{V_{GS}}\right)^2 + \left(\frac{Ve_g}{M_p}\right)^2$$

$$1 \geq \left(\frac{119\text{ kN}}{598\text{ kN}}\right)^2 + \left(\frac{119\text{ kN}(273\text{ mm})}{57.3\text{ kNm}}\right)^2 = 0.0396+0.321=0.361$$

9. Check torsion (likely not required as beam is fully braced):

$$M_{ta} = V\frac{(t_b+t_p)}{2}$$

$$M_{ta} = 119\text{ kN}\frac{(13.0\text{ mm}+9.52\text{ mm})}{2} = 1.34\text{ kNm}$$

$$M_{tn} = \left(0.6F_y - \frac{V}{Lt_p}\right)\frac{Lt_p^2}{2} > M_{ta}$$

$$M_{tn} = \left(0.6(455) - \frac{119\text{ kN}}{230(9.52\text{ mm})}\right)\frac{230\text{ mm}(9.52\text{ mm})^2}{2} = 2.28\text{ kNm} > 1.34\text{ kNm}$$

BCSA/SCI DESIGN PROCEDURE (2002)

Sample calculation for specimen 3B-10-U-0

Loads:

Shear Capacity: 164 kN

Axial Load: 0 kN

Given:

Plate:

t_p = 9.52 mm

d_p = 230 mm

s = 80.0 mm

e_g = 273 mm

L = 233 mm

F_y = 455 MPa

F_u = 507 MPa

Bolts:

F_{ub} ≥ 830 MPa

R_n = 177 kN

d_{BH} = 20.6 mm

n = 6

n_h = 3

Weld:

D = 6.00 mm

Beam:

d_b = 318 mm

Column:

w = 10.9 mm

F_{yc} = 385 MPa

Calculations:

1. Show that it is a "long" shear tab:

$$0.15 \leq \frac{t_p}{L}$$

$$0.15 \leq \frac{9.52 \text{ mm}}{233 \text{ mm}} = 0.0409 \text{ mm}$$

2. Check geometry of the connection:

   a. Bolt Strength

$F_{ub} \geq 800$ MPa

830 MPa ≥ 800 MPa

   b. Check plate depth with respect to the beam depth

$d_p \geq 0.6d_b$

230 mm ≥ 0.6(318 mm) = 191 mm

   c. Check end distance

$e_n \geq 2d$

35 mm ≥ 2(19.1 mm) = 38.1 mm (NOT MET)

   d. Check bolt spacing

$s \geq 2.5d$

35 mm ≥ 2.5(19.1 mm) = 47.6 mm

   e. Check bolt hole diameter

$d_{bh} \geq d+2$

20.6 mm ≥ 19.1+2 = 21.05 (NOT MET)

   f. Check maximum plate thickness

$t_p \leq 0.42d$

9.52 mm ≤ 0.42(19.1 mm) = 8.02 mm (NOT MET)

   g. Check minimum plate thickness

$t_p \geq 6$ mm

9.52 mm ≥ 6 mm

   h. Check weld size

$D \geq 0.8t_p$

$6\text{ mm} \geq 0.8(9.52\text{ mm}) = 7.62\text{ mm (NOT MET)}$

3. Check bolt group capacity: two vertical bolt lines

$I_{BG} = \sum X_i^2 + Y_i^2$

$I_{BG} = 4[(40\text{ mm})^2+(80\text{ mm})^2]+2[(40\text{ mm})^2+(0\text{mm})^2] = 35400\text{ mm}^2$

$M_{BG} = V\left(L+\frac{s}{2}\right)$

$M_{BG} = 164\text{ kN}\left(233\text{ mm}+\frac{80\text{mm}}{2}\right) = 44.8\text{ kNm}$

$R_n \geq \sqrt{\left[\left(\frac{V}{n}+\frac{M_{BG}X_{i\text{-max}}}{I_{BG}}\right)^2+\left(\frac{M_{BG}Y_{i\text{-max}}}{I_{BG}}\right)^2\right]}$

$R_n \geq \sqrt{\left[\left(\frac{164\text{ kN}}{6}+\frac{(52.0\text{ kNm})(40\text{ mm})}{35400\text{ mm}^2}\right)^2+\left(\frac{(52.0\text{ kNm})(80\text{ mm})}{35400\text{ mm}^2}\right)^2\right]}$

$177\text{ kN} \geq 128\text{ kN}$

4. Check the shear capacity of the plate

   a. Gross shear

$A_g = 0.9[2e_n + (n_h - 1)s]t_p$

$A_g = 0.9[2(35.0\text{ mm}) + (3 - 1)80.0\text{ mm}](9.52\text{ mm}) = 1970\text{ mm}^2$

$V_{GS} = 0.6F_yA_g$

$V_{GS} = 0.6(455\text{ MPa})(1971\text{ mm}^2) = 538\text{ kN}$

   b. Net shear

$A_n = A_g - n_h(d_{bh})t_p$

$A_n = 1971\text{ mm}^2 - 3(20.6\text{ mm})(9.52\text{ mm}) = 1382\text{ mm}^2$

$V_{NS} = 0.7F_y(1.1)A_n$

$V_{NS} = 0.7(455\text{ MPa})(1.1)(1382\text{ mm}^2) = 484\text{ kN}$

   c. Block shear: not critical for this connection

5. Check the shear/moment interaction

$V \leq 0.75[\min\{V_{GS}, V_{NS}\}]$ for a low shear connection

$164\text{ kN} \leq \min\{528\text{ kN}, 484\text{ kN}\} = 484\text{ kN}$

$$M_y = \frac{F_y t_p d_p^2}{6}$$

$$M_y = \frac{455\ \text{MPa}(9.52\ \text{mm})(230\ \text{mm})^2}{6} = 38.2\ \text{kNm}$$

$$M = VL = 164\ \text{kN}(233\ \text{mm}) = 38.2\ \text{kNm} \geq M_y$$

6. Check the lateral-torsional buckling capacity (See Annex B of BS5950 for definitions)

$$\lambda_{lt} = 2.8\left[\frac{Ld_p}{1.5t_p^2}\right]^{0.5} = 2.8\left[\frac{233\ \text{mm}(230\ \text{mm})}{1.5(9.52\ \text{mm})^2}\right]^{0.5} = 55.6$$

$$P_e = \frac{\pi^2 E}{\lambda_{lt}} = 605.4\ \text{MPa}$$

$$\lambda_{lo} = 0.4\left(\frac{\pi^2 E}{F_y}\right)^2 = 25.6$$

$$2\lambda_{lo} = 51.3 < \lambda_{lt}$$

$$\eta_{lt} = 14\lambda_{lo}/1000 = 0.359$$

$$\Phi_{lt} = \frac{F_y + (\eta_{lt}+1)P_e}{2} = 639\ \text{MPa}$$

$$F_{cr} = \frac{P_e F_y}{\Phi_{lt} + (\Phi_{lt}^2 - P_e F_y)^{0.5}} = 275\text{MPa}$$

$$M_{cr} = \frac{F_{cr} t_p d_p^2}{6(0.6)} = 38.4\ \text{kNm}$$

$$M = 38.2\ \text{kNm} \geq 38.4\ \text{kNm}$$

7. Beam capacity checks not required.

8. Check column web capacity:

$$V_{CW} = 0.6F_{yc}(0.9wd_p)$$

$$V_{CW} = 0.6(385\ \text{MPa})(0.9)(10.9\ \text{mm})(230\ \text{mm}) = 521\ \text{kN}$$

$$V_{CW} \geq 0.5V = 0.5(164\ \text{kN}) = 82\ \text{kN}$$

TAMBOLI DESIGN PROCEDURE (2010)

Sample calculation for specimen 3B-10-U-200C

Loads:

Shear Capacity: V = 180 kN (Net-section interaction)

Axial Load: N = 200 kN C

Given:

Plate:

t_p = 9.52 mm

d_p = 230 mm

s = 80.0 mm

e_g = 273 mm

L = 233 mm

F_y = 455 MPa

F_u = 507 MPa

E = 189 GPa

Bolts:

R_n = 177 kN

d_{BH} = 20.6 mm

n = 6

n_h = 3

Weld:

D = 6.00 mm

X_u = 490 MPa

Beam:

t_b = 13.0 mm

Calculations:

1. Determine resultant load and its angle:

$$P = \sqrt{V^2 + N^2} = \sqrt{(180\text{ kN})^2 + (200\text{ kN})^2} = 269\text{ kN}$$

$$\beta = \tan^{-1}\frac{N}{V} = \tan^{-1}\frac{200\text{ kN}}{180\text{ kN}} = 48.0\text{ deg}$$

2. Check bolt group capacity: (AISC Table 7-8)

$C = 1.96$ ($\beta = 45$ deg, $e_g = 254$ mm)

$C = 1.68$ ($\beta = 45$ deg, $e_g = 305$ mm)

$C = 1.96 + (1.68 - 1.96)*(273 - 254)/(305 - 254) = 1.86$ ($\beta = 45$ deg, $e_g = 273$ mm)

$C = 2.52$ ($\beta = 60$ deg, $e_g = 254$ mm)

$C = 2.21$ ($\beta = 60$ deg, $e_g = 305$ mm)

$C = 2.52 + (2.21 - 2.52)*(273 - 254)/(305 - 254) = 2.40$ ($\beta = 60$ deg, $e_g = 273$ mm)

$C = 1.86 + (2.4 - 1.86)*(48.0 - 45)/(60 - 45) = 1.97$ ($\beta = 48.0$ deg, $e_g = 273$ mm)

$$V_{BG} = \sqrt{(CR_n)^2 - N^2} = \sqrt{(1.97(177\text{ kN}))^2 - (200\text{ kN})^2} = 285.6\text{ kN}$$

3. Check plate thickness for ductility requirement:

$C' = 401$ (in mm)

$M_{OBG} = R_n C' = 149\text{ kN}\ (401\text{ mm}) = 59.8\text{ kNm}$

$$t_{max} = \frac{6M_{OBG}}{F_y d_p^2} = \frac{6(59.8\text{ kNm})}{455\text{ MPa}\ (230\text{ mm})^2} = 14.9\text{ mm} > 9.52\text{ mm}$$

4. Check the gross shear, axial, and bending capacity of the plate:

   a. Axial capacity

$k = 0.65$

$$r = \frac{t_p}{\sqrt{12}} = \frac{9.52\text{ mm}}{\sqrt{12}} = 2.75\text{ mm}$$

$$F_e = \frac{\pi^2 E}{(ke_g/r)^2} = \frac{\pi^2(189\text{ GPa})}{(0.65(233)/2.75)^2} = 616\text{ MPa}$$

$$F_{cr} = \left(0.659^{F_y/F_e}\right)F_y = \left(0.659^{455\text{ MPa}/616\text{ MPa}}\right)455\text{ MPa} = 334\text{ MPa}$$

$$N_{GS} = F_{cr}t_p d_p = (334\text{ MPa})(9.52\text{ mm})(230\text{ mm}) = 731\text{ kN}$$

   b. Bending capacity

$$\lambda = \frac{d_p\sqrt{F_y}}{t_p\sqrt{47500+112000\left(\frac{d_p}{2L}\right)^2}} = \frac{230\text{ mm}\sqrt{455\text{ MPa (0.145ksi/MPa)}}}{9.52\text{ mm}\sqrt{47500+112000\left(\frac{230\text{ mm}}{2(233\text{ mm})}\right)^2}} = 0.717$$

$$Q = 1.34 - 0.486\lambda = 1.34 - 0.486(0.717) = 0.992$$

$$F_{cr} = QF_y = 0.992(455\text{ MPa}) = 451\text{ MPa}$$

$$V_{PB} = \frac{F_{cr}t_p d_p^2}{4e_g} = \frac{451\text{ MPa}(9.52\text{ mm})(230\text{ mm})^2}{4(233\text{ mm})} = 244\text{ kN}$$

c. Shear capacity

$$V_{GS} = 0.6F_y t_p d_p = 0.6(455\text{ MPa})(9.52\text{ mm})(230\text{ mm}) = 598\text{ kN}$$

d. Gross section interaction

$$1 \geq \left(\frac{V}{V_{GS}}\right)^2 + \left(\frac{N}{N_{GS}} + \frac{8V}{9V_{PB}}\right)^2 = \left(\frac{180\text{ kN}}{598\text{ kN}}\right)^2 + \left(\frac{200\text{ kN}}{731\text{ kN}} + \frac{8(180\text{ kN})}{9(244\text{ kN})}\right)^2 = 0.955$$

5. Check the net shear, axial, and bending capacity of the plate:

a. Shear Capacity

$$V_{NS} = 0.6F_u t_p(d_p - n_h d_{BH}) = 0.6(507\text{ MPa})(9.52\text{ mm})(230\text{ mm} - 3(20.6\text{ mm})) = 487\text{ kN}$$

6. Net section interaction (axial net section not required if axial load is compression)

$$1 \geq \left(\frac{V}{V_{GS}}\right)^2 + \left(\frac{N}{N_{GS}} + \frac{8V}{9V_{PB}}\right)^2 = \left(\frac{180\text{ kN}}{487\text{ kN}}\right)^2 + \left(\frac{200\text{ kN}}{731\text{ kN}} + \frac{8(180\text{ kN})}{9(244\text{ kN})}\right)^2 = 1.00$$

7. Check weld capacity:

$$A_w = \frac{2d_p D}{\sqrt{2}} = \frac{2(230\text{ mm})(6\text{ mm})}{\sqrt{2}} = 1951\text{ mm}^2$$

$$V_w = 0.6X_u A_w(1+0.5(\sin\beta)^{1.5}) = 0.6(490\text{ MPa})(1951\text{ mm}^2)(1+0.5(\sin 48\text{ deg})^{1.5})$$

$$V_w = 757\text{ kN}$$

8. Block shear check will not govern

APPENDIX B:UNSTIFFENED EXTENDED SHEAR TAB LOAD–DEFORMATION CURVES

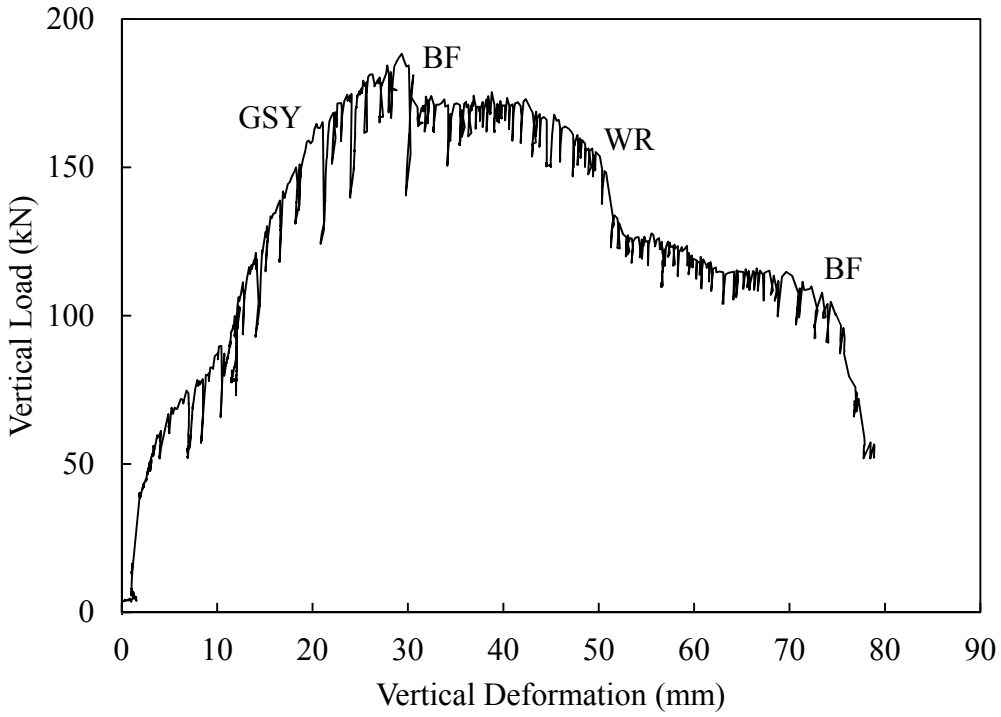

Figure B-1: Specimen 2B-10-U-0

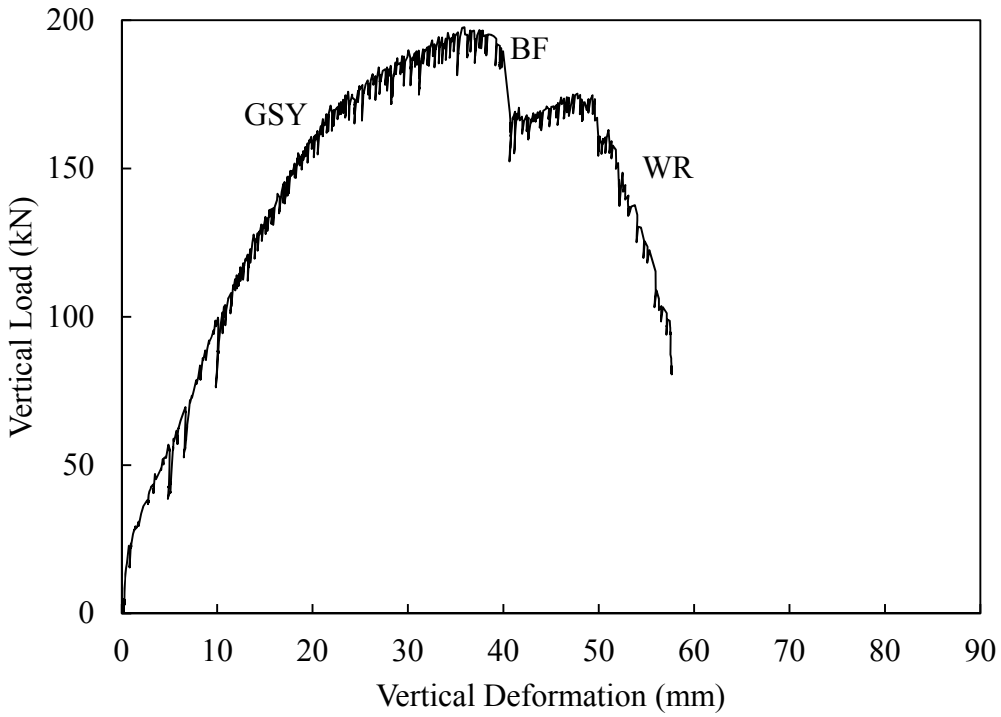

Figure B-2: Specimen 2B-10-U-00

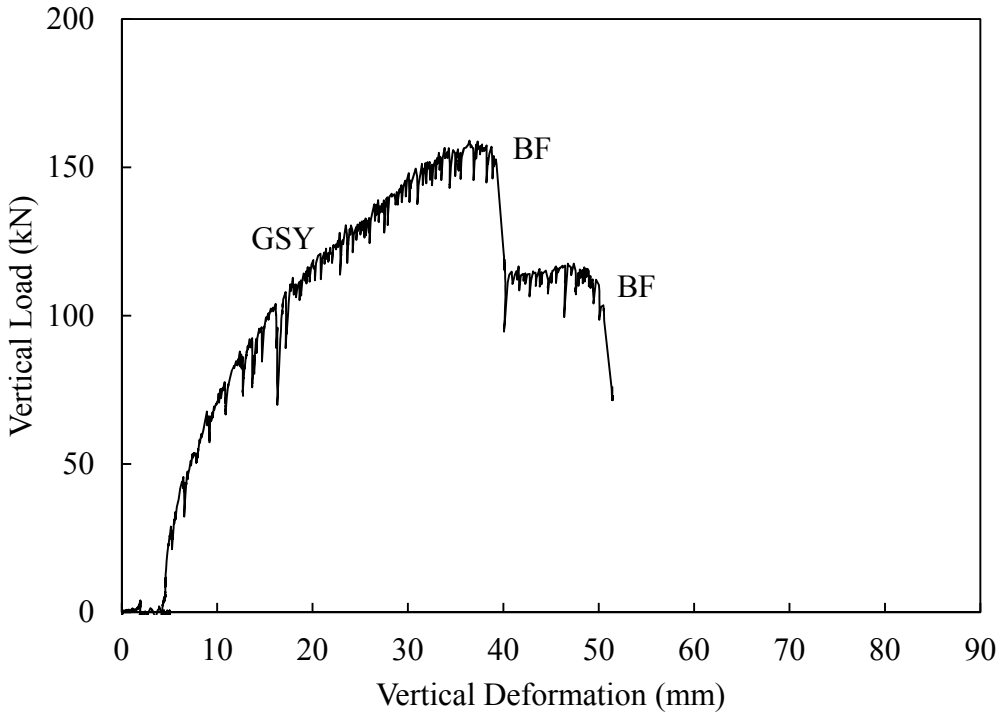

Figure B-3: Specimen 2B-10-U-200C

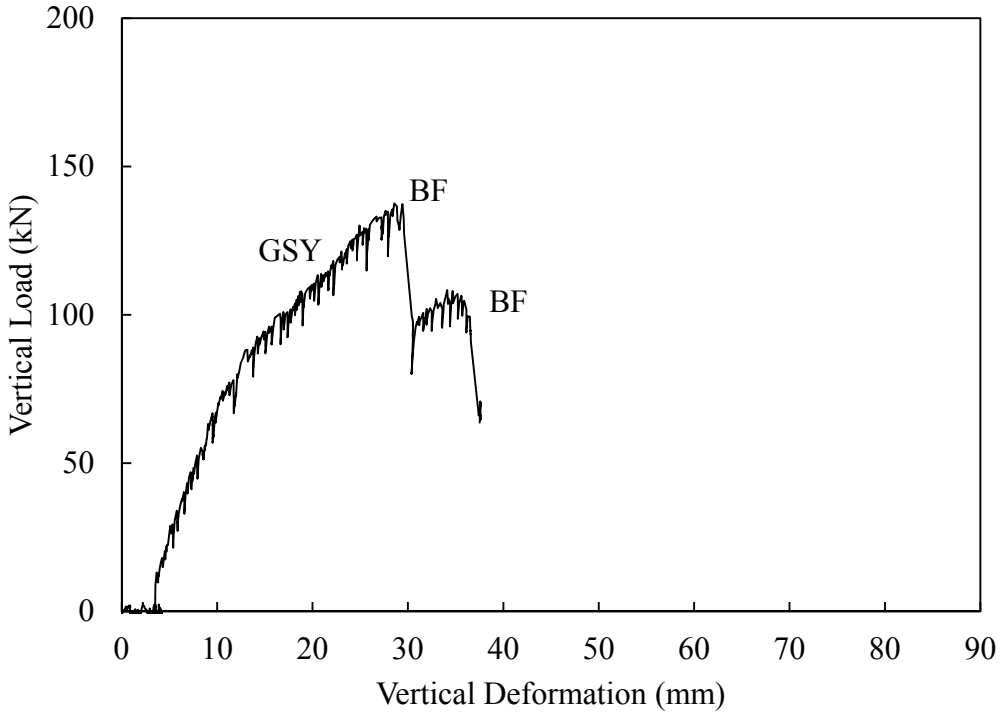

Figure B-4: Specimen 2B-13-U-200C

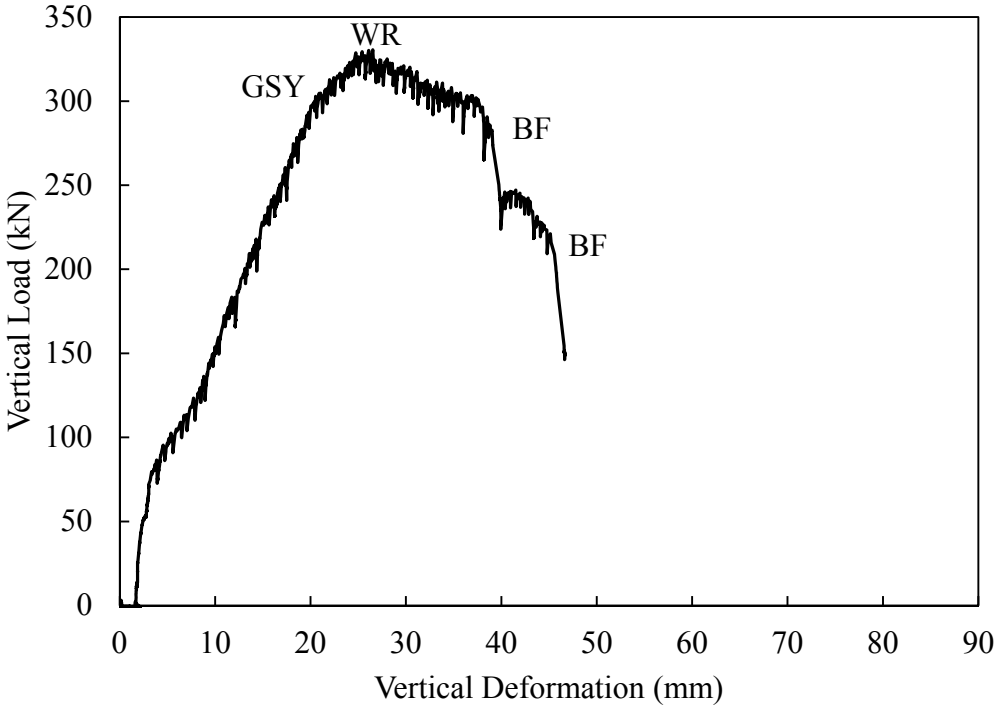

Figure B-5: Specimen 3B-10-U-0

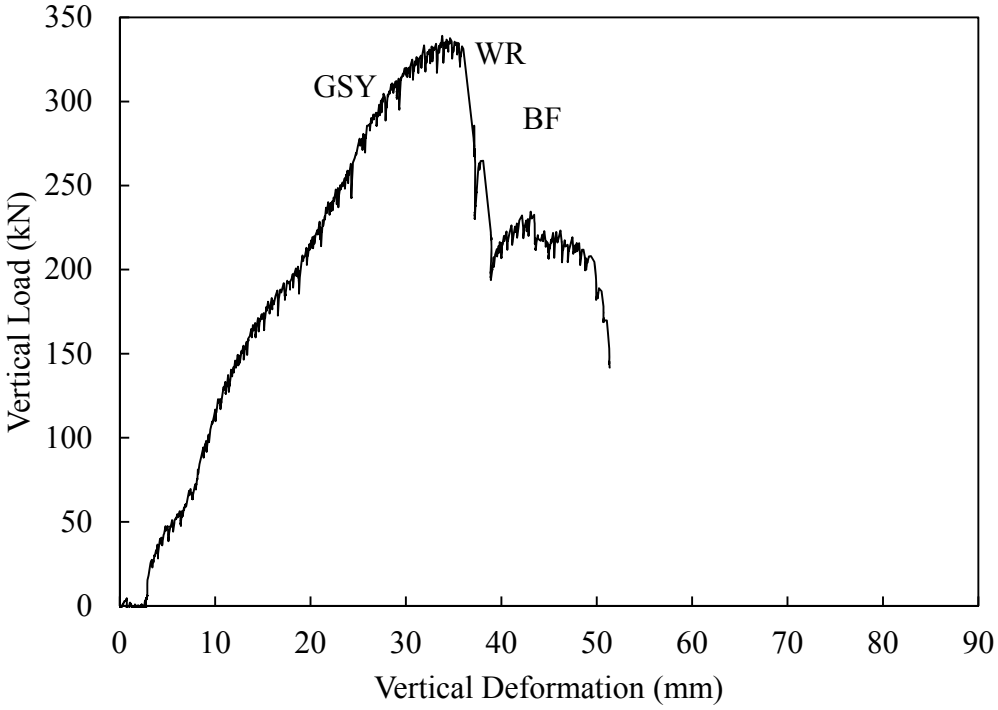

Figure B-6: Specimen 3B-10-U-200C

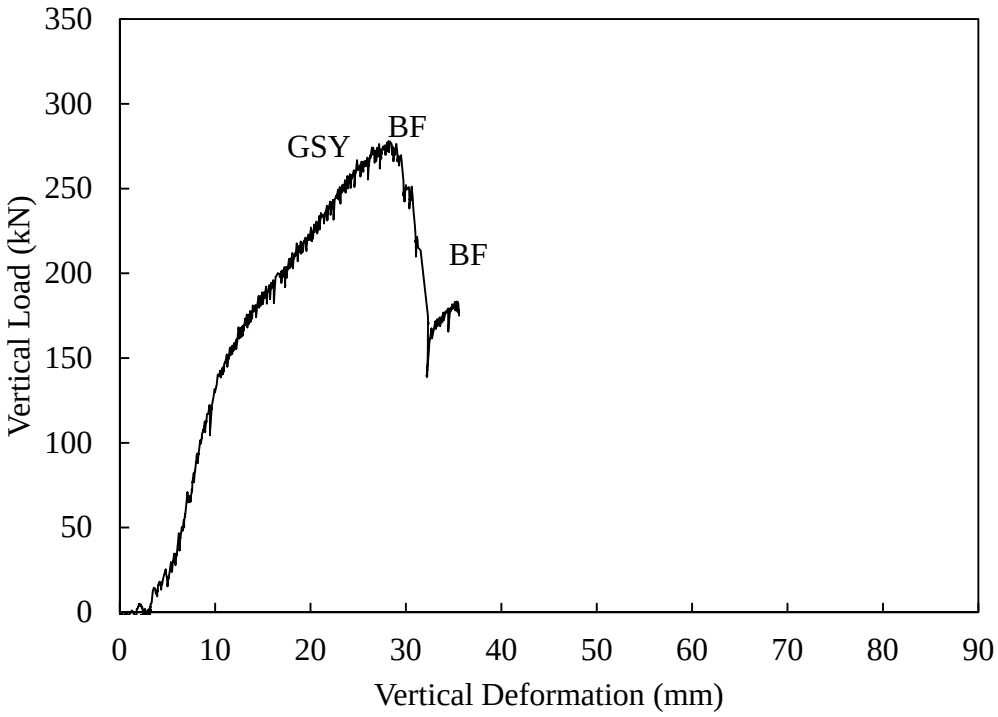

Figure B-7: Specimen 3B-10-U-300C

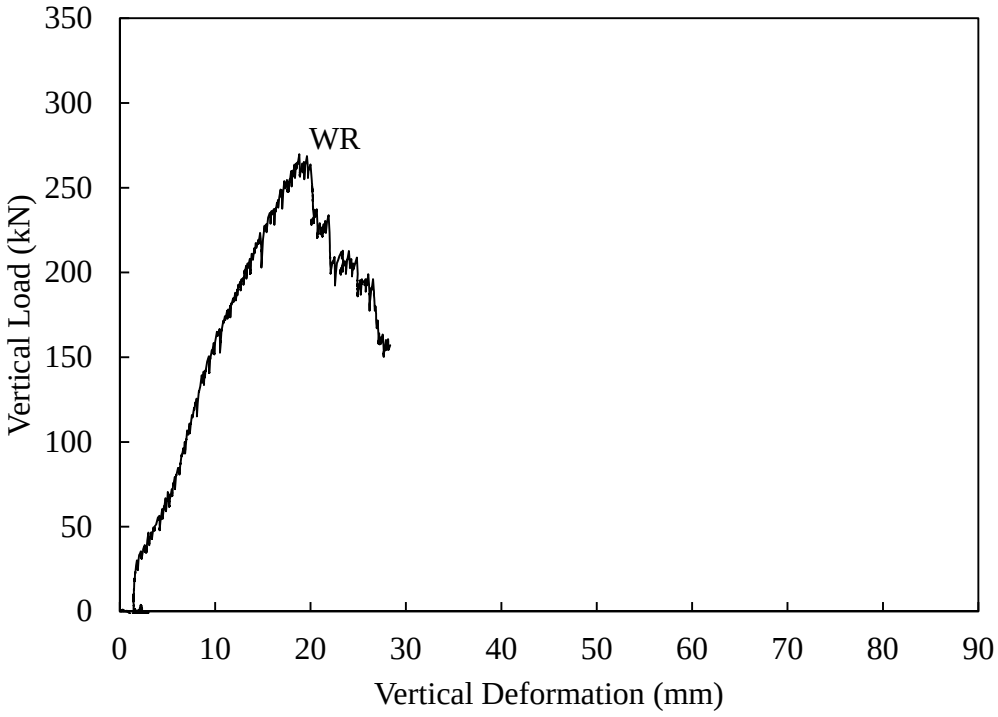

Figure B-8: Specimen 3B-10-U-200T

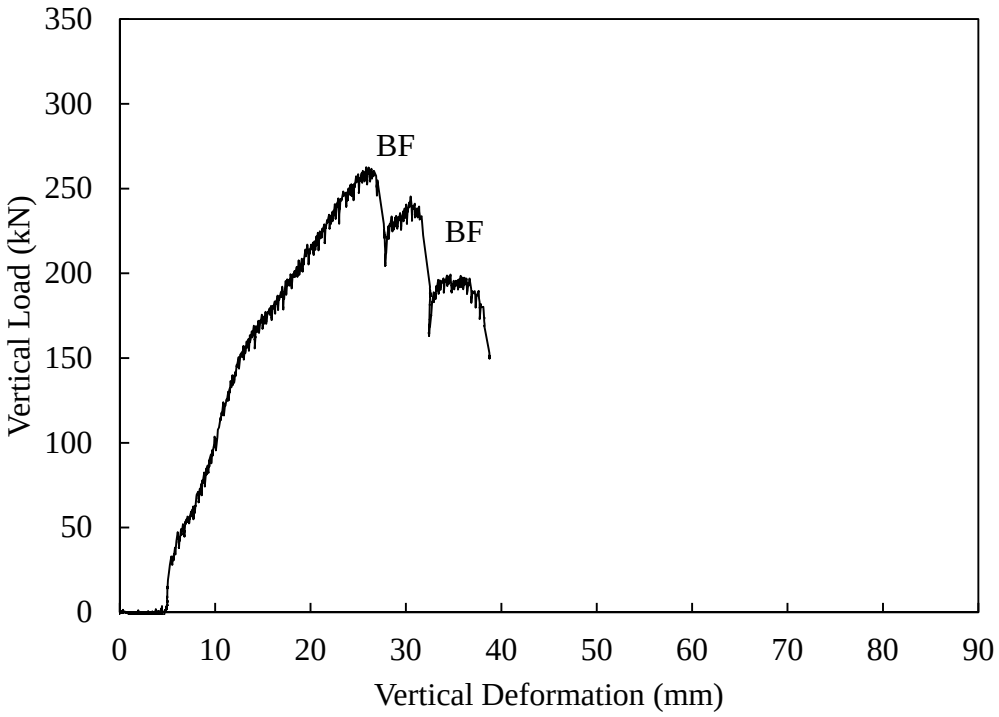

Figure B-9: Specimen 3B-13-U-200C

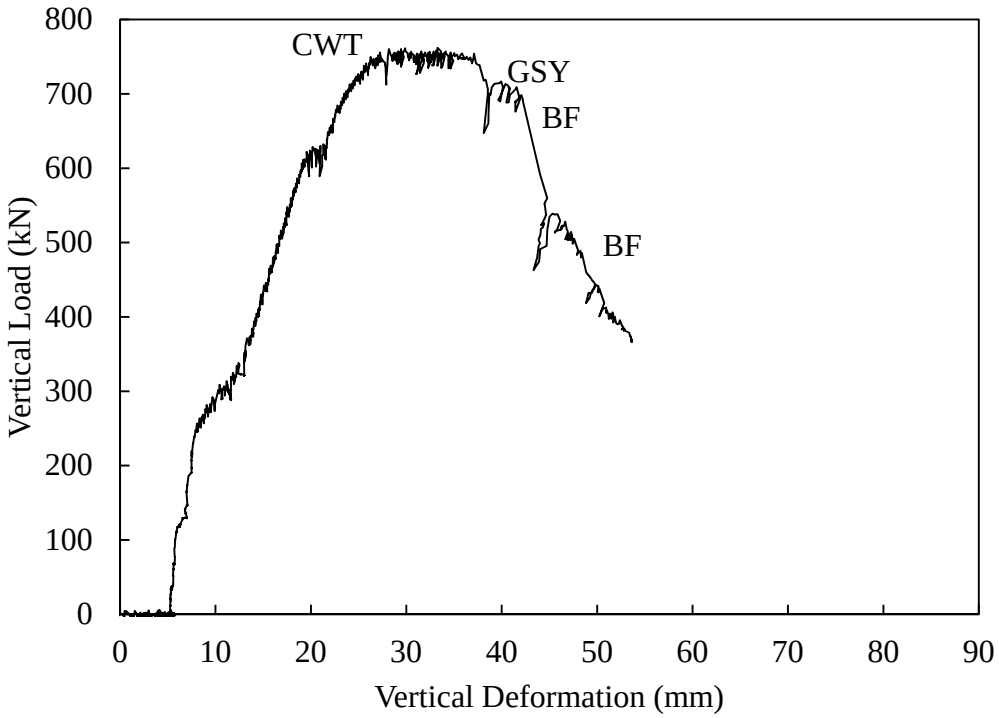

Figure B-10: Specimen 5B-10-U-0

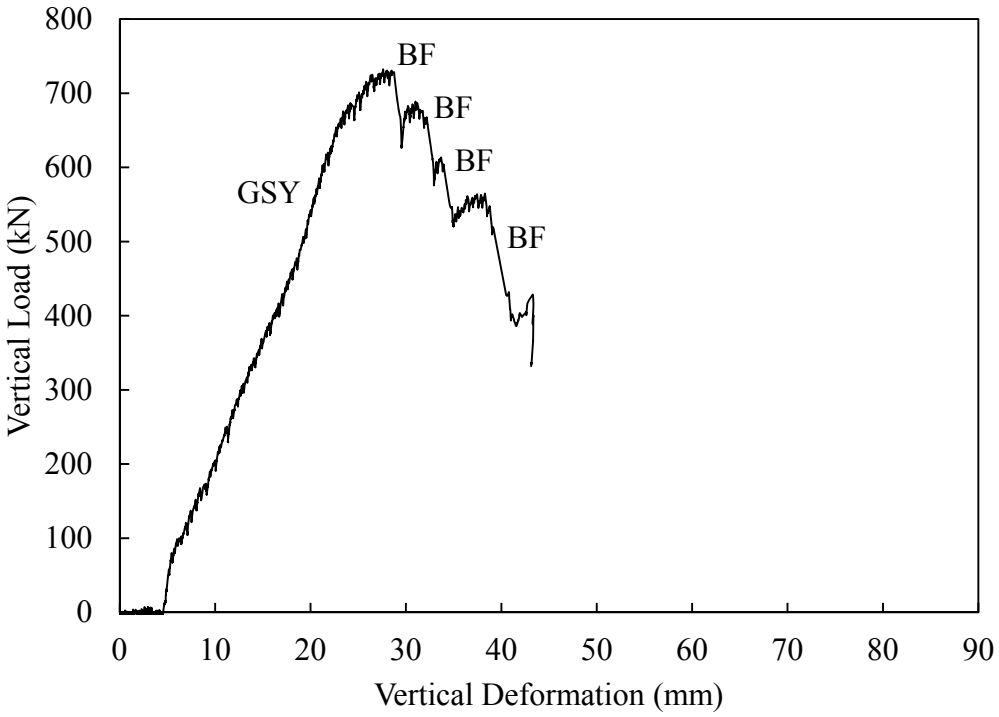

Figure B-11: Specimen 5B-10-U-300C

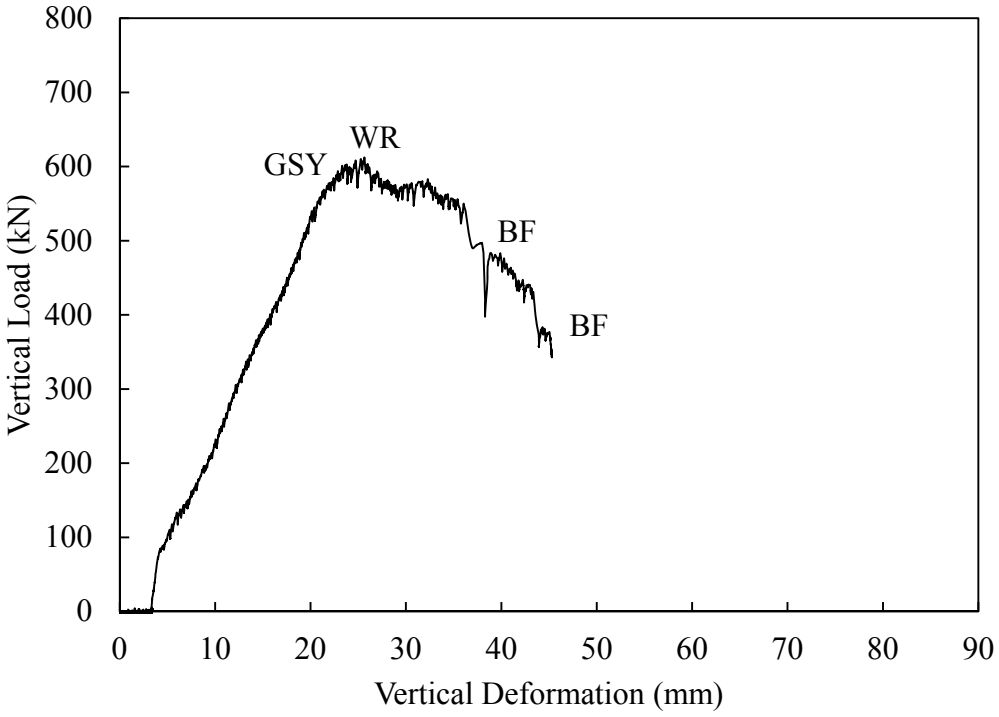

Figure B-12: Specimen 5B-10-U-200T

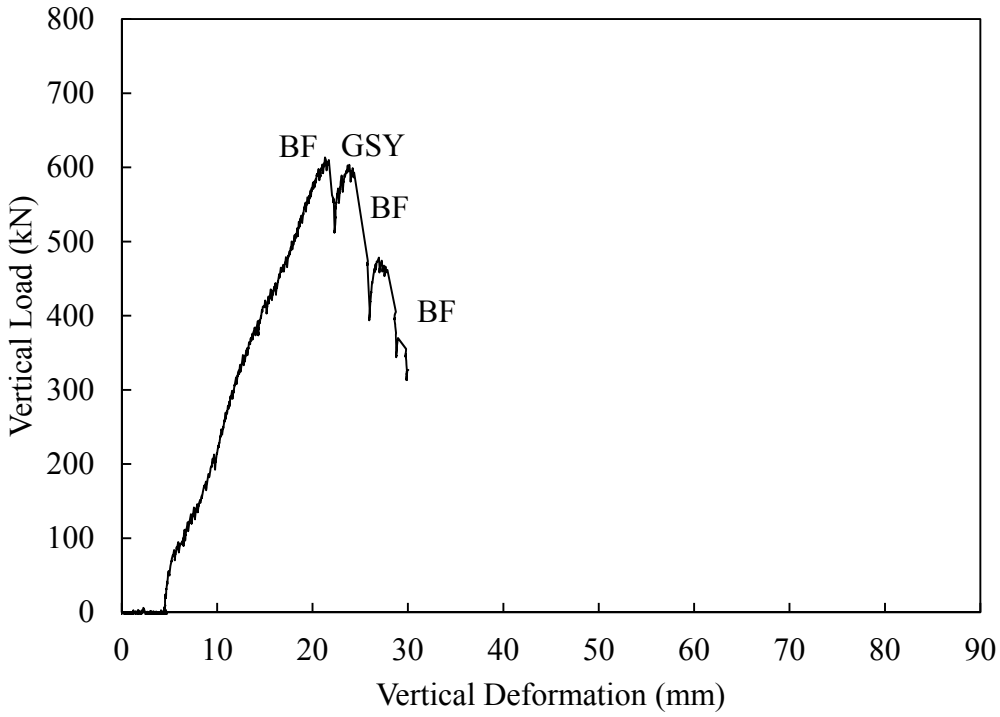

Figure B-13: 5B-13-U-300C

APPENDIX C: STIFFENED EXTENDED SHEAR TAB LOAD–DEFORMATION CURVES

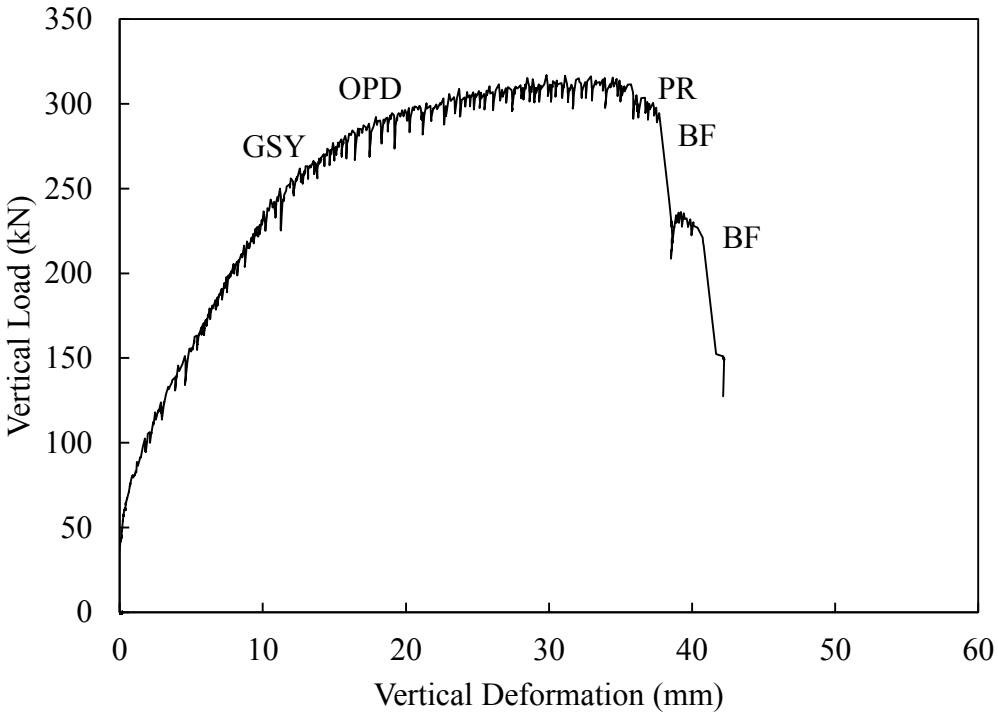

Figure A-1: Specimen 2B-10-S-0

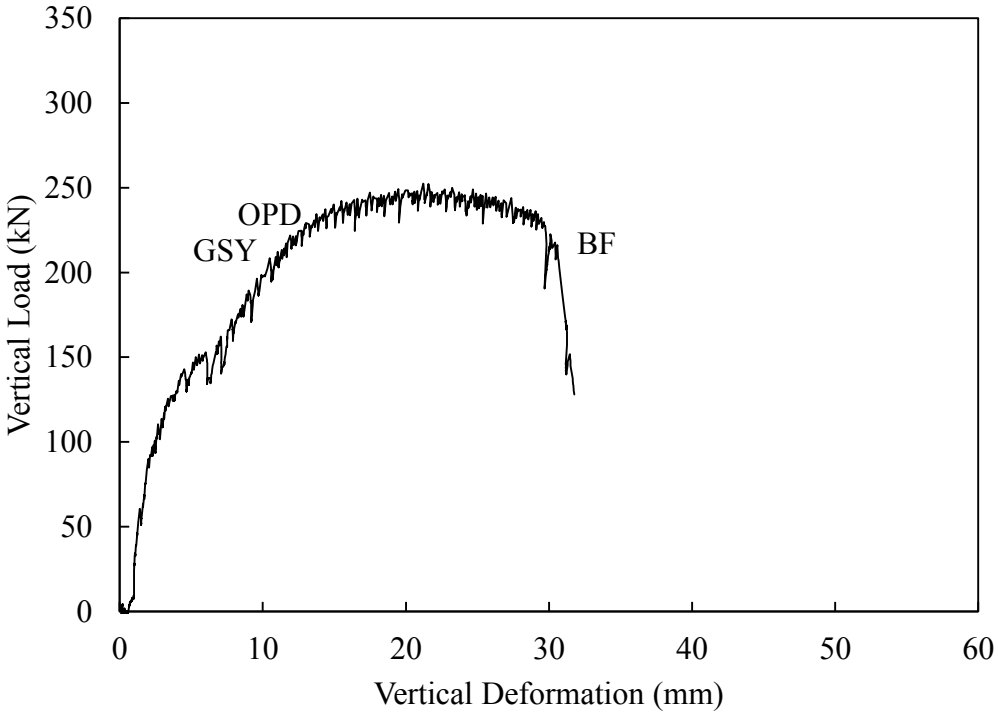

Figure A-2: Specimen 2B-10-S-200C

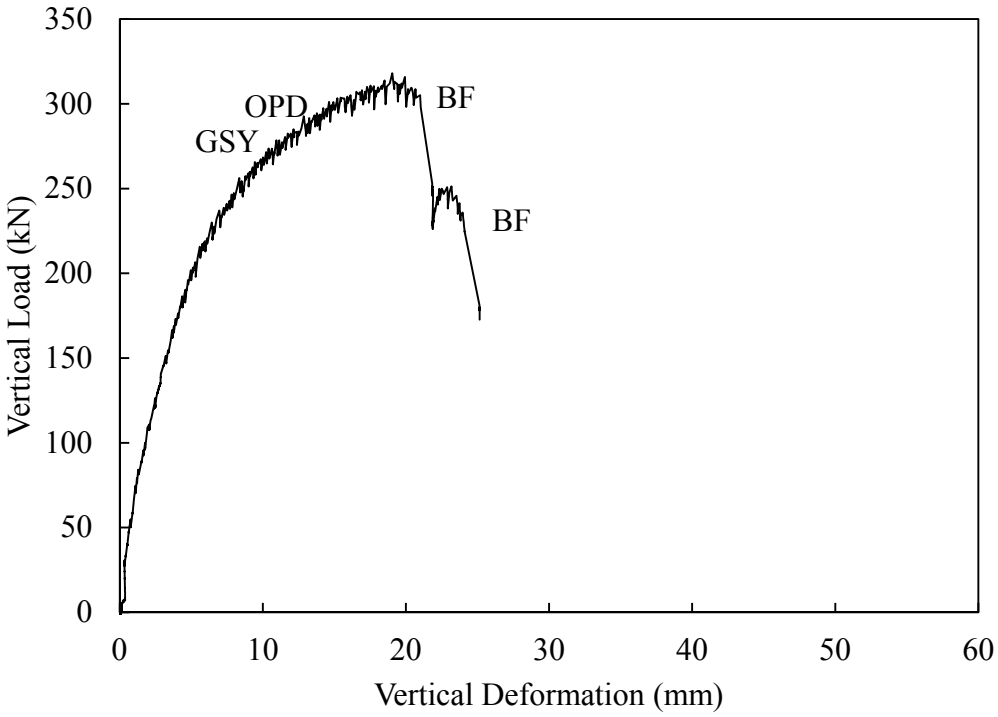

Figure C-3: Specimen 2B-13-S-200C

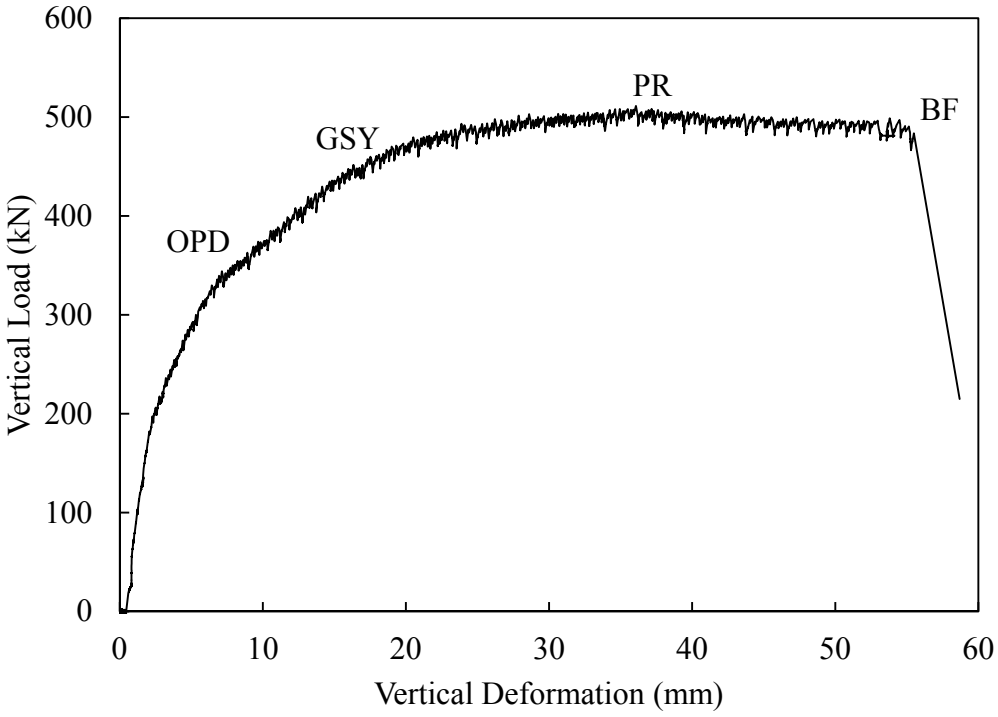

Figure C-4: Specimen 3B-10-S-0

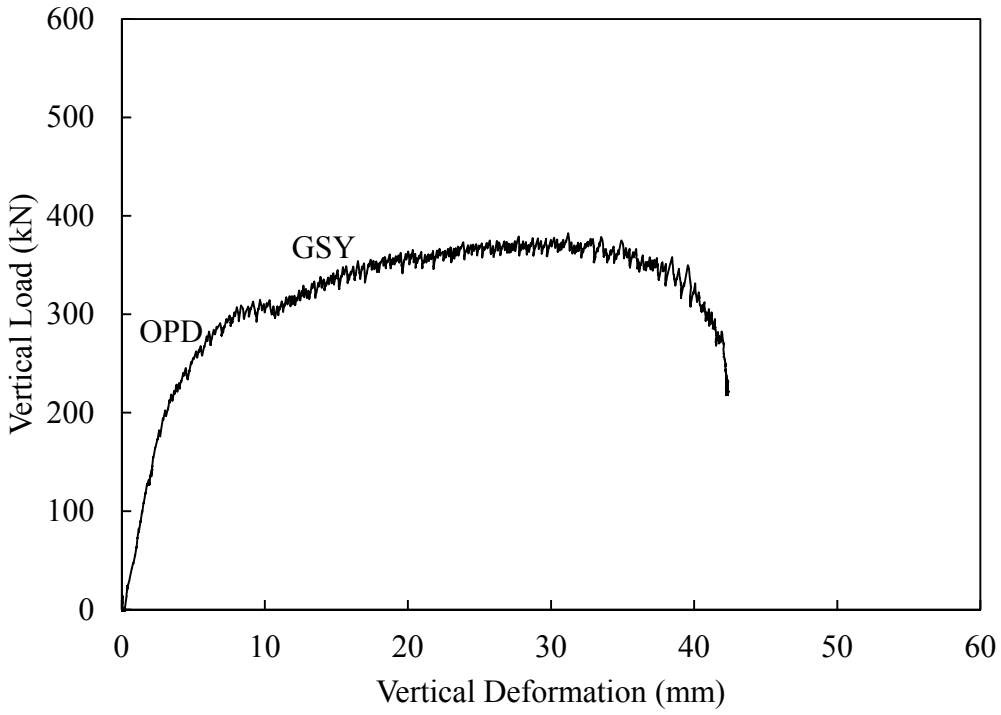

Figure C-5: Specimen 3B-10-S-200C

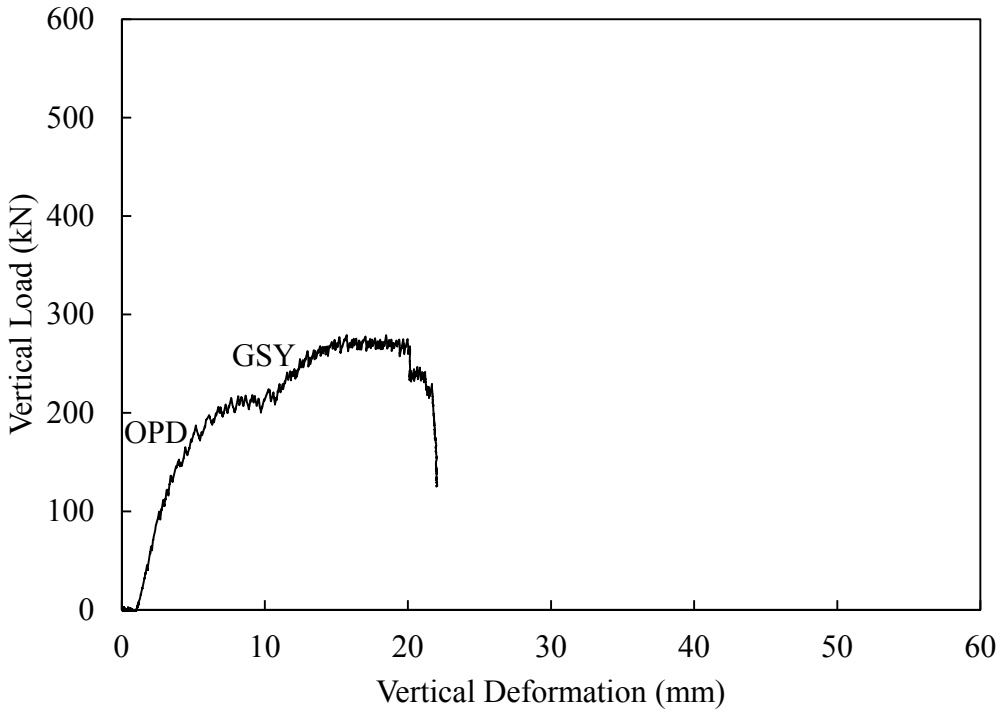

Figure C-6: Specimen 3B-10-S-300C

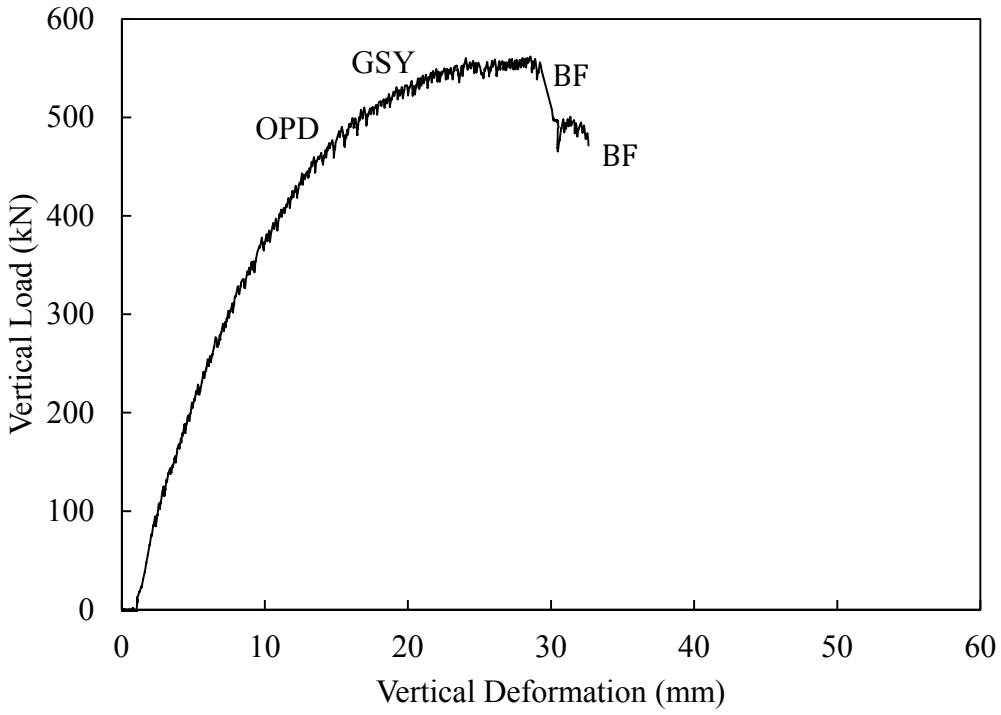

Figure C-7: Specimen 3B-13-S-200C

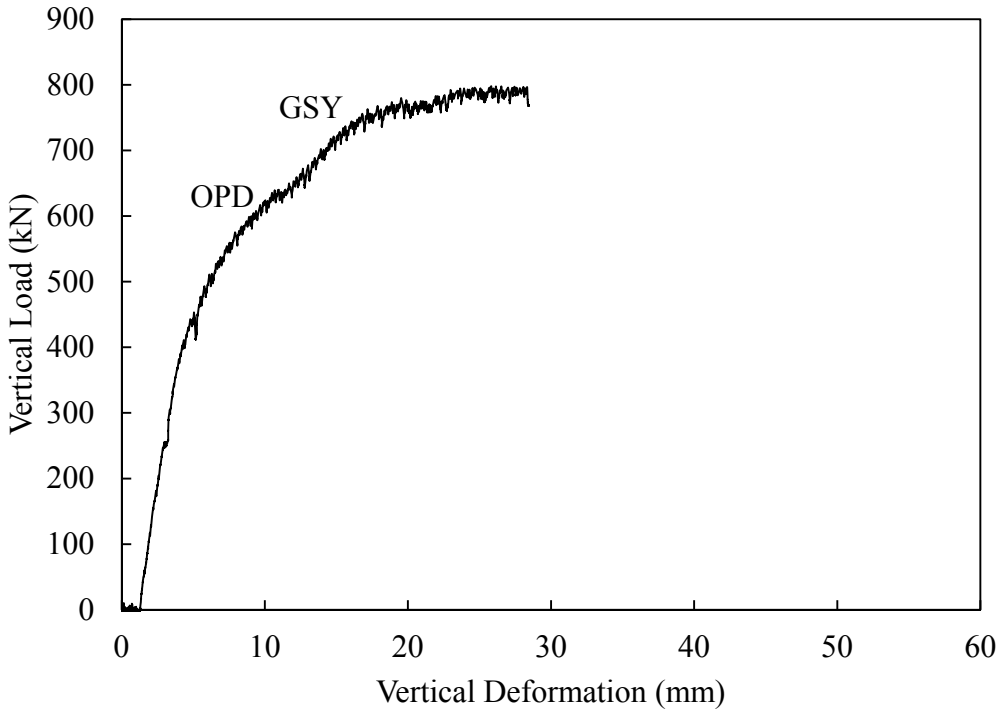

Figure C-8: Specimen 5B-10-S-300C

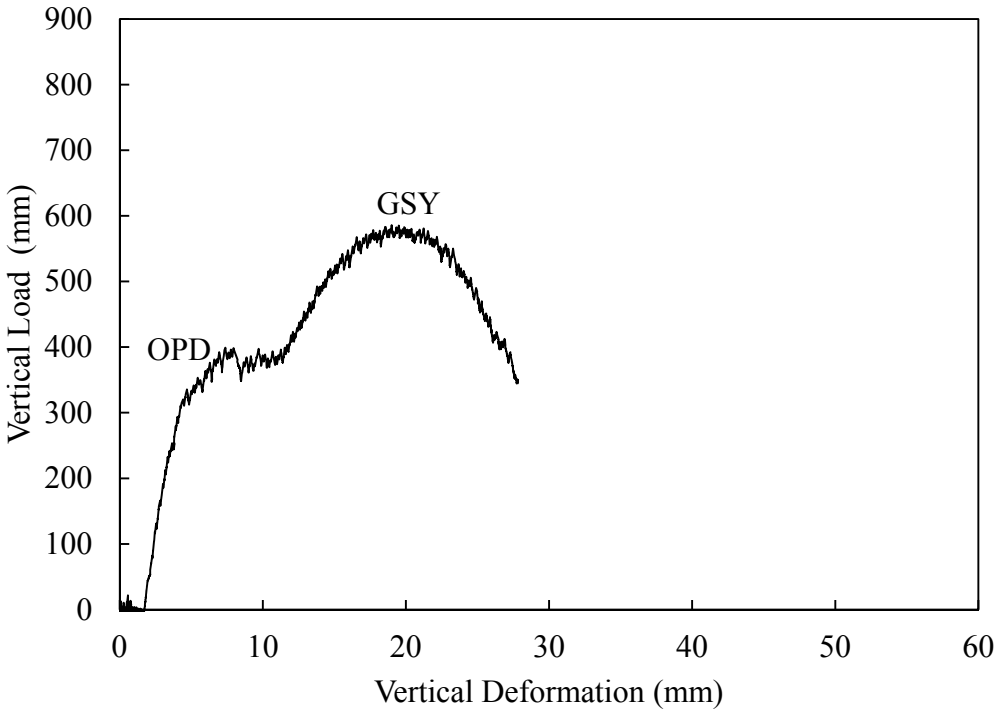

Figure C-9: Specimen 5B-10-S-400C

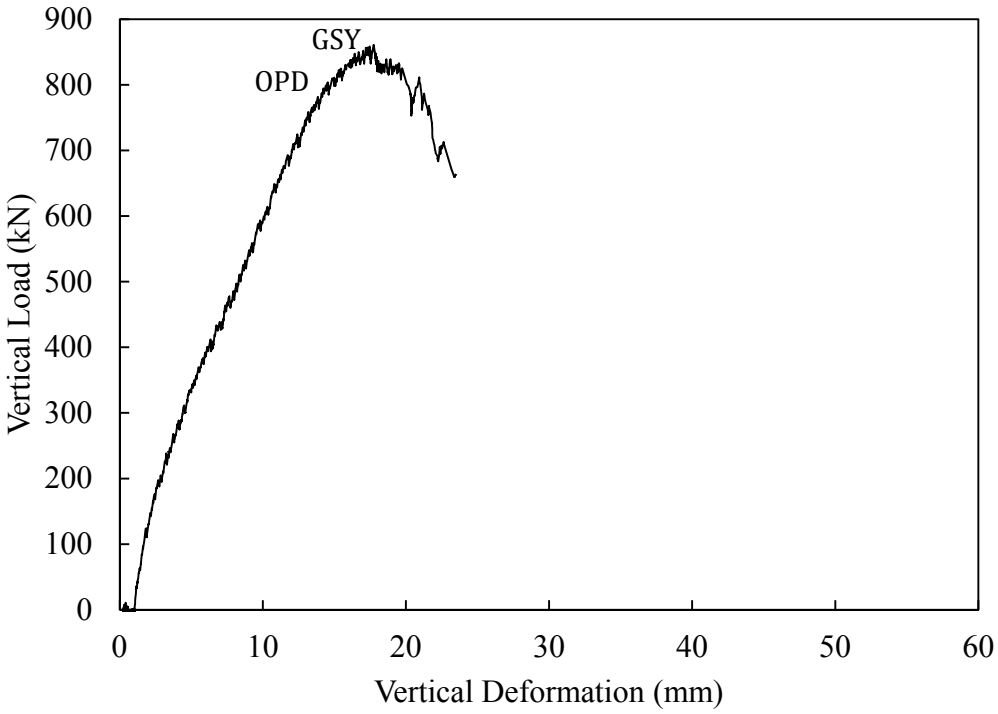

Figure C-10: Specimen 5B-13-S-500C